

Characterisation of the *MAD* and *17-4*
branching regulators of *Arabidopsis*

Danielle Taylor

Doctor of Philosophy

University of York

Biology

September 2013

Abstract

Aerial morphology in higher plants is highly variable and demonstrates the ability of plants to adapt to prevailing conditions. Regulation of shoot branching is a vital aspect of plant growth, controlling shoot system architecture. The phytohormones; auxin, cytokinin, and strigolactone are closely involved in the regulation of bud outgrowth, and therefore shoot branching, and the mechanisms by which they do this are of great scientific interest.

The *MAX (MORE AXILLARY GROWTH)* pathway in *Arabidopsis* consists of a series of genes involved in strigolactone biosynthesis and signalling. Mutations in these genes have been used to great effect to elucidate the manner of auxin-mediated inhibition of shoot branching via the *MAX* pathway.

The purpose of this study was twofold: Firstly, to characterise plants heterozygous for the semi-dominant *mad (more apical dominance)* mutation, which suppresses the *max1* branching phenotype and secondly, to characterise the *17-4* mutant, which displays an increased branching phenotype similar to that of *max2*. Various physiological and genetic techniques were applied to this end.

MAD/mad is not a general mediator of strigolactone signalling as it only affects the *max1* branching phenotype. *MAD/mad* partially restores wild-type branching to all of the *max* mutants, suggesting that it acts either downstream of, or in parallel to, *MAX2*. The *MAD* locus is within a 370kb region on the p-arm of At. Chromosome 3. Among the 230 genes in this region are three of considerable interest, *MES17*, *SPY*, and *AT3G11130.1* all with the potential for a role in the regulation of bud outgrowth and therefore all potential candidates for the *MAD* gene.

17-4 was isolated in a screen looking for mutants with high levels of branching in low nitrate conditions, and has striking morphological similarity to the well characterised *max2* mutant. Complementation testing showed that *17-4* was not one of the currently recognised *max2* alleles. This does not rule *17-4* out as a novel allele of *max2*. Increased branching in *17-4* is probably a result of increased auxin transport capacity and resistance to auxin-mediated suppression of bud outgrowth. *17-4* is not involved in strigolactone biosynthesis but appears to be involved in strigolactone signalling.

Contents

Abstract	2
Contents	3
List of figures	6
List of tables	8
Acknowledgements	9
Authors declaration	10
1. Introduction	11
1.1 General Introduction	11
1.2 Lateral organ formation and axillary meristems	12
1.3 Activity of axillary meristems	15
1.4 The canalisation hypothesis	16
1.5 Auxin	18
1.5.1 Auxin Transport	19
1.5.2 Auxin signalling	21
1.6 Cytokinins	25
1.6.1 Cytokinin biosynthesis and degradation	26
1.6.2 Cytokinin transport and signalling	27
1.6.3 Cytokinin and auxin interactions	28
1.7 Strigolactones and the <i>MAX</i> pathway	30
1.7.1 Strigolactone biosynthesis	31
1.7.2 Strigolactone transport	35
1.7.3 Strigolactone perception and signalling	36
1.8 Dorsoventral polarity in leaves	39
1.9 Nutrient supply	41
1.10 Shade avoidance	42
1.11 Thesis aims	42

2. Materials & Methods	44
2.1 Chemical Stocks	44
2.2 Plant lines and growth conditions	44
2.3 Sterile growth conditions	46
2.4 Antibiotic Selection	48
2.5 Physiological Crossing	48
2.6 Gathering physical data	49
2.7 Auxin transport assay	49
2.8 Split plate assay	50
2.9 Micrografting	51
2.10 Weck Jar branching assay	51
2.11 N deprivation and Crowding response experiments	51
2.12 Screen to isolate mutants with <i>max1</i> , or higher, branching levels	52
2.13 Leaf Cross sections	52
2.14 Scanning Electron Microscopy	53
2.15 GUS staining	54
2.16 Genetic Mapping	54
2.17 Marker Design	54
2.18 DNA and RNA extraction	55
2.19 RT-PCR	55
2.20 cDNA synthesis	55
2.21 PCR	57
2.22 Restriction Digests	58
2.23 Agarose Gel Electrophoresis	58
2.24 Primers	59
3. Characterisation of the <i>MAD</i> extragenic suppressor of the <i>max1</i> phenotype	61
3.1 Morphology of <i>MAD/mad</i> and <i>mad/mad</i>	61
3.2 The <i>mad</i> mutation in other genetic backgrounds	68
3.3 The <i>mad</i> leaf phenotype	70
3.4 Fertility in <i>MAD/mad</i> and <i>mad/mad</i>	79
3.5 Auxin status of <i>MAD/madmax1</i>	81
3.6 The effect of crowding on the <i>MAD/mad</i> phenotype	85
3.7 Mapping the <i>MAD</i> locus	97
3.8 Discussion	101
4. Characterisation of the <i>I7-4</i> mutant phenotype	107
4.1 Isolation of the <i>I7-4</i> mutant	107
4.2 Other mutants isolated in the screen	108

4.3	Auxin status of <i>17-4</i>	117
4.4	The effect of exogenous GR24 on <i>17-4</i>	119
4.5	Riciprocal micrografting of Col and <i>17-4</i>	121
4.6	Discussion	124
5. Conclusion		128
6. References		133

List of figures

	Page number
1. Representation of typical dicot and monocot architecture.	12
2. The auxin transport canalisation hypothesis.	17
3. Representation of auxin transport in vascular associated cells in the stem.	20
4. The conserved structure of ARFs and Aux/IAs.	23
5. Auxin signalling	24
6. Key elements in the cytokinin biosynthetic pathway and common cytokinins	27
7. GR24 and 5-deoxystrigol structures.	32
8. The <i>MAX</i> pathway in <i>Arabidopsis</i> – strigolactone biosynthesis, signalling and effects.	34
9. Strigolactone biosynthesis and signalling, a general overview	38
10. Cross section of a mature <i>Arabidopsis</i> leaf.	40
11. <i>Arabidopsis</i> Aerial Morphology	46
12. Split plate assay	50
13. Comparative aerial morphology of Col, <i>max1</i> , <i>MAD/mad</i> , and <i>mad,max1</i>	62
14. Comparative heights of Col, <i>max1</i> , <i>MAD/mad</i> , and <i>mad,max1</i>	63
15. Leaf and petiole lengths of Col, <i>max1</i> , <i>MAD/mad</i> , and <i>mad,max1</i>	64
16. Rosette and cauline branch number of Col, <i>max1</i> , <i>MAD/mad</i> , and <i>mad,max1</i>	65
17. Comparative aerial morphology of Col, <i>MAD/mad</i> and <i>mad</i>	66
18. Rosette branching in the <i>max</i> mutants, <i>axr1</i> and <i>MAD/mad,max</i> and <i>MAD/mad,axr1</i> double mutants	70
19. The <i>mad</i> leaf phenotype	71
20. Adaxial leaf surfaces of Col, <i>MAD/mad</i> and <i>mad</i>	74
21. Abaxial leaf surfaces of Col, <i>MAD/mad</i> and <i>mad</i>	75
22. Trichome development	76
23. Cross sections of Col, <i>MAD/mad</i> and <i>mad</i> leaves	77
24. <i>FIL8</i> expression analysis of <i>mad</i> leaves	78

25. Germination rates of Col, <i>MAD/mad</i> and <i>mad</i>	80
26. Col, <i>MAD/mad</i> and <i>mad</i> carpel and pollen morphologies	81
27. Auxin transport in Col, <i>MAD/mad</i> and <i>mad</i>	82
28. Bud auxin response in Col, <i>MAD/mad</i> and <i>mad</i>	84
29. Shoot to Root ratios of Col, <i>MAD/mad</i> and <i>max1</i> (monoculture crowding experiments)	87
30. Secondary branching in Col, <i>MAD/mad</i> and <i>max1</i> (monoculture crowding experiments)	88
31. Root length and lateral root number in Col, <i>MAD/mad</i> and <i>max1</i> (monoculture crowding experiments)	90
32. Shoot to Root ratios of Col, <i>MAD/mad</i> and <i>max1</i> (polyculture crowding experiments)	92
33. Secondary branching in Col, <i>MAD/mad</i> and <i>max1</i> (polyculture crowding experiments)	94
34. Root length and lateral root number in Col, <i>MAD/mad</i> and <i>max1</i> (polyculture crowding experiments)	95
35. <i>MAD</i> , GAPC linkage.	97
36. Location of the <i>MAD</i> locus	100
37. Postulated mechanism of bud outgrowth with relation to <i>MAD</i>	104
38. 28 day old Col, <i>max2</i> and <i>17-4</i>	110
39. 6 week old Col, <i>max2</i> and <i>17-4</i>	111
40. 6 week old Col, <i>max1</i> , <i>max2</i> and <i>17-4</i>	112
41. Average heights for Col, <i>max1</i> , <i>max2</i> and <i>17-4</i>	113
42. Average cauline internode lengths and total heights for Col, <i>max1</i> , <i>max2</i> and <i>17-4</i>	114
43. Average leaf and petiole lengths for Col, <i>max1</i> , <i>max2</i> and <i>17-4</i>	115
44. Average rosette branches for Col, <i>max1</i> , <i>max2</i> and <i>17-4</i>	116
45. Auxin transport in Col, <i>max1</i> and <i>17-4</i>	118
46. Bud auxin responses in Col, <i>max1</i> and <i>17-4</i>	119
47. Rosette branching in Col, <i>max1</i> , <i>max2</i> , <i>max3</i> , <i>max4</i> , and <i>17-4</i> with exogenous GR24	121
48. Reciprocal micrografting of Col and <i>17-4</i>	123
49. Postulated mechanism of bud outgrowth with relation to <i>17-4</i>	127
50. Postulated mechanistic model of the regulation of bud outgrowth incorporation potential roles for both <i>MAD</i> and <i>17-4</i> .	129

List of Tables

	Page number
1. Genes involved in the <i>Arabidopsis</i> <i>MAX</i> pathway with orthologs	35
2. Plant lines used in this study	44-45
3. Primer used in this study	59-60
4. Comparative effects on <i>Arabidopsis</i> morphology of the <i>mad</i> mutation	68
5. Treatments applied to Col, <i>MAD/mad</i> and <i>mad</i> in the crowding levels and nitrate deprivation experiments	86
6. Markers used in initial <i>MAD</i> mapping	98
7. Markers used in the fine-structure mapping of <i>MAD</i>	99
8. Mutants isolated in the nitrate deprivation screen	109

Acknowledgements

I would like to thank the following people for their ongoing support, encouragement and help throughout my PhD project, and the writing of this thesis:

My supervisors:

Professor Ottoline Leyser

Dr Richard Waites

The staff in the Leyser Laboratory, University of York, particularly:

Petra Stirnberg

Tom Bennett

Sally Ward

Lisa Williamson

My friends and family, particularly:

Rich Snarr

Gillian Mooney

Eddie Snarr

Authors declaration

I declare that, except where explicit reference is made to the contribution of others, that this thesis is the result of my own work. This work has not previously been presented for an award at this, or any other, University. All sources are acknowledged as References.

Introduction

1.1 General Introduction

Plants are sessile organisms. As a result of this they cannot simply remove themselves from unfavourable environments. In order to achieve the developmental plasticity required for them to survive in prevailing conditions, including abiotic factors such as nutrient supply and light quality and biotic factors such as herbivory (reviewed in deJong, M. and Leyser, O. (2012)), plants need to have architectural flexibility. This is facilitated by the indeterminate nature of plant development. Adapting aerial morphology by controlling shoot branching is a good example of this flexibility put into practice. To be able to produce these responses plants need to be able to integrate signals, environmental or otherwise, in order to regulate development. What these signals are, and how they are perceived and processed, are the subject of a vast amount of current plant science research. One of the plant model organisms used for this research is the Eudicot *Arabidopsis thaliana*. A short life-cycle (approximately 6 weeks), self-fertilisation with prolific seed production, a predominantly mapped genome and the wealth of genomic resources available make *Arabidopsis* a model genetic organism (reviewed in (Mienke, D.W. *et al.* (1998), (Koorneef, M and Mienke, D. 2010)).

Shoot branches arise from axillary meristems, found in leaf axils. All vegetative axillary meristems have the same developmental potential as the main shoot apical meristem (SAM) but are tightly regulated. Most axillary meristems will form a bud, but development will stop and the bud will be held in a dormant state. Axillary meristem activity is tightly regulated by both environmental and inherent physiological factors. Whether or not a bud grows out or is held in a dormant state is therefore the result of complex and dynamic signal integration (Shimizu-Sato, S. and Mori, H. (2001)). Plant hormones are an important factor in the regulation of bud activity (Janssen, B.J. *et al.* (2014)). Phytohormones enable both systemic and local co-ordination of development by acting as long-distance signalling molecules.

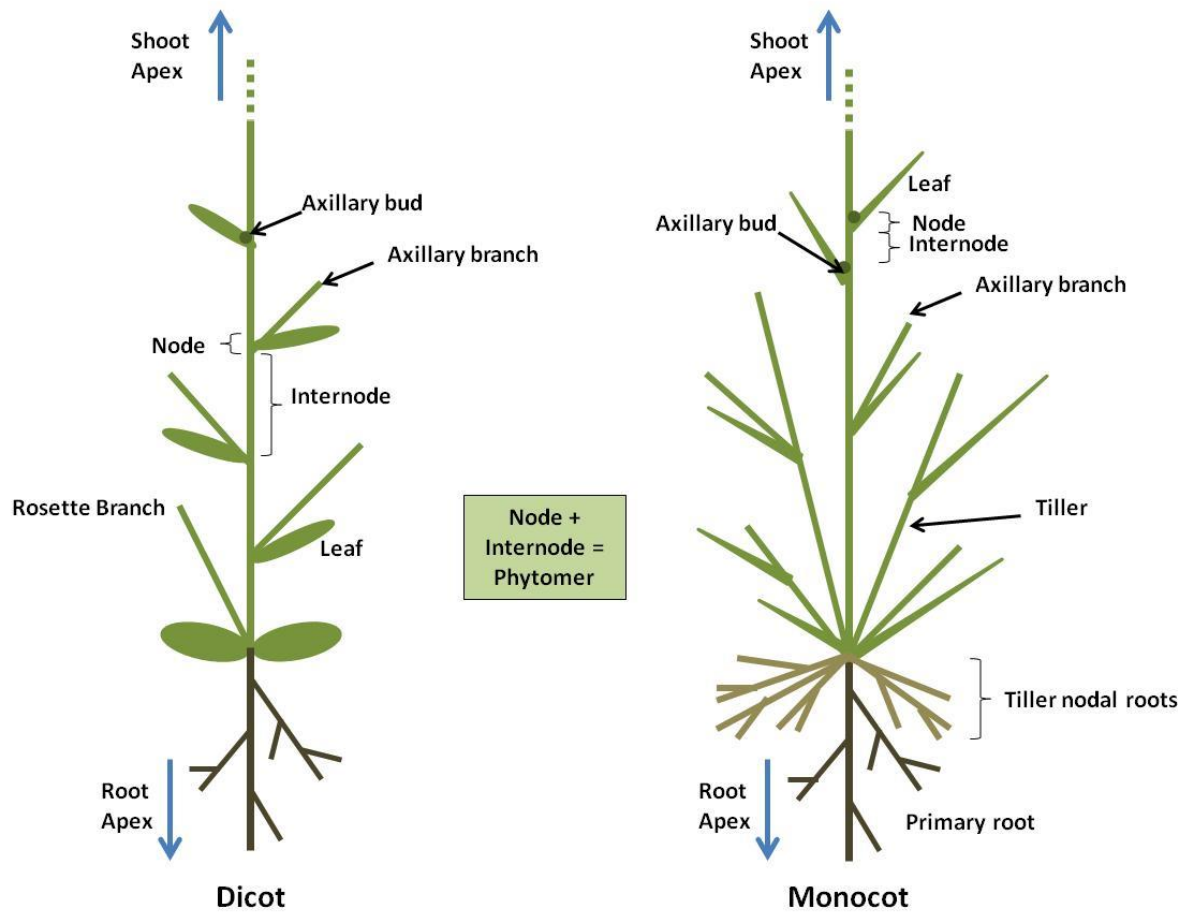


Figure 1. Representation of typical dicot and monocot architecture. The primary shoot axis, with the SAM at its apex, establishes phytomers, consisting of an internode, and node, comprising both an axillary meristem and a lateral leaf. The axillary meristems develop into axillary buds which have the potential to form secondary branches. These branches can, in turn, act in the same way as the primary branch and form higher order branches. The root also has the potential to form lateral roots. Monocot plants can also produce tillers, which are axillary branches formed by the basal nodes of monocots which

1.2 Lateral organ formation and axillary meristems

During embryogenesis the apical-basal axis is determined, with the shoot apical meristem (SAM) at the apical pole, and the root apical meristem (RAM) at the basal pole. Both of these are primary meristems. Plants exhibit modular growth and which is exemplified in the shoot by the production of phytomers. Phytomers are repetitive sections of the plant shoot that include an internode, and a node, that comprise a leaf and its associated axillary meristem (AM). These AMs give the plant the potential for higher order aerial development. AMs may develop into a bud, which has the potential to form a secondary growth axis in the form of a

secondary branch which in turn, can have AMs which form tertiary branches and so on. This mode of development can lead to highly complex aerial morphology and is determined by the number of AMs produced and the ability of these AMs to produce a branch (Bennett, T. and Leyser, O. (2006), DeSmet, I. And Juergens, G. (2007), Janssen, B.J. *et.al.* (2014), Kerstetter, R.A. and Hake, S. (1997), McSteen, P. and Leyser, O. (2005), Schmitz, G. and Theres, K. (2005), Sussex, I.M. and Kerk, N.M. (2001).

As mentioned above, AMs are the starting point for axillary branches. They form at the base of the adaxial side of the leaf in the centre of the boundary zone (BZ). The BZ is an area of cells between the developing leaf and the SAM. It also plays an important role in meristem maintenance and organogenesis (Zadnikova, P. and Simon, R. (2014)). The transcription factor LATERAL ORGAN BOUNDARIES1 (LOB1), which induces the expression of BAS1, encoding a protein which inactivates brassinosteroid activity, is active during the establishment of the BZ (Bell, E.M., *et.al.* (2012)). Brassinosteroids influence cell expansion and division (Fridman, Y. and Savaldi-Goldstein, S. (2013)). The reduction of brassinosteroid activity, mediated by LOB1, results in a reduction in cell size and division rate in the BZ (Bell, E.M., *et.al.* (2012), Gendron, J.M. *et.al.* (2012)). Auxin levels in the BZ are depleted by the outward orientation of the PIN-FORMED1 (PIN1) auxin efflux protein. On the SAM side of its expression domain, PIN1 changes orientation during BZ development from orientation towards the leaf primordium to orientation towards the SAM (Wang, Q. *et.al.* (2014), Wang, Y. *et.al.* (2014)). The change in orientation of PIN1 is dependent on PINOID (PID) kinase as is controls PIN1 apical-basal membrane location (Furutani, M., *et.al.* (2004)). Both *pin1* and *pid* mutant plants have defects in AM formation showing the importance of correct, PID-mediated PIN orientation (Wang, Q. *et.al.* (2014), Wang, Y. *et.al.* (2014)).

The development of secondary branches from AMs is also affected by *RPS10B*. This gene was isolated in a *max2-1* suppressor screen (see chapter 1.7 for more information on MAX2) and encodes the ribosomal protein S10e (Stirnberg, P. *et.al.* (2012)). Levels of proteins which are involved in the regulation of auxin distribution and, by proxy, auxin-mediated patterning of organ boundaries, may be imbalanced. These include the Aux/IAA auxin signalling proteins (see chapter 1.5.2 for more information on Aux/IAAs) which may be affected by the *rps10b-1* mutation.

BZ tissue markers in *Arabidopsis* are the NAM-ATAF1/2-CUC2 (NAC) transcription factors CUP SHAPED COTYLEDONS1,2 and 3 (CUC1, 2 and 3) (Spinelli, S.V. *et.al.* (2011)) which

act redundantly during meristem formation. The tomato gene *GOBLET* (*GOB*) is a *CUC* gene ortholog (Busch, B.L. *et.al.* (2011)). The expression of the *CUC* genes is necessary for both the development of the SAM and the creation of the BZ. Brassinosteroids act to downregulate *CUC* expression giving low brassinosteroid levels a dual purpose in the BZ, reducing cell expansion and division and permitting *CUC* gene expression (Bell, E.M. *et.al.* (2012), Gendron, J.M. *et.al.* (2012))

Cells in the SAM are kept in an undifferentiated state, whilst cell in both the BZ and the leaf primordium differentiate. The homeobox class I KNOX gene *SHOOT MERISTEMLESS* (*STM*) acts to maintain the identity of meristematic cells (Long, J.A. *et.al.* (1996)). The MYB transcription factor AS1 and the LATERAL ORGAN BOUNDARY DOMAIN (LBD) transcription factor AS2 act to down regulate *STM* when cells start to differentiate (Ikezaki, M. *et.al.* (2010)). *STM* continues to be expressed at low levels in BZ cells during an early phase of BZ development (Long, J. and Barton, M.K. (2000)). During this time, cell in the BZ retain the ability to return to a meristematic state. It is during this phase that the AM is initiated (Grbic, V. and Bleecker, A.B. (2000)). At this time, *STM* expression is high in the centre of the BZ. In *Arabidopsis* this *STM* expression is dependent on the GRAS transcription factor LATERAL SUPPRESSOR (*LAS*) (Greb, T. *et.al.* (2003)). *LAS* orthologs are found in tomato (*LS*) (Schumacher, K. *et.al.* (1999)), and rice (*MONOCULM1* (*MOC1*)) (Li, X.Y. *et.al.* (2003)). The initiation and further development of the AM is controlled by several factors that each have partially redundant functions. As well as *LAS*, the MYB factors REGULATOR OF AXILLARY MERISTEMS (*RAX*) in *Arabidopsis*, BLIND (*BD*) and POTATO LEAF in tomato are involved in AM development (Busch, B.L. *et.al.* (2011), Keller, T. *et.al.* (2006), Schmitz, G. *et.al.* (2002)). The basic helix-loop-helix (bHLH) protein REGULATOR OF AXILLARY MERISTEM FORMATION (*ROX*) in *Arabidopsis* and its orthologs LAX PANICLE1 (*LAX1*) in rice, and BARREN STALK1 (*BA1*) in maize, is also involved in AM development (Gallavotti, A. *et.al.* (2004), Komatsu, *et.al.* (2003), Ritter, M.K. *et.al.* (2002), Yang, F. *et.al.* (2012)).

These observations resolve a long running debate in axillary meristem biology involving two ideas about their origin. The *de novo* formation theory suggests entirely new initiation in leaf axils, as suggested by the anatomy of AM formation in some leaves, such as those before the floral transition in *Arabidopsis*. However, in other axils, such as those formed during the floral transition in *Arabidopsis*, AMs are immediately morphologically distinct and appear to form directly from the primary SAM. This is the basis for the detached meristem theory (review

Bennett, T. and Leyser, O. (2006)). Experiments on *LAS*, *RAX* and *ROX* genes have shown that even in axils with slow developing AMs, BZ cells appear to remain in a state that is not fully differentiated from which the AM can be initiated. This provides evidence that, even for plants like *Arabidopsis*, where the meristem is only detectable at a later stage of development, the meristem is a detached meristem and is not formed *de novo* (Bennett, T. and Leyser, O. (2006), Leyser, O. (2003)).

1.3 Activity of Axillary Meristems

Axillary meristem activity is a major determinant of plant shoot architecture. Axillary branching is usually inhibited via the shoot apex in a process known as apical dominance (review Leyser, O. (2005)). The principle of long distance control from a remote site of necessity requires a signal that moves basipetally from the shoot apex. The signal was identified as auxin by Thimann and Skoog in 1933 (Thimann, K.V. and Skoog, F. (1933)). However, auxin from the primary apex does not enter the bud (Booker, J. *et.al.* (2003), Hall, S.M. and Hillman, J.R. (1975), Morris, D.A. (1977)). In light of this, a second messenger was postulated. Cytokinin and strigolactones are the two best candidate for this (cytokinins and strigolactones are covered in more detail in chapters 1.6 and 1.7 respectively). Cytokinins have a distinct effect on bud outgrowth, allowing escape from apical dominance even in the presence of an intact shoot apex (Sachs, T. and Thimann, K.V. (1964)). Cytokinin acts antagonistically with auxin with respect to control of bud outgrowth. A reduction in stem cytokinin levels maintains buds in a dormant state. A reduction of auxin levels in the stem, as a result of decapitation, results in increased levels of cytokinin biosynthesis (Bangerth, F. (1994)). In pea, the expression of cytokinin biosynthesis genes *PsIPT1* and *PsIPT2* is induced near axillary buds after decapitation (Tanaka, M. *et.al.* (2006)). From there, cytokinin may be transported into the adjacent axillary buds. This has been demonstrated in pea where increased levels of the cytokinin zeatin were found in axillary buds post-decapitation (Turnbull, C.N.G. *et.al.* (1997)). However, it has recently been shown that increased transcription from *IPT* genes is not required for release from apical dominance in *Arabidopsis* (Müller, D. *et.al.* (2015)).

Shoot architecture can also be affected by exogenous factors, such as nutrient availability or shading which can have a profound effect on a plants aerial morphology (Casal, J.J. *et.al.* (1986), deJong, M. *et.al.* (2014), Lopez-Bucio, J. *et.al.* (2002), Yoneyama, K. *et.al.* (2013)). Responses in the plant shoot to alterations in nutrient supply most likely involve a long distance

signal acropetal signal from root to shoot. Cytokinin is a good candidate for this as a main site for its biosynthesis is the root tips (Miyawaki, K. *et.al.* (2004), Nordström, A. *et.al.* (2004)). Strigolactones are equally good candidates. Analysis of mutants with increased branching phenotypes; *max* in *Arabidopsis*, *rms* in pea, *dad* in petunia and *d* in rice are all either strigolactone deficient or strigolactone insensitive (Gomez-Roldan, V. *et.al.* (2008), Umehara, M. *et.al.* (2008)). Cytokinin and strigolactone both regulate bud outgrowth. The effects of these two phytohormones was intergrated into a model known as autocorrelative inhibition. This model combines the second messenger theory with the canalization theory and postulates a scenario where buds compete for establishment of an auxin transport route from bud to stem (Balla, J. *et.al.* (2011), Li, C.J. and Bangerth, F. (1999), Sachs, T. (1981)).

1.4 The Canalisation Hypothesis

Auxin transport canalisation was first proposed by Sachs in 1975 (Sachs, 1975). His hypothesis stated that vascularisation occurred due to the gradual restriction of auxin flow into distinct channels. This hypothesis states that there is passive movement of auxin from an auxin source to an auxin sink, and that a positive feedback loop is in effect whereby the active transport of auxin reinforces this passive movement. The canalisation model demonstrates how vascular differentiation can occur in specific cells from within a field of initially similar cells.

The canalisation effect is shown in figure 2. Auxin travels from an auxin source. Competent cells transport the auxin from the source to a sink, ie the stem, and in doing so establish an auxin flux. This flux is hypothesised to upregulate and polarise auxin transporters, such as PIN1. This further encourages auxin transport in a positive feedback loop thus auxin transport is sustained in files of cells. These files of cells differentiate into vascular tissue thereby creating a vascular link from bud to stem. This hypothesis has since been supported by studies showing that PIN1 biosynthesis and polarisation is increased along paths of auxin flux (Paciorek, T. *et.al.* (2005)).

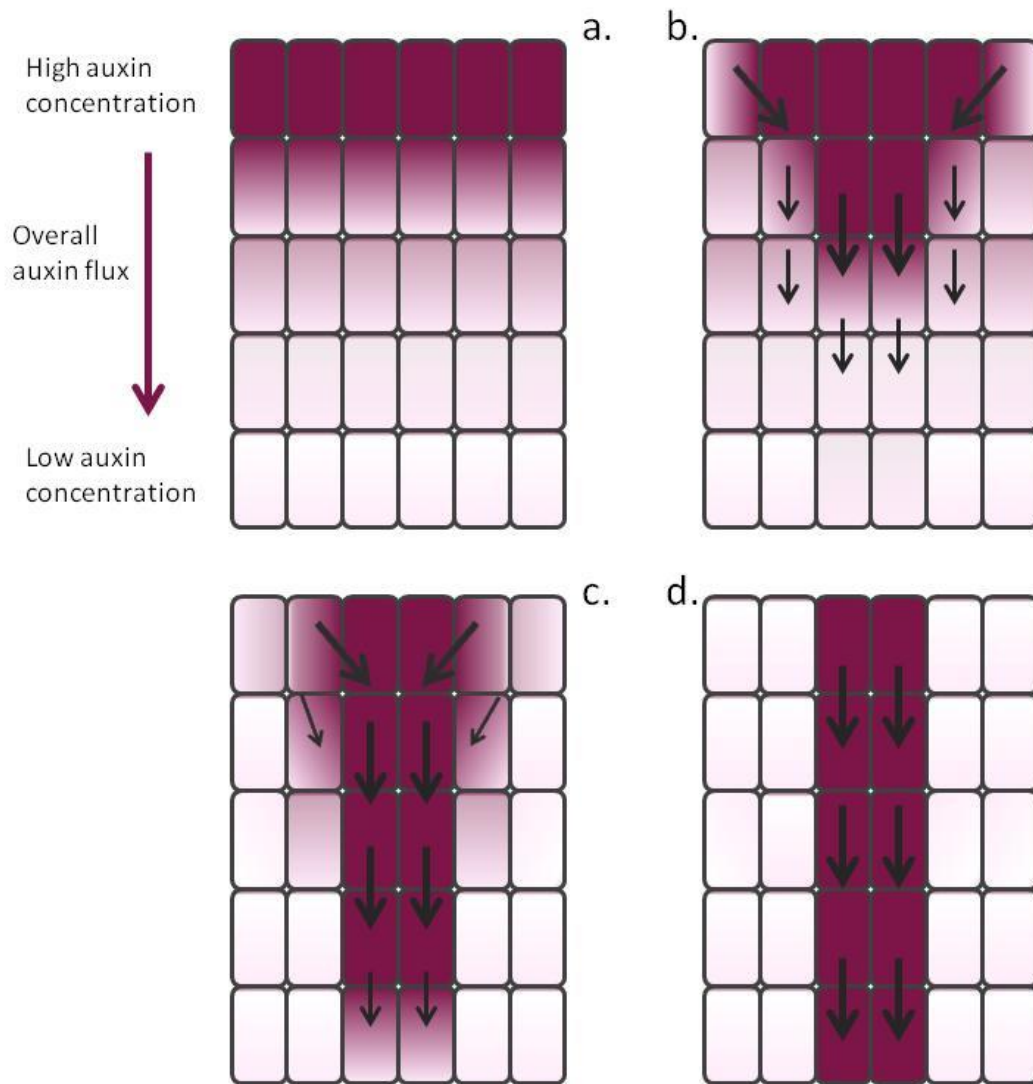


Figure 2. The auxin transport canalisation hypothesis.

- a. An area of undifferentiated tissue with auxin (red) moving from the top of the section to the bottom. The auxin is moving from an area of high concentration (source) to an area of low concentration (sink).
- b. Competent cells with polarised PIN1 auxin efflux proteins at the basal cell membrane start to actively transport auxin.
- c. At this stage the formation of distinct channels of auxin transport can be seen. From the initial flow of auxin continuous transport has been established. The level of auxin flux within the central cells is such that most of the auxin is being transported within this channel.
- d. At this stage directional auxin transport outside of the main channel is negligible. The high auxin flux of the central cells increase PIN1 expression and basal localisation and positive feedback of auxin flux is perpetuated. The auxin within the cells that comprise the auxin channel enables cell differentiation into vascular cells thus connecting the bud to the stem.

When the main source of auxin, ie. the plant stem, is removed, auxin levels in the main stem decrease. This results in extra capacity in the stem for auxin transport which allows auxin flux from bud to stem to increase, resulting in escape from apical dominance and bud outgrowth. When a few buds have grown out and have established auxin flow into the main stem the capacity for auxin in the main stem once more drops and apical dominance resumes. This prevents further buds from growing out.

1.5 Auxin

The phytohormone auxin is directly involved in a multitude of processes key to plant growth and development. The first of the hormones discovered to play a role in regulation of shoot branching, auxin was first recognised as an exogenous repressor of bud outgrowth in 1933 by Thimann and Skoog (Thimann.K, and Skoog.F, 1933). Since that date the field of auxin biology has expanded rapidly, with many areas as yet unexplored.

Despite all plant tissues having the capacity to produce auxin (Ljung, K. *et al.* (2001)), it is produced primarily at the shoot apex and particularly in young, developing leaves. Determining the sites of auxin production has proved to be a far simpler matter than elucidating the exact nature of its complex biosynthesis. Research in this area has been hampered by the fact that Loss of Function (LoF) mutants in auxin biosynthesis genes have very extreme, often lethal, phenotypes; in addition the enzyme families are large with significant functional redundancy. The severe nature of some of these mutants only serves to emphasize the ubiquity of auxin in regulating plant development (Cheng, Y. *et.al* (2006)(2007)). Auxin can be synthesised via either a tryptophan-dependent or a tryptophan-independent pathway (Mano, Y. and Nemoto, K. (2012)). It was initially thought that all auxins were synthesised from tryptophan but experimentation revealed auxin production in several tryptophan deficient mutants, suggesting a second set of potential tryptophan-independent auxin production pathways. Some members of the *YUCCA* gene family are known to play a role in auxin biosynthesis and other potential pathways have been identified based on presumptive intermediary molecules between tryptophan and auxin. These include the IAOx (Indole-3-acetaldoxime) pathway and the more recently determined IPA (Indole-3-pyruvate) pathway (Tao.Y, *et al*, (2008)). It is not known which, if any, of these pathways are used in different circumstances, although it is thought that the IAOx pathway is not the primary method of production as IAOx has not been detected in

monocots thus far (Sugawara.S, *et al.* (2009)). Once produced it is possible to sequester auxin in conjugated form with certain amino acids until it is required.

1.5.1 Auxin transport

Auxin is a molecule that is produced locally, but utilised globally. The suggestion that auxin is a mobile signalling molecule arose from the observation that auxin is distributed throughout the plant and causes effects at a distance from its synthetic location. The famed experiment by Thimann and Skoog in 1934 demonstrated that auxin applied to a decapitated shoot apex could repress the outgrowth of axillary buds. Removal of the apex, and therefore a major auxin source, results in derepression of bud outgrowth. (Cline, M.G. (1996)) replacement of the apex with another source of auxin, such as the synthetic auxin Naphthalene acetic acid (NAA), will result in repression of outgrowth being restored (Hillman, J.R. (1977)). This method of long distance control from a remote apical site has become known as apical dominance.

The small size of the auxin molecule confers on it a natural mobility and it can move, with bulk flow, through the phloem. Specific directional auxin transport was first detected using radiolabelled auxin to track the molecule's basipetal movement along the stem (*review* Goldsmith (1968)). Later experiments showed auxin transport to occur in vascular associated cells with auxin travelling along these conduits to its point of action (Booker, J. *et al.* (2003)). It should be noted that in shoot branching control auxin is in some sense active throughout and not merely at the node. This regulated movement of auxin around the plant is referred to as polar auxin transport (PAT) and is explained using the chemiosmotic model. The chemiosmotic or 'acid trap' hypothesis states that there are distinct pools of IAA within a plant. The first pool is contained within the apoplast. The second pool is contained within the cell cytoplasm, or symplast. There exists a pH differential between the apoplast and symplast with the former having a slightly acidic pH of 4.5 and the latter a neutral pH 7. In the acidic apoplast a significant fraction of IAA is in its protonated, and therefore uncharged, form. IAAH can enter the cytoplasmic space passively across the cell membrane. In addition, auxin can enter cells via an H⁺ symporter such as the AUX1 carrier protein (Yang, Y. *et al.* (2006)). AUX1 is a transmembrane carrier protein that has auxin binding capacity (Carrier, D.J. *et al.* (2008)), and has proven involvement in transporting IAA into the cytoplasm (Yang, Y. *et al.* (2006)). In the neutral pH of the cytoplasm auxin is virtually all deprotonated and as an ion, is therefore unable

to exit the cell passively. This implies the presence of proteins capable of transporting out of cells. These auxin efflux complexes have been shown to include members of the Pin-formed (PIN) family of proteins (Galweiler, L. *et al* (1998)). The *PIN* family encodes proteins of which several are involved in auxin export (PIN1-PIN4, PIN6 and PIN7). In the stem, PIN1 is located on the basal membrane of cells involved in auxin transport, a fact consistent with the lower levels of free IAA found in *pin1* mutant shoots (Okada, K. *et al.* (1991)). Once the IAA has been exported out of the cell the acidic environment results in its reprotonation, allowing passive transport into the next cell. It can also diffuse in the apoplast, so not all of it will go in immediately at the apical end of the next cell. The overall result is directional flux of auxin. In the root the PIN1 complexes are constantly endocytosed in endocytotic vesicles and recycled to the plasma membrane. The protein GNOM is involved in targeting these vesicles to the correct membranes and is therefore involved in PIN1 localisation (Geldner, N. *et al.* (2003)). ABCB-type transporters also contribute to auxin efflux but are not exclusively found on the basal cell membrane (Geisler, M. *et al.* (2005)).

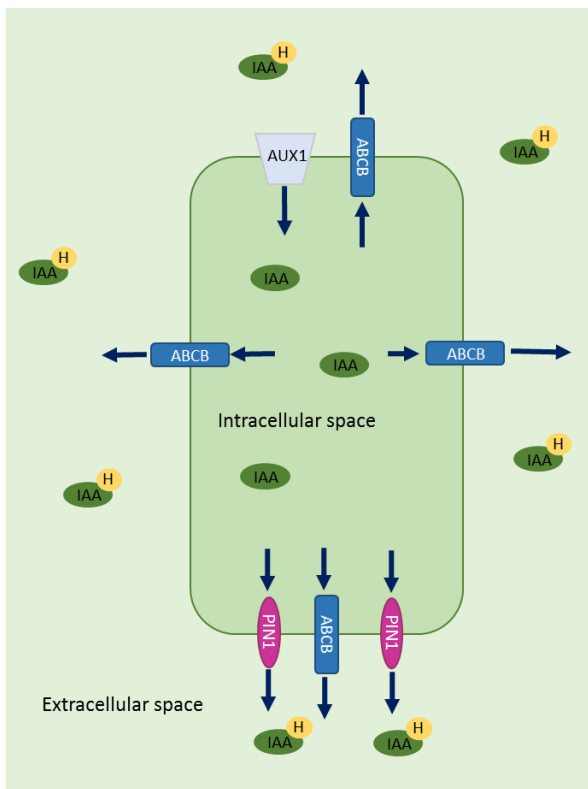


Figure 3. Representation of auxin transport in vascular associated cells in the stem.

Much of the extracellular auxin is found in a protonated form (IAAH). In this form auxin can enter the cell by passive movement. Uptake can also be catalysed by a H^+ symporter such as AUX1. Once in the cell the neutral pH of the cytoplasm deprotonates the IAAH to IAA. IAA can only exit the cell via a basally localized auxin efflux complex, such as PIN1. IAA can also exit the cell via ABCB-type transporters. ABCB transporters have been found to be uniformly localised in four different species and regulate cellular auxin homeostasis (Cho, M and Cho H-Y. (2013)).

1.5.2 Auxin Signalling

Understanding of the auxin signal transduction pathway has greatly increased in the past 25 years. Technological developments have allowed the clarification of the events from auxin perception to changes in gene expression levels. Microarray experiments designed to highlight changes in expression levels in response to auxin revealed hundreds of auxin regulated genes. Amongst the gene families identified before the invention of microarrays are four clearly defined gene families; ACC synthase (involved in ethylene synthesis), GH3s, SAURs (small auxin upregulated RNAs), and Aux/IAAs (Auxin/Indole-3-acetic acid inducible genes). Members of these gene families all have an auxin response element (ARE) within their promoter regions (Ulmasov *et al.* 1995, Hagen and Guilfoyle. 2002). The presence of an ARE confers auxin responsiveness and members of the gene families mentioned above all show a rapid and marked upregulation upon the addition of auxin. A TGTCTC element found within the ARE has been shown to be sufficient to upregulate expression of reporter genes in response to auxin (Wang, *et.al.* 2005).

Auxin Response Factors

Auxin Response Factors (ARFs) are a family of proteins which bind to the AREs in the promoters of auxin inducible genes (Ulmasov *et.al.* 1997). There are currently 23 known ARFs in the *Arabidopsis thaliana* genome (reviewed in Guilfoyle, T. J. and Hagen, G.(2007)). ARF proteins have an amino-terminal DNA binding domain and carboxy-terminal dimerisation domains (known as domains III and IV, capable of both homo- and hetero-dimerisation) (Tiwari, S. B. *et.al.* 2003). The amino acid content of the central region, inbetween the DNA binding domain and domains III and IV, determines whether the ARF will act as a transcriptional activator or a transcriptional repressor. The majority of ARFs act as transcriptional repressors. These ARFs have either serine-rich (S-rich), serine-proline-rich (S-P-rich), serine-glycine-rich (S-G-rich), or serine-proline-leucine-rich (S-P-L-rich) middle regions. The remaining ARFs act as transcriptional activators and have glutamine-rich (Q-rich) middle regions.

Aux/IAAs

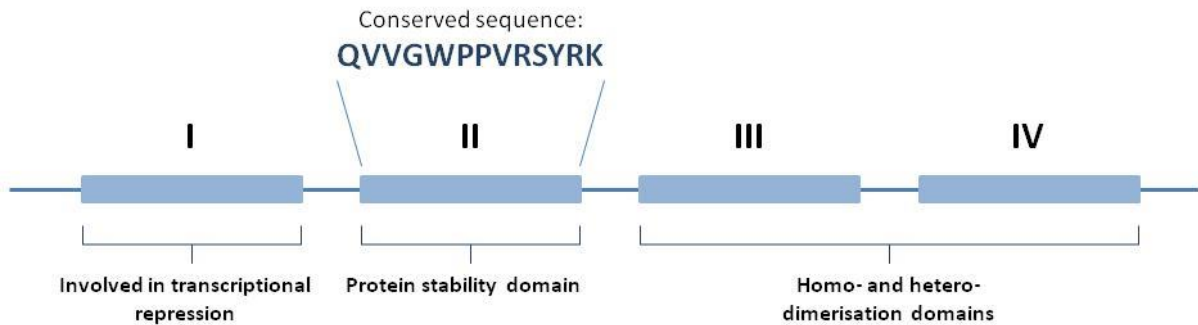
Aux/IAAs, like ARFs, are modular proteins with dimerisation domains. ARFs and Aux/IAAs can form both homo- and hetero-dimers within members of the same protein family and between the two family groups (Kim, Harter, and Theologis. (1997)). 29 members of the *Aux/IAA* gene family have been discovered to *Arabidopsis thaliana*. The *Arabidopsis* genome sequence is very high quality so it is probably safe to assume that this is the final total. The structure of Aux/IAA proteins comprises two carboxy-terminal dimerisation domains III and IV. At the amino-terminus are situated domains I and II, both highly conserved across family members. Domain I is a transcriptional repression domain whereas domain II is involved in the protein instability characteristic of Aux/IAA proteins. The regulated instability of Aux/IAA proteins is an essential feature that enables auxin regulated transcription.

The role of targeted protein degradation in auxin signalling

As mentioned above, the regulation of Aux/IAA protein stability has an important role in auxin signalling. This was highlighted with molecular analysis of the auxin-resistant mutant *tir1* (*transport inhibitor response1*). Wild-type *TIR1* was found to encode an F-box protein (Ruegger, *et al.* (1998)). F-box proteins are a large family of proteins, numbering almost 700 in the *Arabidopsis* genome. As *TIR1* has been shown to be involved in auxin signalling it is known as an auxin-related F-box protein (AFB), of which there are 5 in *Arabidopsis*.

F-box proteins are an integral subunit of a larger complex known as a SCF-type ubiquitin-protein-ligases. These complexes target proteins for degradation via the 26S proteasome (Vierstra, R.D. (2003)). SCFs consist of three main subunits from which they take their name; Skp1, Cullin, and an F-box protein. Rbx1 is another subunit which forms a dimer with Cullin. It is this Rbx1 Cullin dimer which ubiquitinylates the target protein, marking it for destruction. Skp1 attaches to an F-box motif found at the amino-terminal end of the F-box protein. Skp1 also interacts with Rbx/Cullin thereby linking all the constituent parts together to form the SCF complex. The F-box protein is the subunit that confers specificity on the complex as a whole. Different F-box proteins have one of a large variety of protein-protein interaction domains. This allows a wide range of proteins to be recruited to SCFs and targeted for degradation.

Aux/IAA



ARF

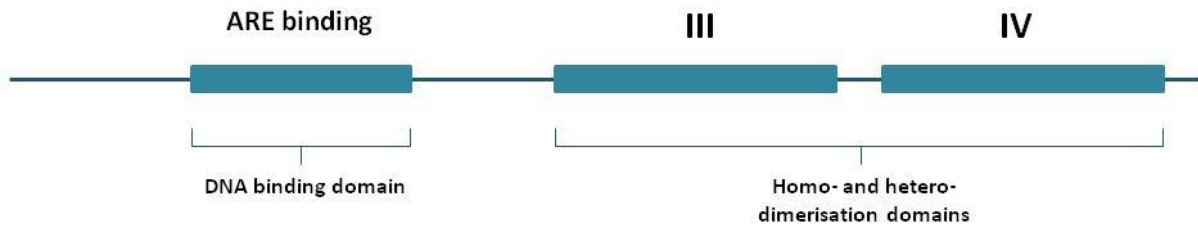


Figure 4. The conserved structure of ARFs and Aux/IAAs.

Aux/IAA proteins have two carboxy-terminal dimerisation domains III and IV. Domains I and II, are highly conserved across family members. Domain I is a transcriptional repression domain whereas domain II confers the protein instability vital for auxin regulated transcription.

ARF proteins contain an amino-terminal DNA binding domain (DBD) and carboxy-terminal dimerisation domains (III and IV) (Tiwari, S.B. *et al.* 2003). The amino acid content of the region inbetween the DBD and domain III identifies the ARF will act as a transcriptional activator or a transcriptional repressor.

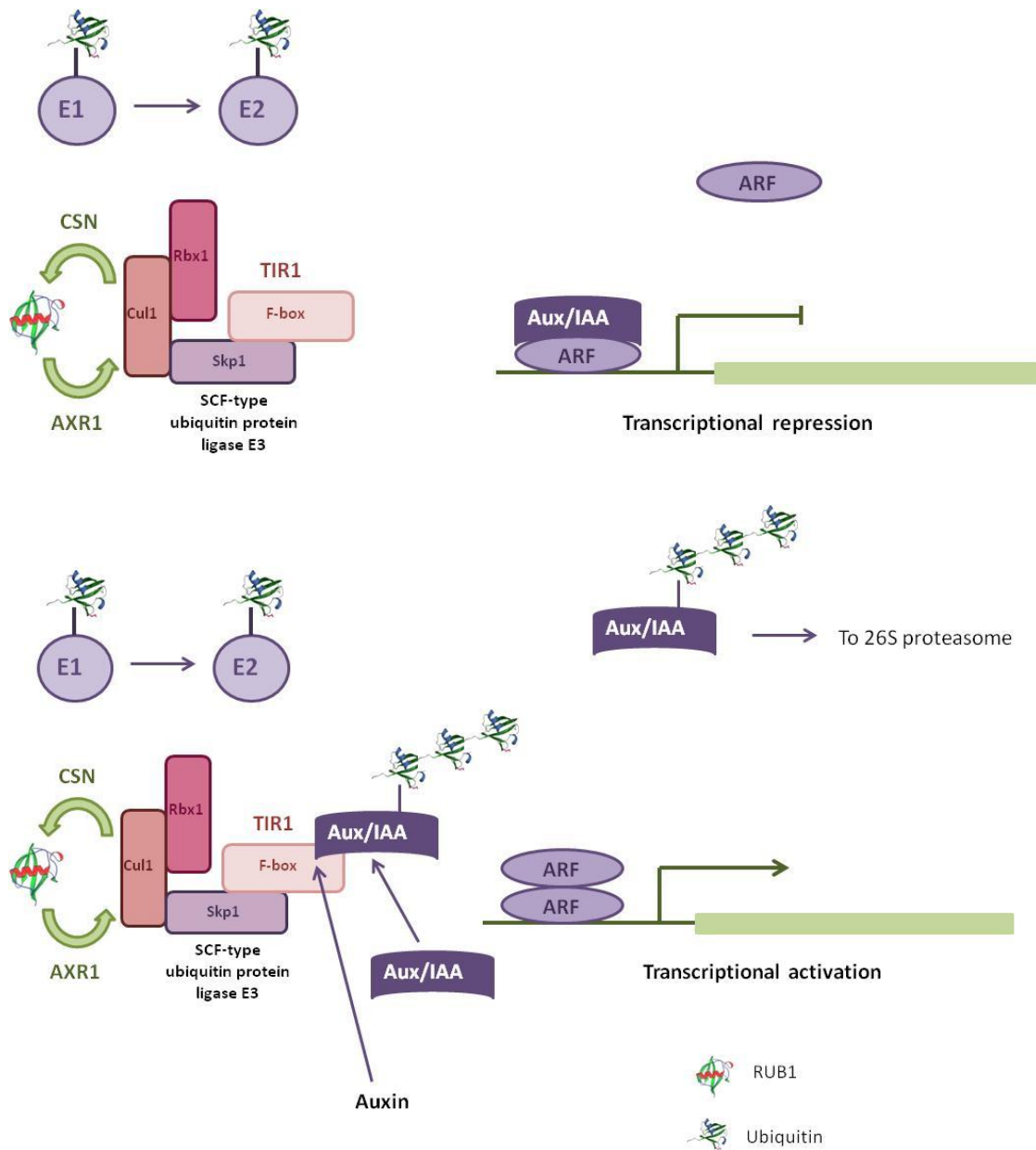


Figure 5. Auxin signalling.

In the top diagram auxin is not present. Aux/IAs dimerise with ARFs at the promoters of auxin inducible genes resulting in transcriptional repression and therefore, inhibition of gene expression.

In the bottom diagram auxin is present, it acts as a ligand to TIR1, which allows TIR1 to recruit Aux/IAs to the SCF complex. Activated ubiquitin is transferred from E1 to E2 and attached to the appropriate Aux/IAA by the SCF, acting as an E3, a ubiquitin-protein ligase. Repeating this results in a poly-ubiquitin chain which marks the Aux/IAA for destruction by the 26S proteasome. ARFs are free to homodimerise, allowing transcription.

Mutations in *AXR1* and *AXR6* both result in auxin resistant phenotypes. *AXR1* encodes a subunit of the RUB1 activating enzyme (Poza, J.C. *et al.* (1998)) whereas *AXR6* encodes Cullin1 (Hellmann, H. *et al.* (2003)). Both RUB1 and Cullin1 are essential to the proper function of the SCF. RUB1 is cycled to and from the SCF in a process that appears to be vital in the formation and subsequent disassembly of the SCF. Upon activation by the RUB1 activating enzyme, RUB1 conjugates to Cullin. RUB1 is removed from the complex via the activity of the COP9 signalosome (Cope, G. and Deshaies, R. (2003)).

The basic mechanism of auxin mediated control of gene expression is demonstrated in figure 5. In the absence of auxin Aux/IAAs are free to dimerise with ARFs at the promoters of auxin inducible genes. This interaction results in inhibition of gene expression because of the potent transcriptional repression domain found in Aux/IAAs. When auxin is present, it acts as a ligand to the F-box protein TIR1, this allows TIR1 to recruit Aux/IAAs to the SCF complex. Ubiquitin, which has been activated by E1 and transferred to E2 is attached to the target Aux/IAA by the SCF, which acts as an E3, a ubiquitin-protein ligase. This process is repeated until a poly-ubiquitin chain of a sufficient length marks the Aux/IAA for destruction by the 26S proteasome. Without the Aux/IAAs competition for dimerisation sites the ARFs are free to homodimerise, allowing transcription.

The importance of Aux/IAA-ARF relations is especially clear when considering the interaction between IAA12/BODENLOS (BDL), and the Q-rich ARF5/MONOPTEROS(MP). Auxin induced degradation of BDL is essential for the appropriate differentiation of root pole in early stage *Arabidopsis* embryos. Mutations in domain II of BDL result in the stabilisation of the protein. The elevated levels of BDL inhibit differentiation of root cells the outcome being an embryo with no root. (Hamann, T. *et al.* (1999)). A similar phenotype is conferred by loss of MP function (Schlereth, A. *et al.* (2010)).

1.6 Cytokinins

Cytokinins are another class of phytohormones involved in shoot branching as well as a myriad of other plant developmental processes from organ formation and seed germination, to shoot apical meristem formation and maintenance, leaf senescence and, most importantly for this study, control of shoot branching (Mok, D.W. and Mok, M.C. (2001)). They were first identified by Skoog and Miller in 1957 who noted their ability to promote cell division, from

which they derive their name (Skoog, F. and Miller, C.O. (1957)). Cytokinins are derived from adenine. Naturally occurring cytokinins are divided into two groups; those with aromatic side chains, and those with isoprene-derived side chains which are mostly found in plants (Sakakibara, H (2006)).

Unlike auxin, cytokinins can act directly to promote bud outgrowth. Cytokinin travels acropetally from its point of biosynthesis to the node. Application of lanolin containing cytokinin to the bud can result in bud outgrowth (Wickson, M. and Thimann, K. (1958)) and levels of cytokinin have been shown to increase in elongating buds (Emery, R. *et.al.* (1998)).

1.6.1 Cytokinin Biosynthesis and degradation

In *Arabidopsis*, cytokinin biosynthesis is mediated by the *ATP/ADP isopentenyltransferase* (IPT) gene family, specifically *AtIPT1* and *AtIPT3-AtIPT8*. For the following example of cytokinin biosynthesis, the resulting cytokinin will be transZeatin (tZ). The enzymes encoded by the *IPT* genes synthesise the cytokinin precursor isopentenyladenine (Kakimoto, T. (2001), Takei, K. *et al.* (2001a)). The cytochrome P450 monooxygenases CYP735A1 and CYP735A2 then catalyse the hydroxylation of the isopentenyladenine precursor to the inactive tZ-riboside-5'-monophosphate (Takei, K. *et al.* (2004)). Enzymes encoded by the LONELY GUY (LOG) gene family convert the inactive tZ-riboside-5'-monophosphate in the active trans-Zeatin (tZ) (Takei, K. *et al.* (2004)). This is summarised in figure 6.

Cytokinin degradation requires the action of cytokinin oxidases (CKX), encoded by the *CYTOKININ OXIDASE* (*CKX*) gene family (Houba-Hérin, N. *et al.* (1999), Schmülling, T. *et al.* (2003)). Genes required for cytokinin biosynthesis and degradation are widely expressed throughout the shoot and root systems (Nordström, A. *et al.* (2004)). Expression analyses for both *IPT* and *CKX* genes have elucidated specific expression patterns for each gene family (Werner, T. (2003), Miyawaki, K. (2004)).

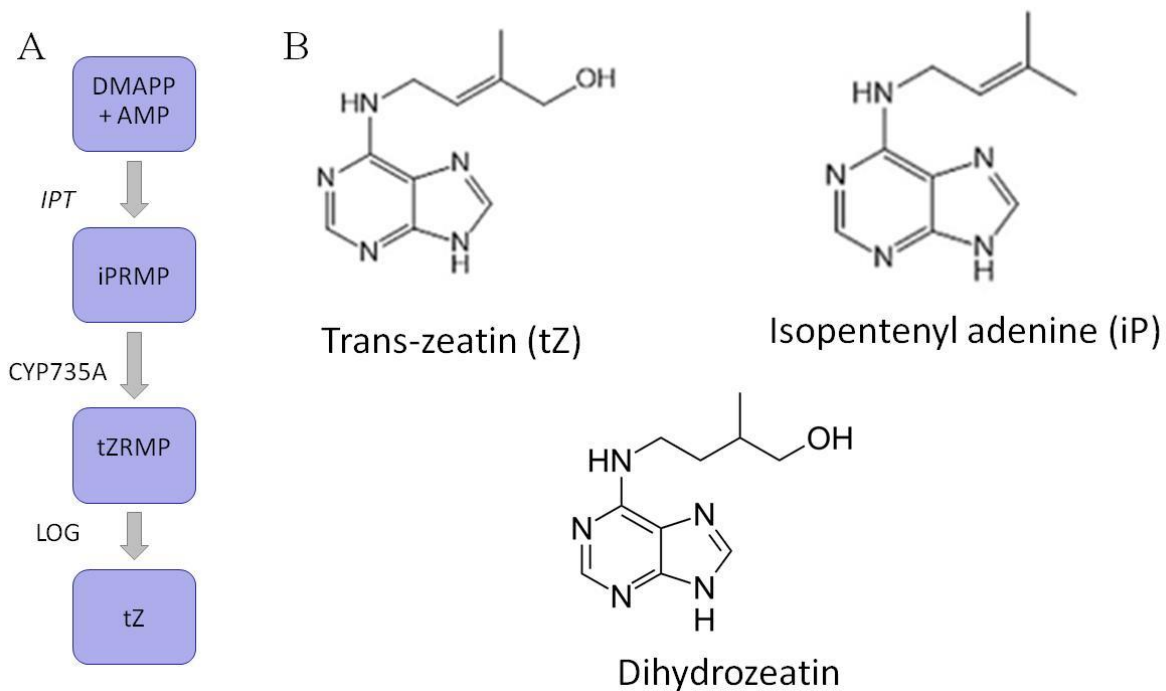


Figure 6. (A) Key elements in the cytokinin biosynthetic pathway. The first step involves the reaction of dimethylallyl diphosphate (DMAPP) with adenosine monophosphate (AMP) to form iP riboside 5'-monophosphate (iPRMP). This reaction is catalysed by members of the *IPT* gene family. The cytochrome P450 mono-oxygenase CYP735A then converts iPRMP to tZ-riboside-5'-monophosphate (tZRMP). The final step involves the catalytic action of enzymes encoded by members of the *LOG* gene family which convert tZRMP into an active cytokinin., in this case, tZ.

(B) Common cytokinins found in plants. Trans-zeatin, Isopentenyl adenine, and Dihydrozeatin, all examples of isoprenoid cytokinins.

1.6.2 Cytokinin transport and signalling

Reciprocal grafting experiments between *ipt1*, *ipt3*, *ipt5*, *ipt7* and wild-type plants showed differences in transport between different cytokinins in the grafted plants. Trans-Zeatin (tZ) was transported acropetally while isopentenyladenine (iP)-type cytokinins moved basipetally (Matsumoto-Kitano, M. (2008)). The use of radiolabelled cytokinins applied to cotyledons has also demonstrated long-distance movement to the root tip through the phloem (Bishopp, A. (2011)). Induction of callose synthesis in the phloem results in the disruption of basipetal flow of cytokinin highlighting the importance of symplastic connections to cytokinin transport (Bishopp, A. (2011)).

Cytokinin signalling involves a two-component signalling pathway. Cytokinin induces autophosphorylation of a histidine kinase (HK) protein. As a result of this a phosphoryl group is transferred from a phospho-accepting histidine residue in the kinase domain of the protein, to an aspartate residue. A histidine phosphotransferase (HP) protein then accepts the phosphoryl group via a conserved histidine. It is then transferred to an aspartate in the receiver domain of a response regulator (RR). This is reviewed more comprehensively in Hwang, I. *et.al.* (2012).

There are 23 functional response regulators in *Arabidopsis* (ARRs) which are divided into three groups, of which two are involved in CK response. Cytokinin mediated phosphorylation of type A ARR has a stabilising effect (To, J.P.C. *et.al.* (2007)) and phosphorylation of type B ARR allows them to bind DNA resulting in the transcription of downstream targets, some of which are type A ARRs (D'Agostino, I.B. *et.al.* (2000)) demonstrating that type A ARRs are under the transcriptional regulation of cytokinin. Type A ARRs are generally thought to have an inhibitory effect on cytokinin signalling.

1.6.3 Cytokinin and auxin interactions

It has long been known that auxin and cytokinin interact, and that these interactions are essential to plant development. As early as 1957 Skoog and Miller controlled *in vitro* organogenesis by varying the ratio of auxin and cytokinin present in growth medium (Skoog, F. and Miller, C.O. (1957)). Cytokinin and auxin act both antagonistically and synergistically to control various aspects of plant development and the mechanisms by which they do so are slowly coming to light.

Cytokinin-mediated regulation of auxin

Cytokinin regulates auxin biosynthesis. Treatment with various cytokinins results in a significant increase in auxin synthesis in the shoot apex, leaf primordial and the root system. This effect was even greater in *arr3*, *arr4*, *arr5* and *arr6*, as a result of their cytokinin hypersensitivity (Jones, B. *et.al.* (2010)). Cytokinin treatment did not have the same effect in *axr3-1* plants, which exhibit auxin response defects owing to increased stabilisation of AXR3/IAA17 (Jones, B. *et.al.* (2010)). A transcriptomics approach highlighted the upregulation of many auxin biosynthetic genes following cytokinin application. Other genes, responsible for auxin storage and degradation were also upregulated in the presence of cytokinin. Cytokinin has also been shown to regulate auxin transport via the PIN auxin efflux

transporters (Laplaze, L., *et al.* (2007)). Expression of *PIN1* and *PIN6* in lateral root primordial was found to be both reduced and diffuse under cytokinin treatment suggesting that cytokinin disrupts patterning during lateral root initiation. Cytokinin treatment also resulted in decreased expression in the shoot of *PIN1*, *PIN2*, *PIN3*, *PIN4* and *PIN7* (Laplaze, L., *et al.* (2007)). *PIN1*, *PIN3*, and *PIN7* are also down-regulated in the vasculature by cytokinin (Dello Ioio, R. *et al.* (2008)). In pea, expression of the *PIN1* and *AUX1* orthologues; *PsPIN1* and *PsAUX1* is rapidly upregulated in response to cytokinin (Kalousek, P. *et al.* (2010)). The *PsPIN1* protein is also basally localised in competent cells in response to cytokinin (Kalousek, P. *et al.* (2010)). These experiments suggest a role for cytokinin in the regulation of PAT and therefore they may regulate apical dominance by proxy.

Auxin-mediated regulation of cytokinin

IPT expression has been shown to respond to auxin treatment (Miyawaki, K. *et al.* (2004)). *IPT5* is upregulated by auxin via *SHY2/IAA3* (Tanaka, M. *et al.* (2006)). Two *IPT* homologs in pea, *PsIPT1* and *PsIPT2* are upregulated in response to exogenous auxin in excised two node assays (Tanaka, M. *et al.* (2006)). Auxin application does not always result in upregulation of cytokinin biosynthesis genes. *Arabidopsis* seedlings treated with auxin exhibit a downregulation in the cytokinin biosynthesis gene *CYP735A1* (Takei, K. *et al.* (2004)).

Auxin can also effect cytokinin degradation via regulation of the *CKX* gene family. *CKX2*, *CKX4*, and *CKX7* are slightly downregulated and *CKX1* and *CKX6* are upregulated in response to auxin but strongly downregulated by NPA addition suggesting that their expression is dependent on PAT or auxin distribution (Werner, T. *et al.* (2006)).

Cytokinin crosstalk with strigolactone

Increased levels of strigolactones in both *Arabidopsis* and pea have been shown to reduce levels of cytokinin in xylem sap samples (Foo, E. *et al.* (2007)). The buds of strigolactone-insensitive plants also display reduced sensitivity to exogenously supplied cytokinin (Dun, E.A. *et al.* (2009)). It is also thought that cytokinin may prevent the upregulation of the strigolactone biosynthesis gene *MAX4* (Bainbridge, K. *et al.* (2005)). This is further supported by experiments in pea; *rms1* (*max4* in *Arabidopsis*), which is deficient in SLs, and *rms4* (*max2* in *Arabidopsis*), which exhibits SL insensitivity. Both mutants have increased levels of *PsIPT1* in the shoot internodes and the nodes (Dun, E.A. *et al.* (2012)). These data seem to suggest that cytokinin and SL act antagonistically to control bud outgrowth. Both cytokinin and SL can induce expression of the TCP transcription factor *BRANCHED1* (*BRC1*). *PsBRC1* is

upregulated by the synthetic SL GR24 and downregulated by cytokinin (Dun, E.A. *et.al.* (2012)).

Cytokinin and nitrate

It has long been established that low nitrate availability increases the proportion of a plants biomass which is allocated to the roots (Drew, M.C. *et.al.* (1975), Scheible, W.R. *et.al.* (1997)) and high nitrate availability is linked to bud activation (De Jong, M. *et.al.* (2014), Ding, Y.F. *et.al.* (1995), Liu, Y. *et.al.* (2011), McIntyre, G.I. (2001), McIntyre, G.I. and Cessna, A.J. (1991), McIntyre, G.I. and Hunter, J.H. (1975)). Nitrate is also known to promote cytokinin synthesis (Takei, K. *et.al.* (2001b), Takei, K. *et.al.* (2002), Takei, K. *et.al.* (2004)). It has recently been postulated that cytokinin may drive bud outgrowth despite high levels of auxin in the stem, added to by actively growing buds and shoots. Data gathered suggests that cytokinin is not required to support branching in low nitrate conditions but may enhance branching when nitrate availability is high (Müller, D. *et.al.* (2015)).

1.7 Strigolactones and the MAX pathway

Strigolactones (SL) form an ancient class of hormones that have only, in recent years, come to light as signalling molecules essential to auxin-mediated inhibition of bud outgrowth. Strigolactones are so named because they were initially identified as a germination stimulant for the parasitic plant *Striga lutea* (witchweed) (Cook, C.E. *et al* (1996)). Plants belonging to the *Striga* genus, as well as those belonging to the closely related *Orobanchaceae* both respond to germination cues in the form of SLs exuded from the roots of host plants. This ensures germination in close proximity to an appropriate host plant. SLs are involved in the recruitment of arbuscular mycorrhizal (AM) fungi from the rhizosphere (Akiyama, K. *et al* (2005)); the environment surrounding the roots of plants, which is host to a wide range of organismal interactions. The appropriation of soil-based nutrients such as phosphorous and nitrogen enabled by AM fungi is critical to the survival of plants such as *Striga* spp. To date 15 SLs have been identified and structurally characterised (Matusova, R. *et al.* (2005), Xie, X. *et al.* (2010))

For the purposes of this study the most interesting aspect of strigolactone biology is the ability to influence shoot branching in higher plants (tillering in monocots) however as endogenous signalling molecules SLs have demonstrated involvement in an expanding list of plant

processes which include: stem elongation, leaf expansion and senescence, root growth, lateral root formation, root hair elongation, and stress responses such as those to drought and salinity. (Agusti, J. *et al.* (2011), Gomez-Roldan, V. *et al.* (2008), Ha, C.V. *et al.* (2013), Kapulnik, Y. *et al.* (2011), Rasmussen, A. *et al.* (2012), Ruyter-Spira, C. *et al.* (2011), de Saint Germain, A. *et al.* (2013), Snowden, K.C. *et al.* (2005), Stirnberg, P. *et al.* (2002), Umehara, M. *et al.* (2008), Woo, H.R. *et al.* (2001))

Genetic screens for shoot branching mutants have isolated plants that are either deficient in SL biosynthesis or SL signalling. Many of the steps in the SL pathway have been elucidated with a clear understanding of the key components of SL biosynthesis. Less is known about SL signalling, both proximal and further downstream, but progress is being made in both of these areas.

1.7.1 Strigolactone biosynthesis

Naturally occurring strigolactones have a basic structure in common. The tricyclic lactone configuration comprises three rings, denoted A, B, and C. An enol-ether bridge connects the aforementioned structure to a D-ring butenolide group (figure 7). The D-ring and enol-ether bridge are invariant, with specificity occurring on the tricyclic lactone sub-section (Magnus, E.M. *et al.* (1992), Zwanenburg, B. *et al.* (2009), (2013)). Genetic screens for increased branching mutants have already identified enzymes responsible for several steps in SL biosynthesis across several species. The *max* mutants in *Arabidopsis*, *ramosus* (*rms*) mutants in *P. sativum* (pea), *dwarf* (*d*) and *high tillering dwarf* (*htd*) in *O. sativa* (rice), and *decreased apical dominance* (*dad*) in *P. hybrida* (petunia). (Arite, T. *et al.* (2007) (2009), Booker, J. *et al.* (2004), Drummond, R.S. *et al.* (2009) (2012), Ishikawa, S. *et al.* (2005), Johnson, X. *et al.* (2006), Lin, H. *et al.* (2009), Simons, J.L. *et al.* (2007), Snowden, K.C. *et al.* (2005), Sorefan, K. *et al.* (2003), Stirnberg, P. *et al.* (2002), Waters, M.T. *et al.* (2012a,b), Woo, H.R. *et al.* (2001)). The above mutants all exhibit increased shoot branching/tillering, low endogenous SL levels, and phenotypic rescue can be achieved with SL addition. Grafting to WT roots also results in phenotypic rescue in the *Arabidopsis* mutants *max3*, *max4*, and *max1*. SL mutants have also been found in *Salix spp.* (willow), *Zea mays* (maize), *Solanum lycopersicum* (tomato), and *Dendranthema grandiflorum* (chrysanthemum) (Dong, L. *et al.* (2013), Guan, J.C. *et al.* (2012), Kohlen, W. *et al.* (2012), Vogel, J.T. *et al.* (2010), Ward, S.P. *et al.* (2013)).

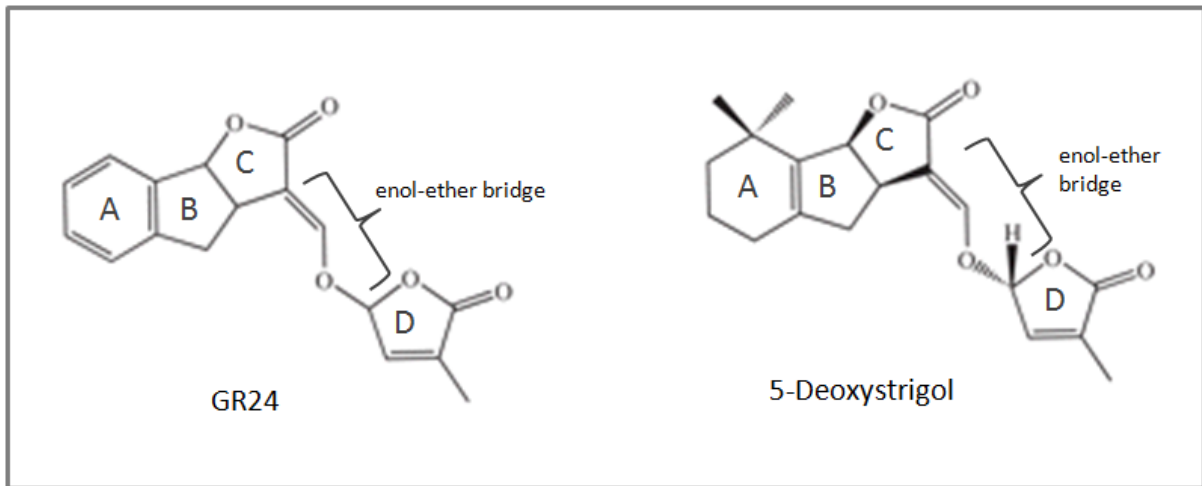


Figure 7. The synthetic strigolactone GR24 and the naturally occurring 5-deoxystrigol, thought to be the simplest of the naturally occurring SLs found in dicots, monocots, and plants of the liverwort genus *Marchantia* (Awad, A.A. *et al.* (2006), Delaux, P.M. *et al.* (2012), Yoneyama, K. *et al.* (2008)). The D butenolide ring and enol-ether bridge are invariant. Specificity occurs on the tricyclic lactone structure comprising three rings; A, B, and C. Hydroxyl groups on the A and/or B ring are associated with increased germination rates (Sato, D. *et al.* (2005), Xie, X. *et al.* (2012)). In *P. sativum*, it has been demonstrated that hydrophobic or acetyl-containing SLs exhibit stronger bud inhibition activity than SLs with hydroxyl groups (Boyer, F.D. *et al.* (2012)).

Strigolactones are carotenoid-derived compounds (Matusova, R. *et al.* (2005)). The initial steps of SL biosynthesis involve the isomerase D27 and the CAROTENOID CLEAVAGE DIOXYGENASES CCD7 (MAX3 in *Arabidopsis*) and CCD8 (MAX4 in *Arabidopsis*). D27, CCD7 and CCD8 are all localised in the plastid and subject the carotenoid precursor to isomerisation and dioxygenase mediated cleavage, producing the substrate for the next part of the pathway (Arite, T. *et al.* (2007), Auldrige, M.E. *et al.* (2006), Booker, J. *et al.* (2004), Lin, H. *et al.* (2009), Sorefan, K. *et al.* (2003), Waters, M.T. *et al.* (2012a)). The first step in SL synthesis is the isomerisation of all-trans- β -carotene to 9-cis- β -carotene (Alder, A. *et al.* (2012)). This reaction in both *Arabidopsis* and rice requires the action of the all-trans- β -carotene/9-cis- β -carotene isomerase D27 (Alder, A. *et al.* (2012), Lin, H. *et al.* (2009), Waters, M.T. *et al.* (2012a)). A CCD7 mediated cleavage reaction converts the 9-cis- β -carotene substrate to 9-cis- β -apo-10'-carotenol which is in turn reorganised by CCD8. CCD8 adds three oxygen molecules and rearranges the backbone of the molecule to form both the enol-ether bridge and the D and A rings (Alder, A. *et al.* (2012)). The resulting carlactone (CL) molecule is an endogenous intermediary in the SL biosynthesis pathway. Isolation of CL in *Arabidopsis* and rice coupled with experiments using C14 radiolabelled CL have verified this (Seto, Y. *et*

al. (2014)). The cytochrome P450 protein MAX1 comes into play downstream of D27, CCD7/MAX3, and CCD8/MAX4. MAX1 is necessary for the production of the active SL 5-deoxystrigol (Booker, J. *et al.* (2005), Kohlen, W. *et al.* (2011), Scaffidi, A. *et al.* (2013). 5-deoxystrigol is thought to be the precursor of other, more complex SLs (Alder, A. *et al.* (2012)). Genes involved in the *Arabidopsis* MAX pathway, along with pea, rice, and petunia orthologues are noted in table 1.

An alternative source of 9-cis- β -carotene, not involving D27 action, is possible. This is supported by the fact that the *d27* branching phenotype is less severe than mutants in genes that act downstream, for example *ccd8/max4* (Lin, H. *et al.* (2009), Waters, M.T. *et al.* (2012a))

The above sequence of events forms the initial steps in the *Arabidopsis* MAX pathway (figure 8). Reciprocal micrografting experiments in *Arabidopsis* (*max1* to *max3*, *max4* and *d27*) had already established the sequence of enzymatic activity and support the existence of a mobile, graft-transmissible SL precursor signal as well as the signal itself. As mentioned above, D27, CCD7/MAX3, CCD8/MAX4 are localised in the plastid. MAX1 is thought to be located in the cytoplasm. In dicots *CCD7* and *CCD8* show high levels of expression in the root tips and epicotyls (Bainbridge, K. *et al.* (2005), Booker, J. *et al.* (2004), Drummond, R.S. *et al.* (2009), Foo, E. *et al.* (2005), Johnson, X. *et al.* (2006), Snowden, K.C. *et al.* (2005)). *MAX1* is expressed in the xylem-associated parenchyma and in the cambial region (Booker, J. *et al.* (2005)). It has been suggested that the vascular localisation of MAX1 means it may be involved in processing a mobile SL precursor, now likely identified as CL, in transit to and/or from the xylem. CL is thought to be between *MAX4* and *MAX1* in the biosynthetic pathway as CL levels in *max1* are very high and, in contrast to *max4*, CL cannot restore wildtype branching levels to *max1* mutants (Scaffidi, A. *et al.* (2013), Seto, Y. *et al.* (2014)).

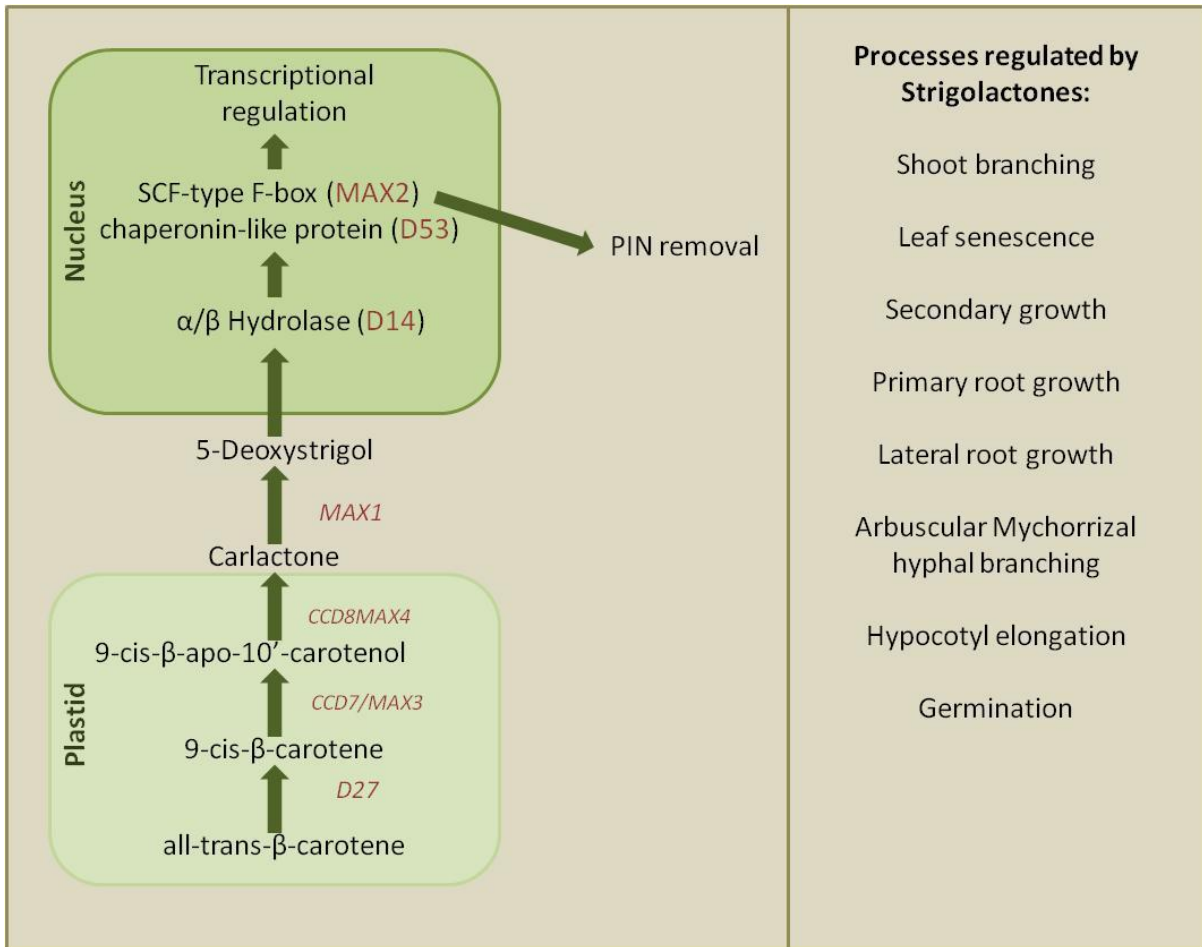


Figure 8. The *MAX* pathway in *Arabidopsis* – strigolactone biosynthesis, signalling and effects.

In the plastid D27 converts all-trans-β-carotene to 9-cis-β-carotene (Alder, A. *et al.* (2012), Lin, H. *et al.* (2009), Waters, M.T. *et al.* (2012a)). MAX3/CCD7 then mediates a cleavage reaction which converts 9-cis-β-carotene to 9-cis-β-apo-10'-carotenol which is in turn reorganised by MAX4/CCD8 (Alder, A. *et al.* (2012)) into the mobile SL intermediary carlactone (CL). MAX1 modifies the carlactone to 5-deoxystrigol (Booker, J. *et al.* (2005), Kohlen, W. *et al.* (2011), Scaffidi, A. *et al.* (2013)). SL is then Perceived by the D14 receptor which forms a complex with D53/SMXLs (D53s are SMXLs in *Arabidopsis*) and SCF^{MAX2} resulting in the degradation of D53/SMXLs, and possibly also D14 (Jiang, L. *et al.* (2013), Zhou, F. *et al.* (2013)). Downstream targets of *MAX2*, such as transcriptional regulation and possibly PIN removal, are affected and the result, in the case of shoot branching, is an inhibition of bud outgrowth. Shoot branching is not the only SL-regulated plant process, others are listed to the right of the diagram.

MAX gene orthologues		Species			
		Pea (<i>Pisum sativum</i>)	Rice (<i>Oryza sativa</i>)	Petunia (<i>Petunia hybrida</i>)	<i>Arabidopsis thaliana</i>
Strigolactone Biosynthesis	CCD7	<i>RMS5</i> (Johnson, X. <i>et al.</i> 2006)	<i>D7/HTD1</i> (Zou, J. <i>et al.</i> 2006)	<i>DAD3</i> (Drummond, R.S. <i>et al.</i> 2009)	<i>MAX3</i> (Booker, J. <i>et al.</i> 2004)
	CCD8	<i>RMS1</i> (Sorefan, K. <i>et al.</i> 2003)	<i>D10</i> (Arite, T. <i>et al.</i> 2007) <i>D27</i> (Lin, H, <i>et al.</i> 2009)	<i>DAD1</i> (Snowden K.C. <i>et al.</i> 2005)	<i>MAX4</i> (Sorefan, K. <i>et al.</i> 2003)
	Cytochrome P450				<i>MAX1</i> (Booker, J. <i>et al.</i> 2005)
Strigolactone Perception	F-box	<i>RMS4</i> (Johnson, X. <i>et al.</i> 2006)	<i>D3</i> (Ishikawa, S. <i>et al.</i> 2005)	<i>DAD2</i> (Hamiaux C, <i>et al.</i> 2012)	<i>MAX2</i> (Stirnberg, P. <i>et al.</i> 2002)

Table 1. Genes involved in the *Arabidopsis* MAX pathway with orthologous genes from Pea, Rice and Petunia. It is worth noting that a *MAX1* orthologue has yet to be identified.

Experiments carried out in *Arabidopsis* involving over-expression of the *MAX2* SL signalling component results in a partial reduction of branching levels in *max1*, *max3*, and *max4* plants (Stirnberg, P. *et al.* (2007)). This suggests that there may be an alternative source of SL available that has not been produced by the *D27/CCD7/CCD8* enzyme chain. The SL Orobanchol has been detected in some of these mutants which supports this theory (Kohlen, W. *et al.* (2011)). In addition, a second, endogenous butenolide signal which appears to be synthesized independently of *CCD7(MAX3)/CCD8(MAX4)* and *MAX1* has been proposed (Nelson, D.C. *et al.* (2011), Scaffidi, A. *et al.* (2013), Waters, M.T. *et al.* (2012b)).

1.7.2 Strigolactone Transport

Reciprocal grafting experiments have demonstrated that SLs travel up the plant from the root to the stem (Beveridge, C.A. *et al.* (1996), Booker, J. *et al.* (2005), Morris, S.E. *et al.* (2001), Napoli, C. (1996), Simons, J.L. *et al.* (2007), Turnbull, C.G. *et al.* (2002)). Consistent with this flux, SLs are present in the xylem sap of *Arabidopsis* and tomato (Kohlen, W. *et al.* (2011)). The PLEIOTROPIC DRUG RESISTANCE1 (PDR1) protein in petunia is currently the only

protein known to facilitate SL transport (Kretzschmar, T. *et al.* (2012)). *PDR1* is expressed highest in the root tips, consistent with a role in SL exudation into the rhizosphere (Sharda, J.N. and Koide, R.T. (2008)). *PDR1* is a member of the ATP BINDING CASSETTE (ABC) family of transporters which are also involved in the transport of auxin and ABA (Petráček, J. and Friml, J. (2009)), Kang, J. *et al.* (2010), Kuromori, T. *et al.* (2010)). Very little SL is found in *Arabidopsis* root exudates, which is not surprising given its non-mycorrhizal nature. Consistent with this, there is no *PDR1* orthologue, in *Arabidopsis* (Kholen, W. *et al.* (2011) (Kretzschmar, T. *et al.* (2012))).

1.7.3 Strigolactone perception and signalling

Whilst the major components of the SL biosynthesis pathway are now established, relatively little is known about downstream signalling. Research in this area is a priority for SL biology and progress is being made all the time.

GR24, a synthetic SL, has been shown to bind the α/β -hydrolase protein D14/DAD2. The increased branching phenotype, typical of SL mutants, is exhibited by the plants with mutations in *D14*; petunia *DAD2*, rice *OsD14*, and the *Arabidopsis* orthologue *AtD14*. The branching phenotype of these mutants cannot be rescued by exogenous SL (Arite, T. *et al.* (2009), Gao, Z.Y. *et al.* (2009), Hamiaux, C. *et al.* (2012), Liu, W. *et al.* (2009), Waters, M.T. *et al.* (2012b)). The exact nature of D14 function is still unclear. As described above, D14 can bind to GR24 and several species have SL insensitive *d14* mutants (Hamiaux, C. *et al.* (2012), Kagiya, M. *et al.* (2013), Waters, M.T. *et al.* (2012b), Zhao, L.H. *et al.* (2013)) consistent with the hypothesis that D14 acts as a receptor for a SL ligand. D14 has also been shown to interact with MAX2 (Hamiaux, C. *et al.* (2013), Jiang, L. *et al.* (2013), Zhou, F. *et al.* (2013)). MAX2 is part of the SCF^{MAX2} ubiquitin ligase complex that targets proteins for ubiquitinylation by the 26S proteasome (Stirnberg, P. *et al.* (2002), Stirnberg, P. *et al.* (2007)). Some of these proteins have recently been identified in rice; members of the D53/SMAX1-LIKE (SMXL) protein family (Jiang, L. *et al.* (2013), Stanga, J.P. *et al.* (2013), Zhou, F. *et al.* (2013)). The D53 protein also appears to interact with D14. The D53 protein is degraded in the presence of the SL analogue GR24, a reaction that is blocked in the dominant *D53* mutant (Jiang, L. *et al.* (2013), Zhou, F. *et al.* (2013)). For the purposes of shoot branching inhibition, D53 seems to

be an important target of SL signalling which, in turn, suggests that D53 acts as a negative regulator of SL responses. This has not yet been proven to be the case.

The smoke-derived molecule Karrikin is closely related to SL and, in *Arabidopsis*, signals through the KAI2 protein. KAI2 is a close relative of D14 and, likely targets the SMAX1 protein for degradation (Stanga, J.P. *et al.* (2013)).

Although the initial stages in SL signalling are now reasonably well consolidated, the downstream signalling events are more controversial. Two direct targets of MAX2 have been suggested; BES1, a brassinosteroid activated transcription factor (Wang, Y. *et al.* (2013)) and DELLA-class transcription factors (Nakamura, H. *et al.* (2013)). These observations were made using biochemical approaches however and genetic data which could have supported these hypotheses are based on highly pleiotropic mutants for BES1, rendering results unreliable, or absent entirely for the DELLAs (Wang, Y. *et al.* (2013)).

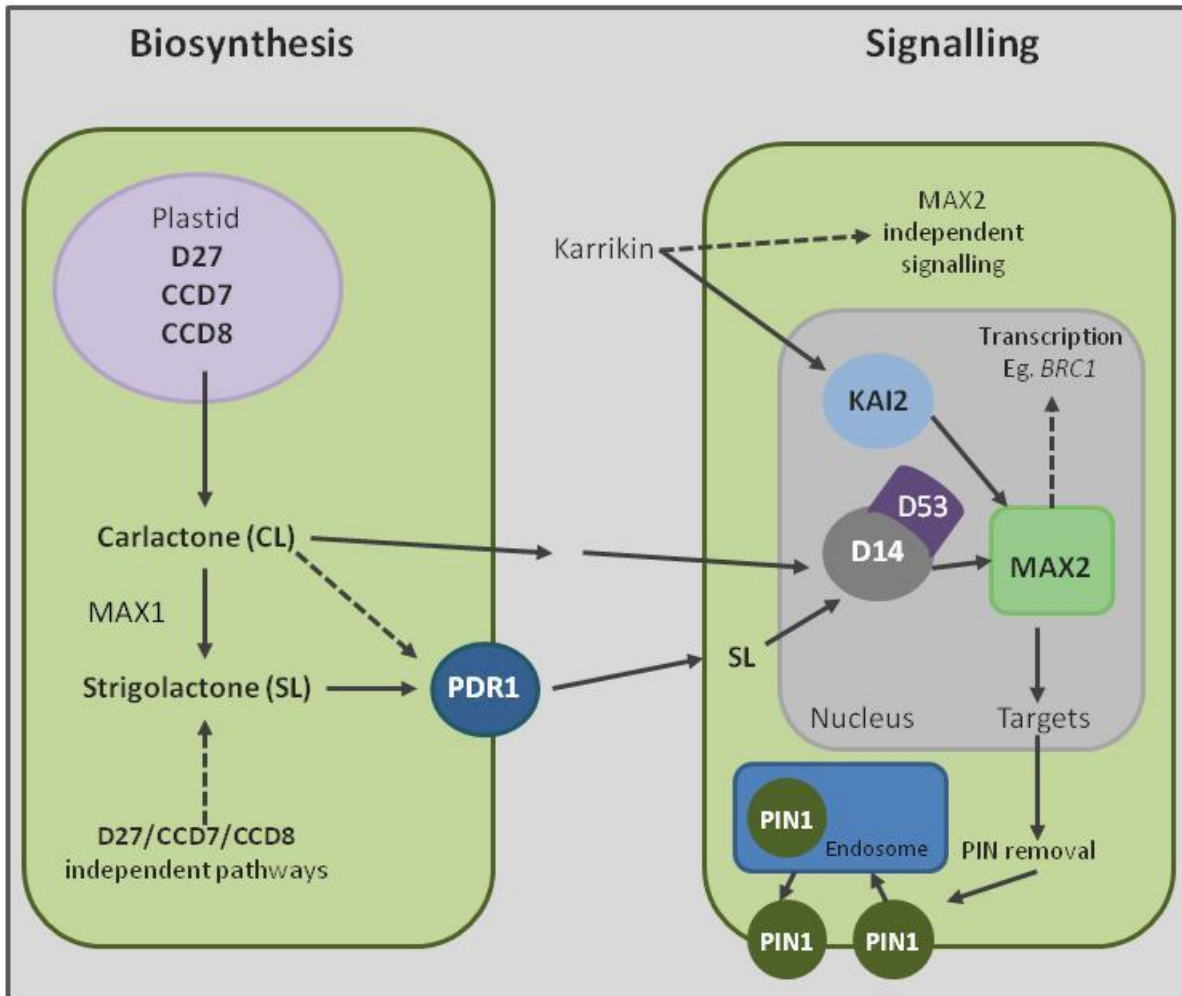


Figure 9. Strigolactone biosynthesis and signalling, a general overview (adapted from Waldie, T., McCulloch, H., and Leyser, O. (2014).

SL biosynthesis involves D27, CCD7, and CCD8 (shown in more detail in figure 8) which are required for CL synthesis. The cytochrome p450 M AX1 converts CL into SL. SL synthesis pathways independent of D27/CCD7/CCD8 should not be ruled out and may contribute to the SL pool. PDR1 is involved in SL transport, enabling exudation of SL into the soil (Kretschmar, T. *et al.* (2012)). There are no PDR1 orthologues in Arabidopsis. The SL-like molecule Karrikin is found in smoke and signals through KAI2. It is thought that both D14 and MAX2 act in the nucleus and are involved SL perception and signal transduction, although it is possible that SL signalling independent of MAX2 also occurs. D14 has been shown to bind to. Although D14 can bind to MAX2 without D53 and SL (Jiang, L. *et al.* (2013), Zhou, F. *et al.* (2013)), D14/D53 are required as a complex to form a substrate for SCF^{MAX2}. D14 and D53 are probably both ubiquitinated as a result of this reaction (Jiang, L. *et al.* (2013), Zhou, F. *et al.* (2013)). PIN removal from the plasma membrane has been postulated as a result of SL signalling which would be an effective means of regulating bud outgrowth by means of an auxin transport-dependent mechanism (Crawford, S. *et al.* (2010), Shinohara, N. *et al.* (2013), Prusinkiewicz, P. *et al.* (2006)). The TCP transcription factor is the best candidate to date for SL mediated transcriptional regulation. In pea *BRC1* is upregulated quickly after the application of SL (Dun, E.A. *et al.* (2012), Braun, N. *et al.* (2012)).

Dotted lines indicate that an action is speculative.

As far as downstream signalling is concerned, *BRC1* appears to be transcriptionally regulated by SL at least in some species. *BRC1* encodes a TCP transcription factor which, in pea, is upregulated after SL treatment (Braun, N. *et al.* (2012), Dun, E.A. *et al.* (2012)). As further supporting evidence, both pea and *Arabidopsis brc1* mutants have an increased branching phenotype which is SL resistant (Aguilar-Martinez, J.A. *et al.* (2007), Braun, N. *et al.* (2012)). *BRC1* only has a limited expression domain, and *brc1* mutants are less branched than SL deficient mutants (Aguilar-Martinez, J.A. *et al.* (2007), Braun, N. *et al.* (2012)) so it is likely that it is only responsible for part of the SL response.

It has also been shown that SL signalling can trigger removal of the PIN1 auxin efflux carrier from the plasma membrane (Crawford, S. *et al.* (2010), Shinohara, N. *et al.* (2013)). In this way it could regulate shoot branching via auxin transport/canalization (pages 15-17) (Prusinkiewicz, P. *et al.* (2009), Shinohara, N. *et al.* (2013)). It has been postulated that PIN2 polarity is also influenced by SL, although the effect is indirect (Pandya-kumar, N. *et al.* (2014)). SL regulation of PIN1 proteins would explain the systemic effects of SL signalling and it would be interesting to investigate the effects of SL on other members of the PIN family. The Leyser lab has now looked at several PIN proteins and so far, only PIN1 responds.

1.8 Dorsoventral Polarity in Leaves

Leaves develop from a primordial population of cells at the flanks of a shoot apical meristem. An *Arabidopsis* leaf has two sides, each with distinct functions (figure 10). The adaxial side of the leaf forms adjacent to the meristem and in the mature leaf faces upwards. This side of the leaf has its main function in photosynthesis and is darker green than the underside due to a higher concentration of chlorophyll. The adaxial surface also has proportionally a lot more trichomes than the abaxial side. The lower, or abaxial leaf surface has many more stomata and the lower internal portion of the leaf is composed of spongy mesophyll, which has ample intercellular air space. These features allow for efficient gas exchange, the primary function of the abaxial leaf structures.

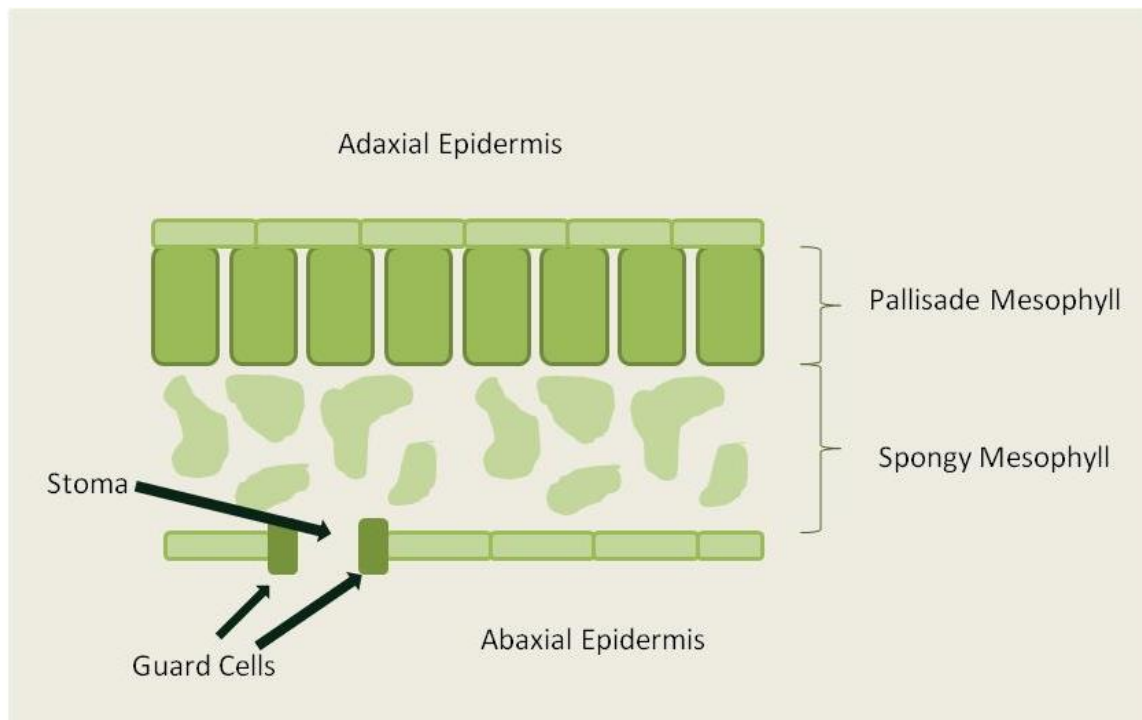


Figure 10. Cross section of a mature *Arabidopsis* leaf. Palisade cells are regular in shape and are found directly beneath the Adaxial epidermis cells. Under the palisade layer is the spongy mesophyll. Cells in this region are irregular and have relatively large intercellular spaces which allow for gas exchange. Gases enter the cell through stomata on the abaxial leaf surface. Guard cells on either side of a stoma can facilitate closure if necessary, for example, to prevent loss of excess fluid in drought conditions.

The differentiation of the primordium into a mature leaf is highly complex so for the purposes of this study only relevant gene families are discussed. The two relevant gene families in this case are the Class III HD-ZIP (*HD-ZIPIII*) transcription factor genes and the *YABBY* gene family. There are five *HD-ZIPIII* genes in *Arabidopsis* with overlapping expression domains which include the meristem, the cotyledons, and the leaves (Baima, S. *et al.* (1995)), (Otsuga, D. *et al.* (2001)) (Prigge, M.J. *et al.* (2005)) Recessive mutations in *HD-ZIPIII* genes are not sufficient to cause morphological phenotypes with the exception of *revoluta (rev)* which has altered axillary and floral meristem function (Otsuga, D. *et al.* (2001)). The *rev* mutant is used in this study as a marker of adaxial cell identity using the promoter::reporter fusion *rev9::GUS*.

There are three members of the *YABBY* gene family in *Arabidopsis*; *FILAMENTOUS FLOWER (FIL)*, *YAB2*, and *YAB3*. All three of these genes are expressed in abaxial leaf cells with expression gradually restricted to the abaxial leaf margins (Sawa, S. *et al.* (1999)), (Siegfried,

K.R. *et al.* (1999)). The *FIL* gene is used in this study as a marker of abaxial cell identity, using the promoter::reporter fusion *fil8::GUS*.

1.9 Nutrient supply

Plants are reliant on their environment to provide them with minerals that are essential for growth such as nitrates (or another N source), potassium and magnesium. When any of these nutrients become less readily available metabolic changes occur. The increase in carbohydrates in the roots results in an increase in root biomass relative to that of the shoot (Linkohr, B. *et al.* (2002)). Stimulating root growth allows for maximum uptake of nutrients from the local environment thereby increasing the plants chances of survival. With growth concentrated in the roots, plants in nutrient poor environments will tend to have a simpler shoot system as resources cannot be used for less important features such as lateral branching. Nutrient shortage can occur either in nutrient poor media or when plants are competing in the same nutrient pool.

Plants take up nitrogen as nitrate (NO_3^-). Nitrate will first be reduced to nitrite (NO_2^-) by nitrate reductase using $\text{NADH} + \text{H}^+$ as a reducing agent. This reaction occurs in the cytoplasm. Secondly nitrite is reduced to ammonium in plastids by nitrite reductase. Free ammonium ions are toxic to plant cells and are rapidly incorporated into organic compounds like amino acids. A link between auxin, and nitrate metabolism and uptake has been suggested several times in recent years. The amount of nitrate that can be taken up by plant roots is dependent on the levels of exogenous auxin in a plant. Higher levels of auxin promote lateral root formation which will allow a greater volume of nitrate uptake. More specifically the *Arabidopsis* dual-affinity nitrate transporter gene *CHLI* was found to be regulated by auxin in both shoots and roots (Guo, F-Q. *et al.* (2002)).

The wildtype response of *Arabidopsis* plants to a low nitrate supply includes a reduction in the level of secondary branches. Another response is a shift in biomass allocation from the shoot to the root. This maximizes nutrient uptake. *max1* plants exhibit a degree of resistance to both the reduction in secondary branching and shift in shoot to root ratio seen in wildtype plants.

1.10 Shade avoidance

As photosynthetic organisms light is vital to plants. It is not just the presence of or the lack of light that plants are receptive to but also the quality of light. Consistent monitoring of the light reaching the plant is achieved using photoreceptors which absorb blue (~475nm), red (655-665nm) and far-red light (725-735nm). In direct sunlight the plant will perceive light with the correct ratio of red to far-red wavelengths (approximately 1.15:1 Red:Far Red (R:FR)). In a crowding situation the light that reaches a plant will have had to pass through, or be reflected from, leaves of nearby plants. Chlorophyll and other pigments in the leaves alter the quality of the light passing through them, absorbing light below 700nm. Red light wavelengths are therefore absorbed by leaves severely reducing R:FR light on the other side.

Typical responses to a drop in R:FR include; rapid stem elongation, reduction of leaf development and an increase in apical dominance, characterised by a decrease in branching. This is known as shade avoidance response (Casal, J.J. (2012)).

1.11 Thesis Aims

The overall aim of this thesis is to contribute to the knowledge of hormonal regulation of shoot branching. Furthering the understanding of these mechanisms will provide a more solid base for further work in the subject to be conducted. The first section of my thesis will concentrate on the *more apical dominance (mad)* mutation. The *mad* mutation was isolated in a screen designed to find suppressors of the *max1* branching phenotype. By characterising the effects of *mad* it will become possible to assign putative roles for *MAD* in the regulation of bud outgrowth. This will either expand current knowledge on strigolactone based control of bud outgrowth, if *MAD* proves to be part of Arabidopsis *MAX* pathway, or highlight an existing, or novel method of control of bud outgrowth. Delineating the *MAD* locus will allow for sequencing. This in turn will allow for any *MAD* orthologs to be identified in the other plant systems with an identified strigolactone biosynthesis and signalling pathway which is involved in shoot branching control (petunia, rice, and pea are the best characterised systems). The second part will concentrate on the outcomes of a screen designed to isolate mutants with an

increased branching phenotype, like that of *max1*, specifically in low nutrient conditions. The aim of this screen is twofold; to find previously undiscovered alleles which may be involved in the control of shoot branching, and to find potential links between shoot branching and nutrient availability. These mutants will be phenotypically characterised with the hope of understanding the mechanism by which bud outgrowth is deregulated.

2. Materials and Methods

2.1 Chemical Stocks

Unless otherwise stated chemical used were from Fisher Scientific (FS), Sigma-Aldrich (S-A) or BDH Chemicals (BDH).

2.2 Plant lines and growth conditions

The plant lines used in this study are detailed in the table below

Line or mutant	Description	Origin
Col-1 (columbia)	Wildtype	Leyser Lab
Ler (landsberg erecta)	Wildtype	Leyser Lab
<i>max1-1</i> (<i>more axillary branching 1</i>)	Increased branching EMS mutation	Stirnberg, van De Sande, <i>et al.</i> 2002 Leyser Lab
<i>max2-1</i>	Increased branching EMS mutation	Stirnberg, van De Sande, <i>et al.</i> 2002 Leyser Lab
<i>max3-9</i>	Increased branching EMS mutation	Booker, Auldridge, <i>et al.</i> 2004
<i>max4-1</i>	Increased branching T-DNA mutation	Sorefan, Booker, <i>et al.</i> 2003
<i>axr1-3</i> (<i>auxin resistant 1</i>)	Increased branching Auxin signalling mutant	Leyser, Lincoln, <i>et al.</i> 1993
<i>mad</i> (<i>more apical dominance</i>)	Decreased branching EMS mutation	Leyser Lab
17-4	Increased branching EMS mutation	Leyser Lab
<i>rev9::GUS</i> (<i>revoluta9::βGlucuronidase</i>)	rev9 promoter, GUS fusion	Bowman Lab

<i>fil8::GUS</i> (<i>filamentousflower8</i>)	fil8 promoter, GUS fusion	Bowman Lab
---	---------------------------	------------

Table 2. Plant lines used in this study, also noted are their uses, and origins. Where possible, references have been given to papers containing further details.

Growth conditions

Seeds were sown onto Levingtons F2 compost at a density of 2 seeds per 4 cm² pot, unless otherwise stated. Seeds were then cold stratified at 4°C for a minimum of 48 hours to aid germination.

Glasshouse grown plants were subject to a 20°C, 16 hr light/15°C, 8 hr dark photoperiod. The light intensity was approximately 150 μmolm⁻²s⁻¹.

Plants grown in growth chambers were also subject to a 20°C, 16 hr light/15°C, 8 hr dark photoperiod but light intensity was approximately 120 μmolm⁻²s⁻¹.

Morphological techniques

Arabidopsis morphology

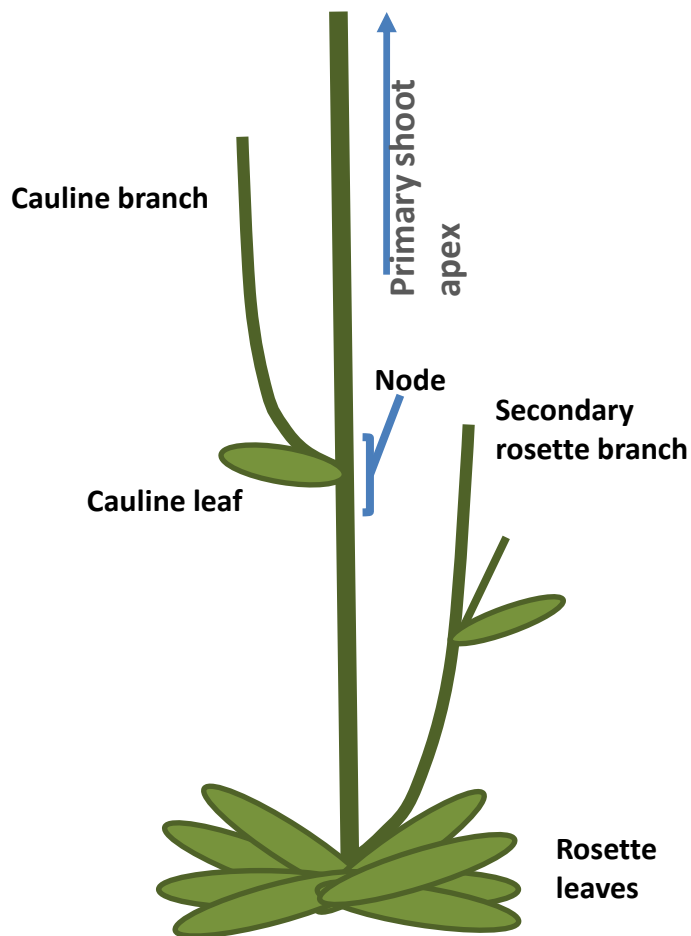


Figure 11. Diagrammatic representation of wildtype *Arabidopsis thaliana* with the main morphological features highlighted. *Arabidopsis* is a typical dicot with hallmark features such as the repetitive growth modules, phytomers, which consist of an inter node and a leaf with its associated axillary meristem. Both rosette branches and cauline branches are secondary axes of growth with the potential to form tertiary axes of growth and so on.

2.3 Sterile growth of plants

Plants to be grown axenically were either grown in Weck jars or in 10 cm² petri dishes. The culture medium used was *Arabidopsis thaliana* Salts (ATS) (Wilson *et al.* 1990).

Reagent	Final Concentration
Potassium nitrate (KNO_3) (BDH)	5 mM
Potassium dihydrogen orthophosphate (KH_2PO_4) adjusted to pH 5.5 with K_2HPO_4 (BDH)	2.5 mM
Magnesium sulphate (MgSO_4) (FS)	2 mM
Calcium nitrate ($(\text{CaNO}_3)_2$) (FS)	2 mM
Orthoboric acid (H_3BO_4) (BDH)	70 μM
Iron-ethylenediaminetetraacetic acid (FeNa-EDTA) (Duchefa)	50 μM
Manganese chloride (MnCl_2) (FS)	14 μM
Sodium chloride (NaCl) (FS)	10 μM
Zinc Sulphate (ZnSO_4) (BDH)	1 μM
Copper Sulphate (CuSO_4) (FS)	0.5 μM
Sodium Molybdenate (NaMoO_4) (BDH)	0.2 μM
Cobalt chloride (CoCl_2) (Fisons)	0.001 μM

The reagents listed in the above table result in an ATS solution with a 9mM nitrate (NO_3^-) concentration. For experiments which required plants undergo nitrate starvation the nitrate concentration was reduced to 1.8mM. This was achieved by substituting 4ml/l of the KNO_3 with 1M potassium chloride (KCl), and 1.6ml/l of the $\text{Ca}(\text{NO}_3)_2$ with 1M calcium chloride (CaCl_2) to replace the nitrate with calcium anions. The optional components in the table below were added when required.

Reagent	Concentration
Sucrose (FS)	10g/l
Technical agar No.3 (Oxoid)	10g/l

Seeds of the appropriate genotype were first sterilised using a chlorine bleach method. This method involves agitating the seeds for 10 minutes in a 10% (w/v) chlorine bleach solution. The seeds are then transferred to a 70% solution of ethanol (F) for 30 seconds before being rinsed in at least 7 changes of sterile dH₂O. The seeds were then cold stratified at 4°C for 48 hours before sowing.

2.4 Antibiotic selection

The antibiotics detailed in the table below were used when antibiotic resistance was to be assessed.

Antibiotic	Application	Concentration
Hygromycin	GUS selection	50 µM

2.5 Physiological crossing

Of the two genotypes to be crossed the physically stronger plant, ie, the wildtype plant or the one with the least detrimental mutant phenotype, was chosen, were possible, to be the maternal plant. Small axillary branches, siliques, and any inflorescences were removed from a chosen branch before a suitable bud was selected. All outer floral organs were removed from the bud so that just the carpel remained. The plants were then left for 24hrs to determine any dead or damaged carpels.

Once viable carpels had been identified stamens from an appropriate flower on the paternal plant, preferably one that was visibly shedding pollen, were removed and the pollen transferred

to the receiving maternal carpel. Successful fertilisation was evident when the siliques grew out within 72hrs.

2.6 Gathering physiological data

When analysing phenotypes comparatively it was necessary to analyse every aspect of the mutant phenotype that was either different to the original mutant (as in the *MAD/mad* mutant which was isolated following the EMS mutagenesis of *max1*) or wildtype. The elements measured are listed in the table below.

Phenotypes analysed
Height
Leaf length (7 th rosette leaf)
Petiole length (7 th rosette leaf)
Stem thickness (when comparing with max1)
Number of rosette branches
Internode length

Data was gathered when all floral activity had ceased. Leaf data was collected when leaf expansion was complete. All data collected was pooled and averaged over a population of no less than 50 plants.

2.7 Auxin transport assay

In order to assess the level of auxin transport in a given stem segment a standard auxin transport assay was used. To this end 15mm stem segments from below the first node were placed, apical end down, into a 0.5xATS solution (no sucrose) with 0.005% Triton-X-100, a detergent to ensure that the apical end of the stem segment remains submerged, and 1 μM ^{14}C -labelled Indole-3-acetic acid (IAA) (American Radiolabelled Chemicals Inc. (specific activity 55mCi/mmol)).

Stem segments were transferred to a controlled environment growth room to incubate for 24 hours after which time the stem segments were removed from the radiolabel mixture and rinsed in 0.5XATS. The basal-most 5mm of the stem segments were removed and placed into 90 well scintillation plates along with 80% methanol, sealed, and left for 48 hours to allow the radiolabel to diffuse from the segments. Half of the methanol was then transferred to another scintillation plate along with 200 μ l scintillation fluid (Microscint, from Packard Biosciences) before the scintillation level was assessed using a scintillation counter (Topcount, from Packard Biosciences).

2.8 Split plate assay

The split plate assay protocol followed was taken from Chatfield *et al.* (2002). Plants of the appropriate genotype were grown axenically, from sterilised seed on ATS nutrient media in 11 Weck jars. Once the plants had moved from vegetative to reproductive growth but had no more than 2 nodes along the primary shoot axis they were deemed ready to use and excised nodal segments were transferred to split plates. Split plates were made by removing a 5mm section from the solidified ATS agar contents (with or without added hormone treatment) of a 10cm² petri dish. Nodes with a bud of no more than 1.5mm, to ensure that the bud had not yet been released from dormancy, were selected. The nodal segments were embedded, apically and basally, into the ATS agar as shown in figure 12. The plates were then transferred to a controlled environment growth room where bud outgrowth was measured over a 10 day period.

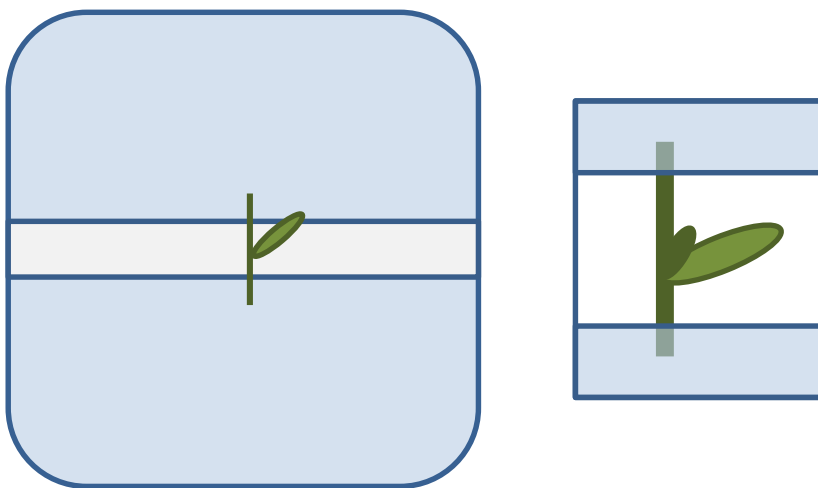


Figure 12. The split plate assay, in which an excised node segment is embedded in between two block of agar with or without hormone treatments applied. As an example, auxin (IAA) in different concentrations can be added to the vascular transport stream from and the effect on bud outgrowth measured over a period of days. Similarly, cytokinin could be added to the xylem transport stream. The effect of hormones or hormone transport inhibitors can be directly measured in this way.

2.9 Micrografting

Under sterile conditions seeds of the appropriate genotype were sown onto 10cm² Petri dishes containing ATS agar (20 seeds per plate in four rows). The sealed plates were placed vertically in a controlled environment growth chamber under standard anoxic conditions (16 hr light/ 8 hr dark, 22/18°C, and 100 μmol/m²/s) and left to grow for 3 days. After three days the seedlings were moved to a different growth cabinet set at 27°C (16/8 hr light/dark, 60 μmol/m²/s) for a further 2 days. The increased endogenous auxin levels at 27°C increases the hypocotyl length making for easier grafting.

Under sterile conditions selected seedlings (long straight hypocotyl and strong root growth) were cut transversely across the hypocotyls (rootstock donor $\frac{3}{4}$ of the way up the hypocotyl, scion donor halfway up the hypocotyl), a silicon tubing collar placed over the hypocotyls of the rootstock and a suitable hypocotyl from an excised scion slotted into the top half of the collar so that the rootstock and scion meet and reconstitute a whole seedling. As well as reciprocal genotype combinations “self grafts” were also performed as a means of control.

The graft junctions were inspected using a dissecting microscope before being returned to the 27 °C growth chamber for 3 to 4 days. Successful grafts were then transferred to soil. After an appropriate length of time the plants were then phenotypically assessed. Once the data was collected the graft union was checked for integrity and adventitious roots to confirm the validity of results

2.10 Weck jar branching assay

Plants were grown axenically on ATS solid media with or without added hormone treatment. Branching levels were assessed after 4 weeks.

2.11 Nitrate deprivation and crowding response experiment

Seeds of each genotype (Col-1, *max1-1* and *MAD/mad*) were sown, in monoculture, at densities of 1 (low density), 4 (medium density), and 16 (high density) per 4 cm² pot in the N-limiting combination of 50% latent buzzard sand and 50% Terragreen. Plants were then supplemented with *Arabidopsis thaliana* salts (ATS) media (700ml initial treatment, 200ml at week 3, 300ml at week 4, and 300ml at week 5) at either 9 mM or 1.8m M N concentrations to provide N sufficient or N limiting conditions respectively.

The plants were also grown in competitive culture to determine any differences in the *max1* and *MAD/mad* genotypes response to the nitrate deprivation and crowding treatments when placed in competition with wildtype (Col-1) *Arabidopsis* plants. For this experiment, plants were grown at densities of 2, 4, and 16 plants per 4 cm² pot with an equal number of each genotype in each pot.

Growing heterozygotes to specific densities required more *MAD/mad* seeds to be sown and the wildtype and *mad* homozygotes to be removed at an early stage.

The plants were measured and harvested at approximately 7 weeks, when the primary apex had ceased activity. Factors measured were; number of secondary rosette branches, root weight (fresh and dry), shoot weight (fresh and dry), primary root length, and number of lateral roots. These measurements allow determination of root shoot biomass ratio and simple analysis of root and shoot architecture.

2.12 Low nutrient screen to isolate mutant with elevated branching levels

In order to identify additional shoot branching mutants, a mutant screen was designed specifically for this project. Col seeds were treated using a standard EMS mutagenesis protocol. Seed was collected from the M1 population and was used throughout the screen.

M2 seed was sown onto a mixture of 50% vermiculite sand and 50% Terragreen. This was supplemented with ATS solution with a low nitrate concentration of 1.8mM. Wildtype *Arabidopsis* plants respond to nitrate deprivation by reducing branching levels and increasing the root to shoot ratio in order to maximize nutrient uptake. The *max* mutants do not behave in this way and remain highly branched even in nitrate concentrations as low as 0.36mM. With this in mind the screen was designed to isolate individual plants that remain highly branched in low nitrate conditions.

Imaging and microscopy

2.13 Leaf cross sectioning

Fifth leaves from 26 day old plants were cut into quarters along the midrib and the leaf length and fixed in 2.5% gluteraldehyde and 4% paraformaldehyde in 0.1M phosphate buffer for 1

hour. Samples were washed in 0.1M phosphate buffer before being covered in 1% Osmium tetroxide for 2 hours, and followed with another phosphate buffer wash. The leaf tissue was then dehydrated through an acetone series; 10 minutes in each of 10%, 20%, 30% etc. through to 100% acetone. The dehydrated tissue was then transferred to a 1:1 mixture of Agar low viscosity resin embedding medium (medium hard thickness): acetone for 1 hour before being transferred into beam capsules and covered with the resin. Samples were cured for 24 hours at 60°C before being stained in 0.1% toluidine blue. Sections were taken using a microtome. Images were obtained a Zeiss LSM510 META compact mounted on an Axiovert 200 inverted microscope.

2.14 SEM images

4 week old *mad* mutant plants were used for the scanning electron micrographs of *mad* mutant leaves. *mad* leaves were mounted onto the specimen holder using an adhesive. The sample was then subjected to cryofixation (flash frozen in liquid nitrogen) before entering a preparation chamber under vacuum in which the sample was coated with a thin layer of gold (SEM requires samples to be able to conduct electricity). The cryofixation step allows samples to undergo imaging without tissue degradation being a factor. For cross-sections whole leaves were freeze fractured in the vacuum chamber before entering the microscope.

Image Capturing Equipment	Application
Nikon Coolpix 4500 digital camera	Whole plant pictures
JEOL 6490LV Scanning electron microscope with cryostage	SEM leaf images

Molecular Biology

2.15 GUS staining

Tissue from plants that were 4 weeks old were incubated in a GUS staining solution which contained 0.5mg/ml X-Gluc (5-bromo-4-chloro-3-indoyl- β -D-glucuronide) (Melford), 50mM sodium phosphate (pH 7.0), 0.05% Triton-X-100, 0.1mM potassium ferrocyanide ($K_4Fe(CN)_6$ (S-A) and 0.1mM potassium ferricyanide ($K_3Fe(CN)_6$ (S-A), for at least 37°C for at least 16 hours (depending on the strength of the reporter). The tissue was destained in 80% methanol(w/v). Images were acquired using an HP Scanjet 4370 digital scanner at a resolution of 600 dpi and the resulting files were processed in Photoshop CS3'.

2.16 Genetic Mapping

Because the mutant gene to be mapped is in the Columbia background it is possible to take advantage of the natural polymorphisms existing between the Col and Ler ecotypes in order to map the mutant gene locus. A mapping population was created by crossing homozygous mutant individuals with Ler. Because of recombination individuals will have a genome with sections of Col-specific DNA and sections of Ler specific DNA. The mutant gene will always be on a section of Col DNA.

Initial mapping involves testing markers spread across the genome for linkage. A 1:1 Col:Ler ratio of alleles indicates no linkage between the marker being tested and the mutant gene. The more Col alleles there are, the stronger the linkage between marker and gene.

Once initial mapping has indicated the rough position of the mutant gene more markers can be designed to narrow down the mapping interval bit by bit. This process is known as chromosome walking. Because recombination frequency is an indicator of physical distance the number of Col alleles at any given marker will reduce the closer they are to the gene. Eventually there will be no recombinants left at markers on either side of the gene. At this point the mapping interval containing the gene is as small as it can get.

2.17 Marker design

Markers were designed using the CEREON database of SSLP (simple sequence length polymorphism) and SNP (single nucleotide polymorphism) polymorphisms.

2.18 DNA extraction

DNA extraction was completed using one of two methods, the first being the DNeasy 96 plant protocol (QIAGEN). 50mg of fresh plant tissue was collected from each plant to be used before following the protocol detailed in the DNeasy 96 plant handbook.

The above method was used to collect DNA from the *mad* mapping population as it allows collection of 96 DNA samples at a time. When fewer extractions were required a Mini prep kit was used instead. This protocol yields DNA concentrations of approximately 20.4µg in 100µl Qiagen elution buffer AE. All DNA samples were stored at -20°C.

RNA extraction

100mg of stem tissue was taken from 5 week old plants and ground in liquid nitrogen. RNA was extracted using the RNeasy kit (QIAGEN). RNA was stored at -80°C

2.19 RT-PCR

RT-PCR was used to assess the expression levels of a given gene. This is achieved by synthesising cDNA from mRNA. The cDNA can be amplified using PCR and the relative amounts of DNA present in the final reaction mix are indicative of the level of gene expression. All samples are compared to expression levels of a constitutively expressed gene such as Actin.

2.20 cDNA synthesis

For synthesis of complementary DNA from mRNA the components in table below were heated to 65°C for 5 minutes before being chilled, the components in the lower table were then added to the reaction mix before incubating at 42°C for 2 minutes. 1 µl of Superscript™ reverse transcriptase was added before a further 42°C incubation, this time for 50 minutes, before a heat inactivation step (70°C for 15 minutes). cDNA was stored at -20°C.

Component	μl in a 12μl reaction mix
RNA	1μg
10mM Oligo dT	1
10mM dNTPs	1
Rnase free dH ₂ O	Enough to make up to 12μl

Component	μl added to cDNA reaction mix
5X first strand buffer	4
0.1M DTT	2
Rnase OUT	1

2.21 Polymerase Chain Reaction (PCR)

Amplification of DNA was carried out using the methods detailed in the tables below

Component	μl in a 10 μl reaction mix
10X buffer	1
2mM dNTPs	0.8
10 μM Forward Primer	0.25
10 μM Reverse Primer	0.25
0.25 units Taq DNA polymerase	0.2
DNA to be amplified	1
dH ₂ O	6.5

Step	Temperature/ $^{\circ}\text{C}$	Length of time	Stage of reaction
1	94	1 minute	Denaturation
2	94	10 seconds	Denaturation
3	X Approx. the lowest annealing temp of the primer pair	10 seconds	Annealing
4	72	1 minute	Extension
5	-	-	Repeat – stages 2 -5 X37 (varies)
6	72	1 minute	Final extension
7	12	Indefinite	

2.22 Restriction digests

Reactions that required a digest step (CAPS markers) had the components in the table below were added to the PCR reaction mix. The reaction mix was then incubated at 37°C for 1 hour.

Component	µl in a 20µl reaction mix
Restriction enzyme (NEB)	0.5
Appropriate 10X buffer (NEB)	2
PCR reaction mix	10
dH ₂ O	7.5

2.23 Agarose gel electrophoresis

Agarose gel electrophoresis was used to separate out DNA molecules based on their molecular weight and charge. This method was primarily for genetic mapping but also for checking if DNA amplification had been successful. The strength of the gel required is dependent on the size difference between the molecules that are to be separated. This study used between 1% and 4% agarose gels. The gels were composed of Tris-borate-EDTA (TBE) (see table below) diluted to a working concentration of 0.5X, with added agarose (FS). A typical gel would be 120ml and to this was added 1µl of 10mg/ml ethidium bromide (S-A) or 2µl of SYBRsafe®(Invitrogen).

Tris-borate-EDTA (TBE) component	Amount in 1l
Tris (Invitrogen)	108g
0.5M EDTA pH8.0	40µl
Orthoboric acid	55g
dH ₂ O	To 1l

To each 5µl of PCR reaction mix 1µl of loading buffer (detailed below) was added.

Component	% (w/v)
Bromophenol blue (Fisons)	0.25
Xylene cyanol FF (BDH)	0.25
Ficoll (S)	40

Gels were run at 90kV for an appropriate length of time (between 1 and 3 hours depending on the strength of the gel and fragment size) before being examined using a uv transilluminator.

2.24 Primers used in this study

Name	Forward Primer	Reverse Primer	Application
CAT3	ACG GTG GTG CTC CAG TCT CCA A	CTC GGG GTA GTT GCC AGA T	Initial mapping of the MAD locus CAPS marker
NPR1	TGA CCG TCT CAC TGG TAC GAA	GCA ACT CTG TAA CAC CAT CAT	Initial mapping of the MAD locus CAPS marker
GAPC	ATC AAC GGT TGG GAC ACG GAA A	CTG TTA TCG TTA GGA TTC GGA A	Initial mapping of the MAD locus CAPS marker
AFC1	ATC ATC GCG ATC GAG CTA GCT T	CTC GGA ACT CTC AAG TCT AAA	Initial mapping of the MAD locus CAPS marker
DET1.1	GAG CAT CAA CAA GAT GAC CAG AA	CCG ACT AAG CAA AGC AAT ACA A	Initial mapping of the MAD locus CAPS marker
KLPNHC	CGT TGC TCG TGG ATT TTG TAA	CAG TAC CGC GAA CAG GAT CTT	Initial mapping of the MAD locus CAPS marker
LFY3	GCC AGT ATT GCC AAC TTT CCA T	AAT CGT CTC CGT TCA GCT CTA A	Initial mapping of the MAD locus CAPS marker

CA1	GTC GGA TGA AGT ACC TGT CTG AA	GGC TTT GAC GTT TCG AGC TA	Initial mapping of the MAD locus CAPS marker
NGA126	GGA CGG GTT TAC TCT GGT T	GCT TGT GAC GTT GCC AAA AT	Initial mapping of the MAD locus SSLP marker
CER470589	GAC CCC TCA AAG ATT ATC TCT T	GAT CTT CAT CTG AGC TTC GGA T	Fine structure mapping of the MAD locus SSLP marker
CER469977	AGC TTA TCA ACT CGT TCT CTT	AGA CCT TCA AGT ACA TGC CGT T	Fine structure mapping of the MAD locus SSLP marker
CER470642	CAG ACT CTC TTA CAG AGT A	GGC ATC TGA ACA CGT TAG	Fine structure mapping of the MAD locus SSLP marker
CER470384	GAA CAG CCT GGA TAG AGT AT	GAC GCA TGT CTG CGA ATA A	Fine structure mapping of the MAD locus SSLP marker
CER464953	GAT GCG CAA GAA TAG GAT	TAG TGA ACA CAA CCA TTG TTA	Fine structure mapping of the MAD locus SSLP marker
CER464637	TTA ACT GAG CAA AGC CAC ATT A	GTA GCA TAG GTA ACA CGT CAG AA	Fine structure mapping of the MAD locus SSLP marker
CER464922	GGT CTT GAC TAG TCG ACG TAA	GGA CGC ATC GTA ATT TAC TA	Fine structure mapping of the MAD locus SSLP marker
PIN1-RT	GAA ACG CTC CGG TGG TGG	GAC CAG GTG ATG CCG AAT A	Amplification of PIN1 from cDNA
D14	ATG AGT CAA CAC AAC ATC TTA GAA GC	TCA CCG AGG AAG AGC TCG C	Amplification of D14 from cDNA

Table 3. Marker and primer details used in this study. Markers used for fine structure mapping of the *MAD* locus were all designed specifically for this study. Primers for the initial mapping of *MAD*, *PIN1-RT*, and *D14* were designed previously and details held by the Leyser lab.

3. Characterisation of the *MAD* suppressor of the *max1* phenotype

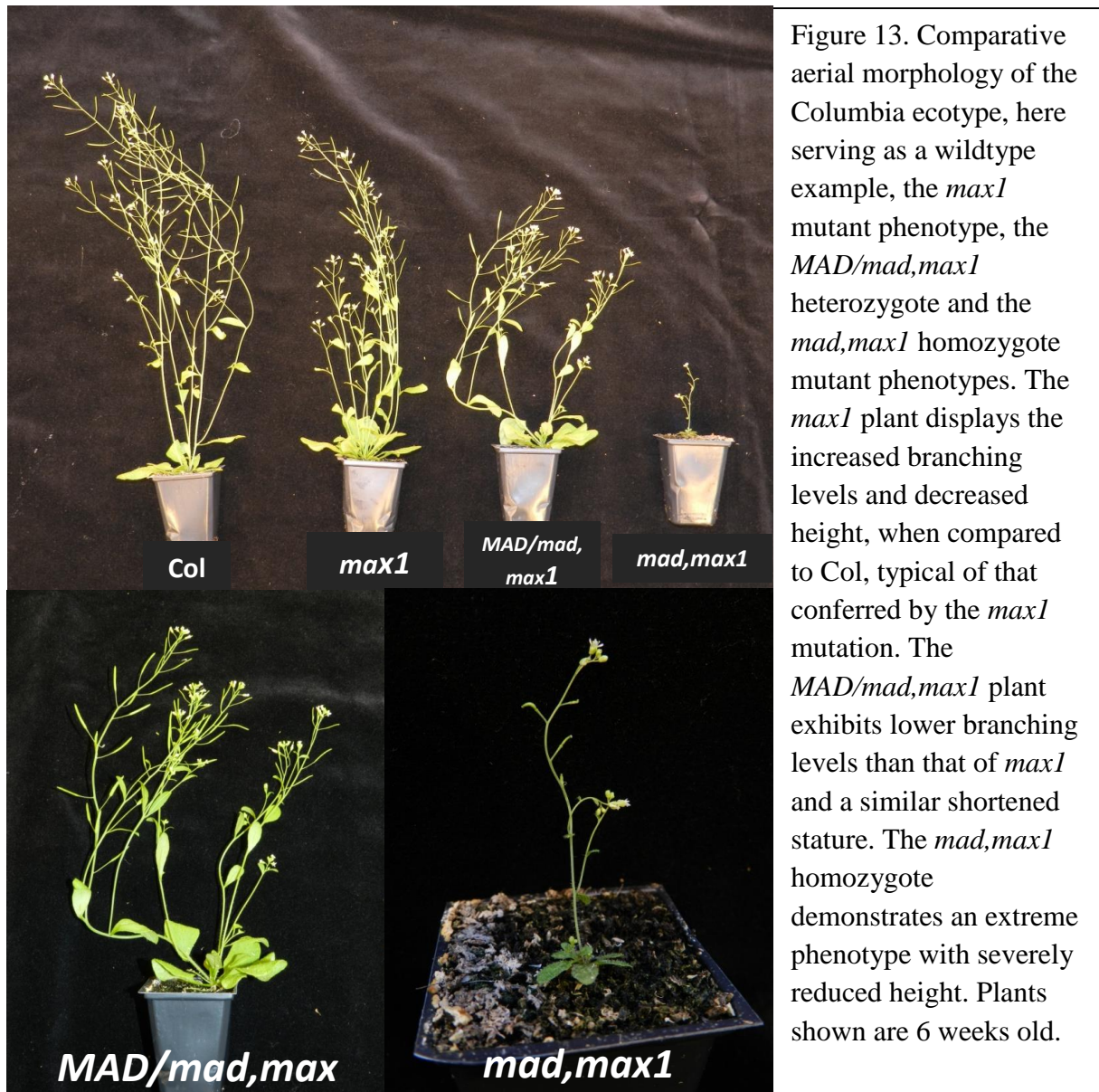
Characterisation of the *MAD/mad* and *mad* Arabidopsis mutant phenotypes

The *mad* mutation was isolated in a screen designed to look for enhancers and repressors of the highly branched phenotype of *max1* mutant plants (typically 4-5 rosette branches per plant) towards wildtype levels (typically between 0 and 2 rosette branches per plant) (designed and implemented by Tom Bennett). This was achieved via EMS mutagenesis of a *max1* seed population. Any individuals grown from the F2 seed with fewer rosette branches than an average *max1* plant were selected for further investigation. *MAD/mad, max1* was one of plants discovered by these means and is the subject of the following study. The total number of mutants isolated was 284, too high a number for individual assessment of each phenotype. Only the most novel and/or relevant were chosen for further investigation. The most promising were; *sideways (swy)* which specifically enhances *max1-1*, *advoluta (adv)* which exhibits a decreased branching phenotype, *crispy (cpy)* which has several highly pleiotropic phenotypes, *depressor (dep)* which has a leaf and shoot phenotype, and the *mad* heterozygote (*MAD/mad*) which decreases *max1* branching without any major pleiotropic phenotypes. The *mad* homozygote however, has a highly pleiotropic phenotype.

3.1 Morphology of *MAD/mad* (*MORE APICAL DOMINANCE/more apical dominance*) and *mad* plants

Comparisons of aerial morphology between *MAD/mad,max1*, *mad,max1*, and the two standards, Col and *max1* demonstrates a partial rescue of the *max1* branching phenotype when in a *mad* heterozygote background (figure 13). This is expected given the nature of the screen. This part of the analysis was carried out with the *mad* mutation in a *max1* background. This enabled an appropriate assessment of the effect of the *mad* mutation on *max1* physiology, particularly on branching levels. Something that cannot be appreciated when *MAD/mad* is present in a wildtype background with already low levels of branching.

The effect of the *mad* mutation is dose dependent with two copies of the mutation resulting in a far more severe phenotype than that of the heterozygote. Whereas in *MAD/mad,max1* the most immediately obvious effect of the *mad* mutation is that of reduced branching compared to *max1*, in *mad,max1* the deleterious effects of *mad* are far more striking. A *mad,max1* genotype results in a very much weakened plant of diminutive stature. This posed a problem for further investigation as the condition of the plant renders most experimentation untenable.



The height differential between *mad,max1* plants and the other genotypes is substantial (figure 14). What is also apparent is the similarity in height of *max1* and *MAD/mad,max1*. The height of *MAD/mad,max1* plants, compared to *max1* plants, appears to be more variable across the population measured (pop. Size = 30) with standard deviations of 27.2 and 19.1 respectively.

Despite this variability there is no significant difference in height between the two genotypes indicating no rescue of the *max1* reduced height phenotype. The extreme loss of height seen in the *mad,max1* mutant is probably attributable to the overall unhealthy nature of the plant. It is therefore not possible to know what effect, if any, two copies of the *mad* allele has on the height of *max1* plants.

Variation is not just found in the overall height of these plants and a more comprehensive set of data takes into account the length of the cauline internodes along the shoot as well as total plant height (figure 14). The location and number of cauline branches has great impact on the aerial structure of flowering plants. When compared to Col, *max1* have nodes occurring closer together, nearer to the bottom of the shoot. The result is a plant with shorter internodes than found in wildtype Col. This feature is also seen in *MAD/mad,max1*. Because *mad,max1* is so much smaller than the other genotypes, and never has more than 2 cauline nodes along the stem, comparative analysis is difficult. The reduction in node number is likely a result of the inherent weakness of the genotype rather than the potential lack of *MAD* activity. This is a dominant mutation so it might not be a result of loss of function.

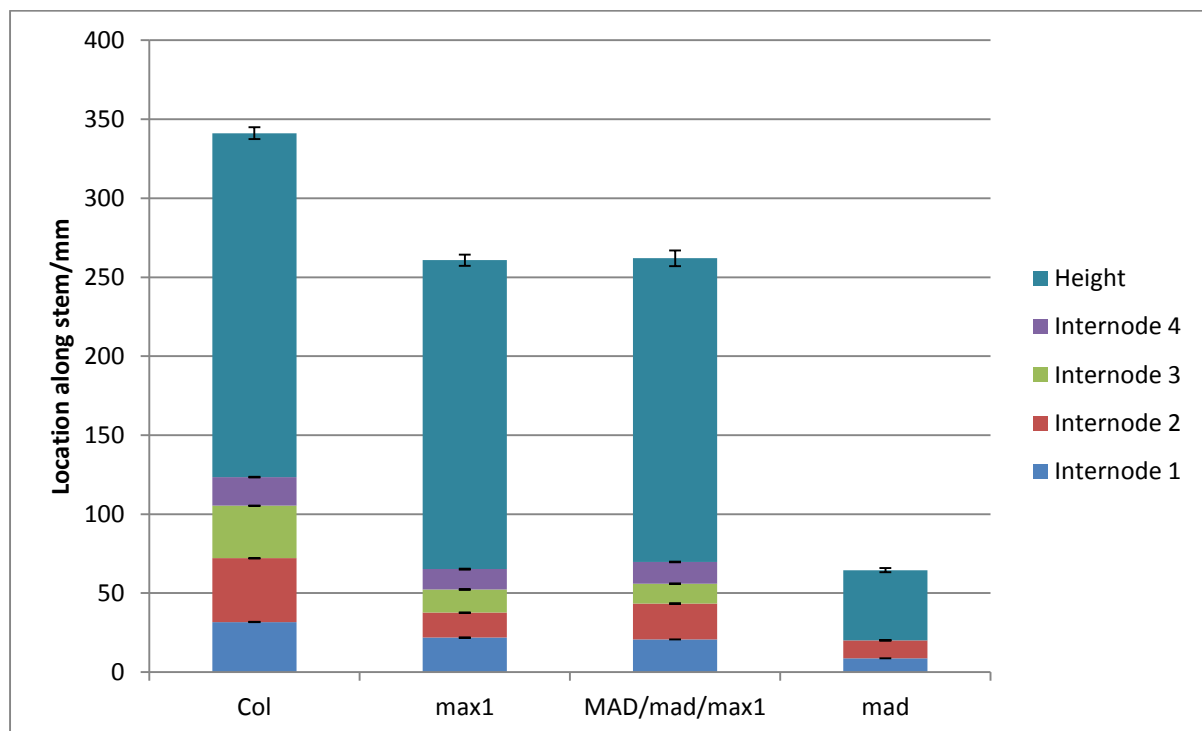


Figure 14. Comparative heights of Col, *max1*, *MAD/mad,max1*, and *mad,max1* with cauline internodal sections detailed along the stem. Plants were grown under standard glasshouse conditions. Measurements were taken at 6 weeks post germination.

Error bars depict standard error. N=30 ANOVA (heights) Col, *max1* sig. = 0.018. Col, *MAD/mad,max1* sig. = 0.024. Col, *mad,max1* sig. = <0.001. *max1*, *MAD/mad,max1* sig. = 0.521. *max*, *mad,max1* sig. = <0.001. *MAD/mad,max1*, *mad,max1* sig. = <0.001

Another noted difference between *max1* and Col is that of the length of rosette leaves with *max1* exhibiting a shorter, more rounded organ than that of Col. This *max1* phenotype is perpetuated in *MAD/mad,max1* with both leaf and petiole length very similar. The *mad,max1* length measurements show a far smaller leaf compared to the other genotypes (figure 15). These data can also be used to measure petiole:leaf length ratio. The petiole:leaf ratio is similar in Col, *max1*, and *MAD/mad,max1* (1:1.9, 1:2.1, and 1:1.6 respectively) whereas the ratio in *mad,max1* (1:2.7) is significantly different. It is not clear whether this is due to the *mad* mutation or just a result of the smaller organ in *mad,max1* plants.

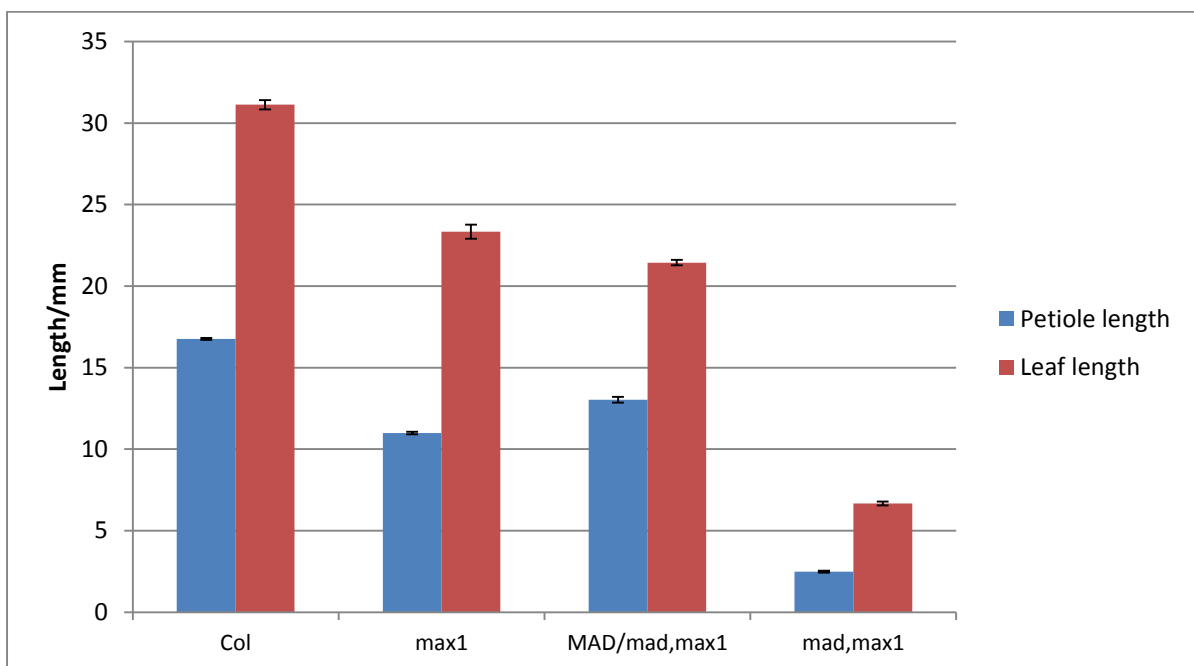


Figure 15. Leaf and petiole length measurements of the seventh rosette leaves of 6 week old plants.

Petiole:leaf ratios: Col 1:1.9 *max1* 1:2.1 *MAD/mad,max1* 1:1.6 and *mad,max1* (1:2.7).

Plants were grown under standard glasshouse conditions.

Error bars depict standard error N=30 ANOVA (leaf length) Col, *max1* sig. = 0.021. Col, *MAD/mad,max1* sig. = 0.014. Col, *mad,max1* sig. = <0.001. *max1*, *MAD/mad,max1* sig. = 0.048. *max*, *mad,max1* sig. = <0.001. *MAD/mad,max1*, *mad,max1* sig. = 0.012. ANOVA (petiole length) Col, *max1* sig. = 0.037. Col, *MAD/mad,max1* sig. = 0.041. Col, *mad,max1* sig. = <0.001. *max1*, *MAD/mad,max1* sig. = 0.084. *max*, *mad,max1* sig. = 0.009. *MAD/mad,max1*, *mad,max1* sig. = 0.007

The most prominent feature of *max1* is an increased rosette branching phenotype. When *max1* is in a wildtype background the average number of rosette branches produced is usually between

3 and 5 (figure 16). In a *MAD/mad* back ground however the branching level is reduced substantially to between 1 and 2 rosette branches. The branching level of *mad,max1* individuals is even lower with plants frequently not producing a single rosette branch. As with all other data the depleted vigour of *mad,max1* plants means that this result should be treated cautiously.

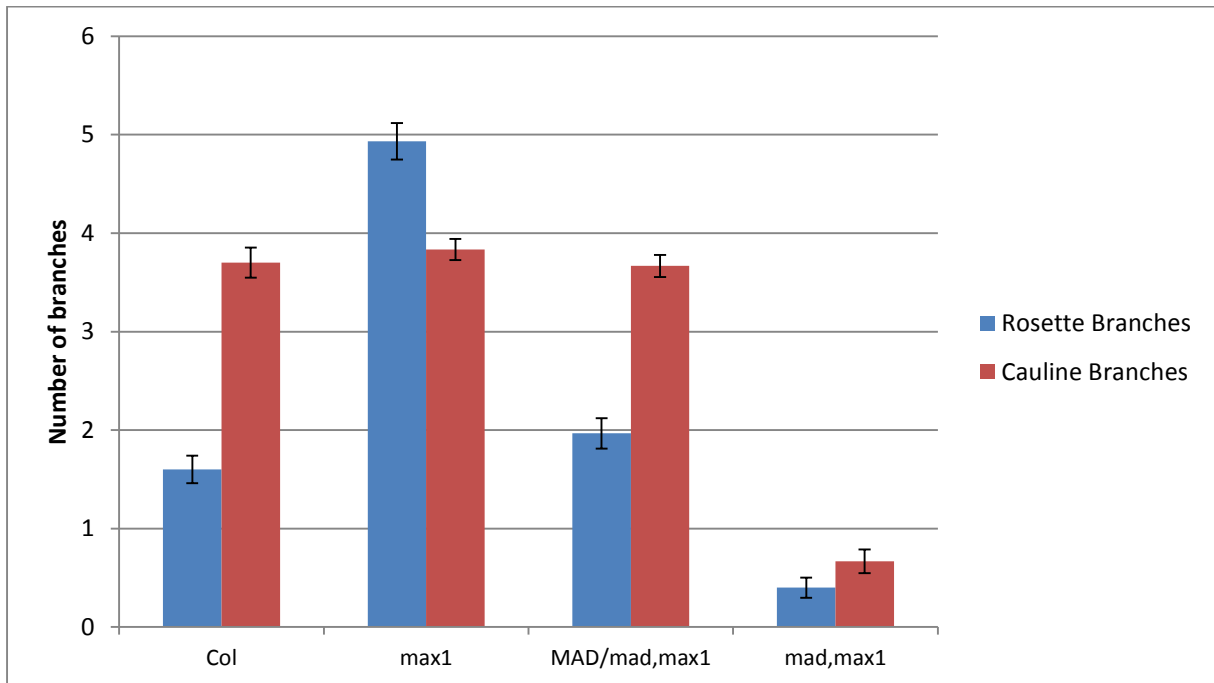


Figure 16. Number of rosette and cauline branches across Col, *max1*, *MAD/mad,max1* and *mad,max1*. A distinct drop in *max1* mediated branching levels can be seen when *max1* is in the *MAD/mad* genetic background. Branching levels in *mad,max1* are very low. The *mad,max1* homozygotes are extremely sickly plants which renders the results of this experiment rather less useful than if the plants were healthy.

Plants were grown under standard glasshouse conditions (pg 45) and measured at 6 weeks old.

Error bars depict standard error. N=30 ANOVA (rosette branches) Col, *max1* sig. = 0.009. Col, *MAD/mad,max1* sig. = 0.171. Col, *mad,max1* sig. = 0.047. *max1*, *MAD/mad,max1* sig. = 0.006. *max*, *mad,max1* sig. = <0.001. *MAD/mad,max1*, *mad,max1* sig. = 0.034. ANOVA (cauline branches) Col, *max1* sig. = 0.214. Col, *MAD/mad,max1* sig. = 0.576. Col, *mad,max1* sig. = 0.081. *max1*, *MAD/mad,max1* sig. = 0.662. *max*, *mad,max1* sig. = 0.041. *MAD/mad,max1*, *mad,max1* sig. = <0.027.

Removal of *max1* from the *MAD/mad* genetic background was essential to allow the effects of the *mad* mutation to be assessed independently of its interaction with the *max1* mutation. This was achieved by backcrossing *MAD/mad* to Col to segregate out the *max* mutation. Four

backcrosses were carried out, simultaneously removing most of the additional EMS-induced mutations that may be present.

The following experiments are replicas of the above but with *MAD/mad* and *mad* as the only mutations present without the *max1* mutation in the background. This allows a clearer analysis of the effects of the *mad* mutation. The results are shown in figure 17.

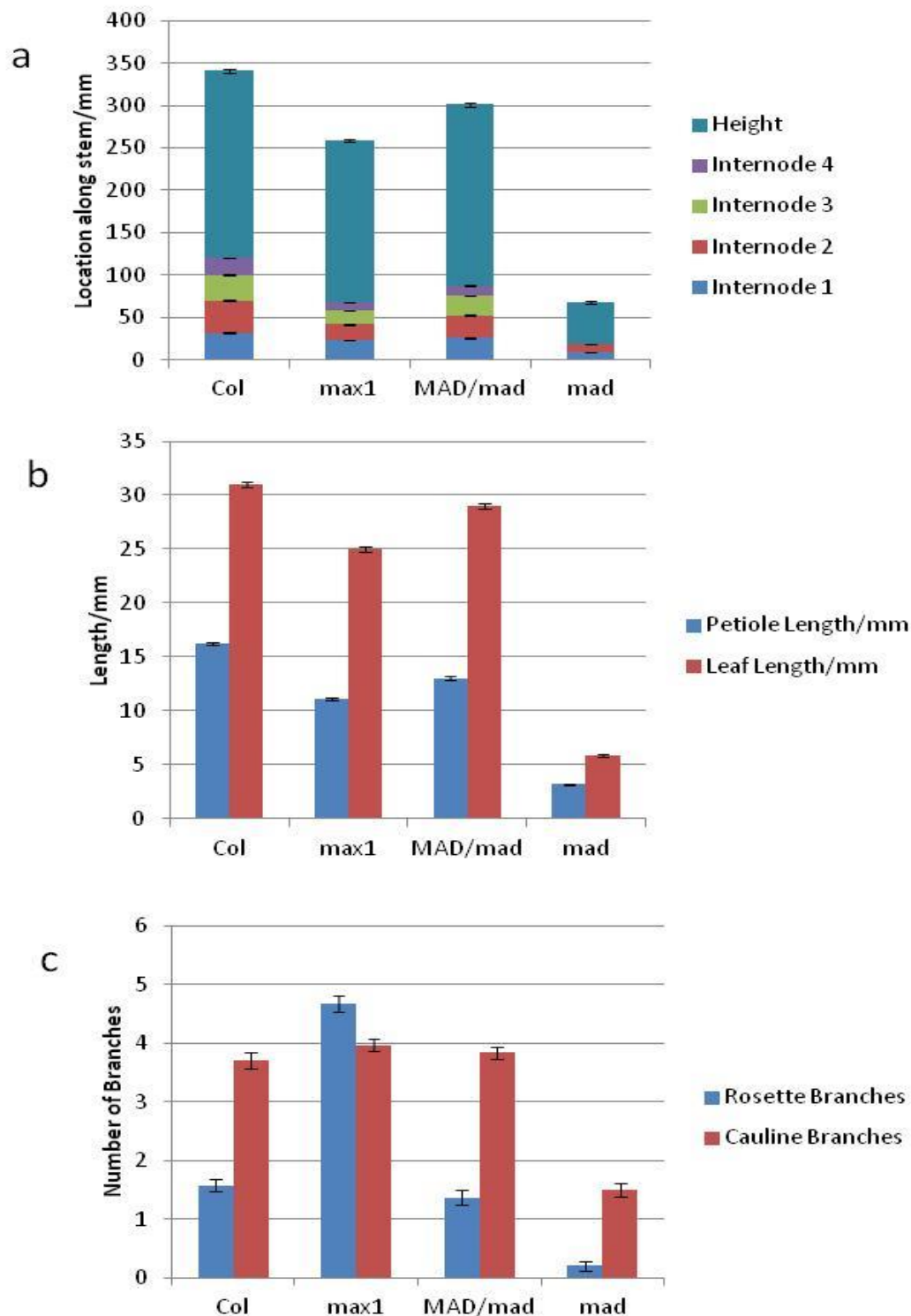


Figure 17. Previous page. Comparative morphological analysis of the *MAD/mad* and *mad* mutants.

a). Heights and internodal sections of Col, *max1*, *MAD/mad* and *mad*. *MAD/mad* is significantly taller than *max1* and internodes 2 and 3 are significantly longer than those of *max1*. Like *mad*, *max1* (figure 14), *mad* is extremely short, with no more than 2 internodes present on any of the plants assessed.

b). Leaf and Petiole lengths of Col, *max1*, *MAD/mad*, and *mad*. The short leaf length seen in *MAD/mad,max1* has been partially restored in *MAD/mad* although not to a wild type length. The *mad* leaf and petiole lengths are very much like those of *mad,max1*.

c). Branching patterns in Col, *max1*, *MAD/mad*, and *mad*. The number of cauline branches is not significantly different between Col, *max1*, and *MAD/mad*. The number is reduced in *mad* but this is most likely a result of the plant being shorter and weaker than the other genotypes. The number of rosette branches seen in *MAD/mad* is not dissimilar to a Col level of branching. This was not the case in the *MAD/mad,max1* mutant where branching levels were reduced but were still higher than wildtype. *mad* mutant plants only produce rosette branches occasionally.

Plants for each of the above experiments were grown under standard glasshouse conditions and measured at 6 weeks old.

Error bars depict standard error. N=30

ANOVA (a) (height) Col, *max1* sig. = 0.011. Col, *MAD/mad* sig. = 0.036. Col, *mad* sig. = <0.001. *max1*, *MAD/mad* sig. = 0.057. *max*, *mad* sig. = 0.006. *MAD/mad*, *mad* sig. = 0.004. ANOVA (b) (leaf length) Col, *max1* sig. = 0.033. Col, *MAD/mad* sig. = 0.047. Col, *mad* sig. = 0.017. *max1*, *MAD/mad* sig. = 0.092. *max*, *mad* sig. = 0.032. *MAD/mad*, *mad* sig. = 0.021. ANOVA (b) (petiole length) Col, *max1* sig. = 0.127. Col, *MAD/mad* sig. = 0.086. Col, *mad* sig. = 0.027. *max1*, *MAD/mad* sig. = 0.177. *max*, *mad* sig. = 0.032. *MAD/mad*, *mad* sig. = 0.018. ANOVA (c) (rosette branches) Col, *max1* sig. = 0.005. Col, *MAD/mad* sig. = 0.314. Col, *mad* sig. = 0.097. *max1*, *MAD/mad* sig. = 0.003. *max*, *mad* sig. = <0.001. *MAD/mad*, *mad* sig. = 0.084. ANOVA (c) (cauline branches) Col, *max1* sig. = 0.512. Col, *MAD/mad* sig. = 0.606. Col, *mad* sig. = 0.021. *max1*, *MAD/mad* sig. = 0.733. *max*, *mad* sig. = 0.018. *MAD/mad*, *mad* sig. = 0.023.

When *MAD/mad* had *max1* removed from its genetic background the phenotype was altered (figure 17 and table 4). Height was partially restored, although not to wildtype levels and there was a distinct increase in the length of the first three internodes. The leaf length also exhibits partial recovery and no longer has the characteristic rounded appearance of the *max1* leaves seen in *MAD/mad,max1* (data not shown).

Rosette branching in *MAD/mad* (1.37 rosette branches on average) is very similar to Col (1.58 rosette branches on average) and both are significantly lower than that of *MAD/mad,max1* (1.97 rosette branches on average). The number of cauline branches is similar across all of the genotypes excluding *mad,max1* and *mad*. The results for *mad* and *mad,max1* are interesting

but problematic as all morphological aspects of these plants will be strongly influenced by their weak nature.

	Genotype					
	Col	<i>max1</i>	<i>MAD/mad, max1</i>	<i>MAD/mad</i>	<i>mad,max1</i>	<i>mad</i>
Height/mm	340.9	259.8	262	301.4	64.6	67.4
Internode 1/mm	31.9	22.7	20.7	26.0	8.8	8.7
Internode 2/mm	39.2	17.2	22.7	26.8	11.3	10.0
Internode 3/mm	31.7	15.5	12.6	23.4	0	0
Internode 4/mm	19.2	11.3	13.7	11.3	0	0
Leaf Length/mm	31.1	24.2	21.4	29.0	6.7	5.9
Petiole Length/mm	16.5	11.1	13.0	13.0	2.5	3.2
Petiole:Leaf Ratio	1:1.88	1:2.18	1:1.65	1:2.23	1:2.68	1:1.84
Rosette Branches	1.58	4.80	1.97	1.37	0.40	0.20
Cauline Branches	3.70	3.90	3.67	3.83	0.67	1.5

Table 4. Comparative effects on plant physiology of the *mad* mutation both in the *max1* genetic background and in a wildtype genetic background.

Values are means taken from 40 samples of each genotype

3.2 The effect of the *mad* mutation in other genetic backgrounds

In order to see if the *mad* mutation was effective at reducing increased branching phenotypes in other branching mutants *MAD/mad* was crossed with the *max* mutants, including *max1* as a control, and *axr1-3*, another highly branched mutant. Once the double mutants had been generated they were grown under glasshouse conditions and had the number of rosette leaves counted at 6 weeks post-germination. The results are shown in figure 18. *MAD/mad* effectively

reduces branching levels in every genotype assessed in this way. The average number of rosette branches in Col is approximately 1.6 (table 4) so the restoration of branching levels is never quite to that of wildtype but is nonetheless very pronounced.

The fact that both the biosynthetic *max* mutants (*1*, *3*, and *4*) and *max2* have their branching levels reduced by *mad* suggest that *MAD* acts either downstream of *MAX2* action or by another route, independent of the *MAX* pathway.

These results suggest several things. *mad/MAD* suppresses only the *max1* branching phenotype, and none of the other *max1* effects, therefore it is not a general downstream mediator of strigolactone signalling. *mad/MAD* suppresses the branching phenotype of all the *max* mutants, therefore it does not simply allow activation of the signalling pathway in a strigolactone-independent way. *mad/MAD* also suppresses the branching phenotype of *axr1*. There is some debate about why *axr1* is branchy, but at least most of it is *MAX*-independent (Prusinkiewicz, P. *et.al.* (2009)). Probably it is due to over-production of auxin by buds making them stronger auxin sources. *mad* can apparently suppress this activation too.

It could be that *mad/MAD* has a general effect on bud activation. Arguing against this, it has no effect on branching in otherwise wild-type plants, although there is some proportionality in its effects, so maybe there are too few branches in wt to see modest suppression.

This can be investigated further by looking at physiology (ie hormone responses etc).

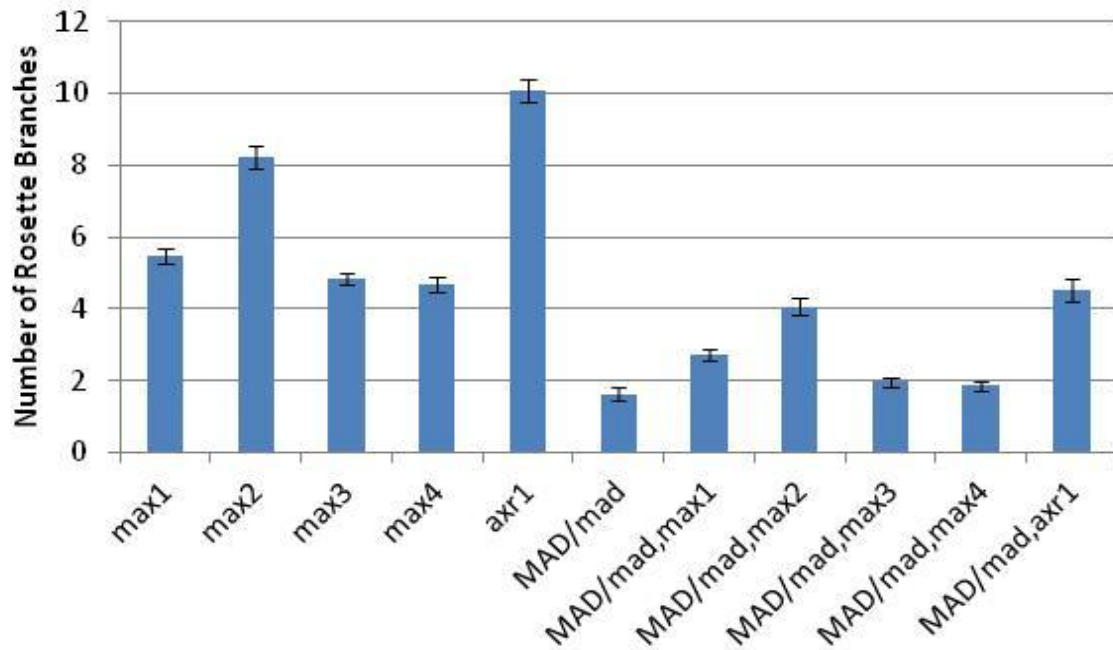


Figure 18. Rosette branching in the highly branched *axr1* and *max* mutants and in their corresponding *MAD/mad* double mutants. The *mad* genotype is sufficient to lower branching levels across all the genotypes tested.

Rosette branching was measured at 6 week post-germination.

Plants were grown under standard glasshouse conditions.

Error bars indicate standard error. N=30 Standard T-test. *max1*, *MAD/mad,max1* sig. = 0.011. *max2*, *MAD/mad,max2* sig. = 0.016. *max3*, *MAD/mad,max3* sig. = 0.032. *max4*, *MAD/mad,max4* sig. = 0.015. *axr1*, *MAD/mad,axr1* sig. = 0.007.

3.3 The *mad* leaf phenotype

Closer inspection of both rosette and cauline leaves of *mad,max1* plants revealed an interesting leaf phenotype which persisted when *mad* was crossed into a wildtype background. The leaves have a very uneven, undulating surface and a serrated edge (figure 19). Non-uniform light reflection, suggests uneven wax distribution across *mad* leaves. The adaxial and abaxial surfaces have different characteristic waxes in the cuticle, so patchy wax might reflect abaxial confusion.

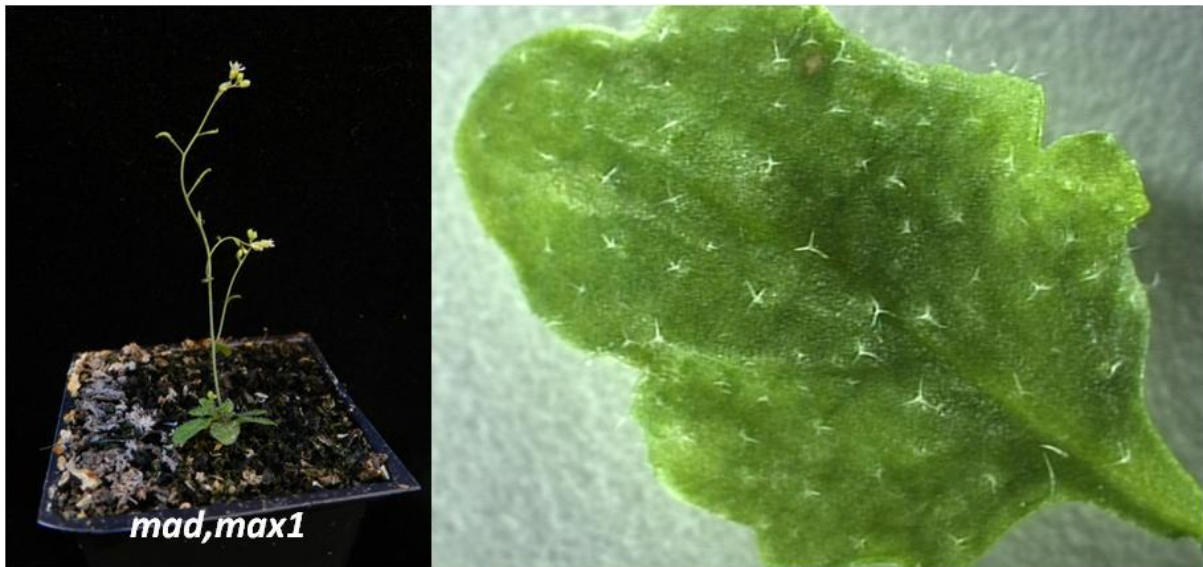


Figure 19. The *mad* leaf phenotype. Leaves exhibit an uneven surface, uneven wax distribution and do not have the smooth outline of a wildtype leaf, instead having a serrated edge. The whole plant image shows a 6 week old *mad,max1* plant, the image on the right shows a X10 magnification of a rosette leaf from a 28 day old *mad,max1* plant. It should be noted that although the images above show *mad,max1* plants the phenotype is still present in a wildtype background (ie. *mad/mad*) and is associated with the *mad* mutation. The phenotype is present in both rosette and cauline leaves but is far more prominent in the former.

Initial leaf preparations using the dehydration method detailed on pages 51-52 were imaged using Zeiss LSM510 META compact mounted on an Axiovert 200 inverted microscope. These images have not been shown as the quality was such that differentiating cell types was made difficult and damage to the delicate *mad* leaves worsened the problem. The solution was to use scanning electron microscopy to enable a more detailed view and minimise damage to the sample during preparation.

Scanning electron micrographs of Col, *MAD/mad*, and *mad* enabled the close structure analysis of leaf epidermal phenotypes. By comparing wildtype leaf epidermis to that of *MAD/mad* and *mad* plants it was possible to specify the effect of the *mad* mutation on the leaf epidermis which, in turn, gave some clue as to what was happening beneath the leaf surface. Features characteristic of the *mad* homozygote leaf phenotype (seen in figure 19) are not visible at low levels of magnification. *MAD/mad* leaves share the same smooth leaf outline and even surface as those of wildtype Arabidopsis. However, although *MAD/mad* leaves appear normal, without the more comprehensive view found at higher magnification, it is impossible to state that the *mad* mutation has no effect on leaf epidermal structure.

Both the adaxial (upper) and abaxial (lower) leaf surfaces have certain characteristics that, for the purpose of this experiment, serve as wildtype markers. The leaf epidermis of wildtype *Arabidopsis* plants is composed of interlocking pavement cells under a layer of waxy cuticle. Despite the irregular cell shape of pavement cells, the overall appearance of the leaf epidermis should appear ordered. Both stomata, with enclosing guard cells, and trichomes should be evenly spaced with the majority of stomata found on the abaxial surface and the majority of trichomes found on the adaxial surface. A morphologically normal *Arabidopsis* trichome has three branches and arises from an ordinary epidermal cell. The trichome precursor cell undergoes a switch from ordinary mitosis to endoreduplication. This results in an increase in ploidy. The first branching event occurs in alignment with the proximodistal axis of the leaf, the second branching event produces a trichome which is asymmetrical with respect to the leaf axis. These events control the orientation of trichomes such that all trichomes should have the same orientation (figure 22).

A detailed assessment of the leaf epidermis comprises data on the three aspects of leaf morphology mentioned above; pavement cell appearance, distribution of stomata, and the morphology, orientation, and distribution of trichomes.

Scanning electron micrograph images of the leaf epidermis of Col, *MAD/mad*, and *mad* plants have allowed comparative analysis of the *mad* phenotype on a cellular level. The wildtype standards for the leaf features mentioned above are exemplified by the Col leaf phenotype. The adaxial surface of Col rosette leaves has an ordered system of pavement cells with morphologically normal, well spaced trichomes (figure 20) which are greater in number on the adaxial leaf surface compared to the abaxial leaf surface. The opposite is true for stomata which are found in far greater number on the abaxial surface. Those found on the adaxial leaf surface of Col plants are well spaced. The appearance of *MAD/mad* adaxial epidermis does not have any significant physical differences from that of Col. The pavement cells are similarly well ordered but occasionally encroach upon the mid-vein, a trait which was not noted in any of the Col samples assessed. Both trichomes and stomata were morphologically normal and well spaced with both features found at the correct comparative density when compared to the abaxial surface. These results support the hypothesis that the leaf phenotype conferred by the *mad* mutation is not present in the *MAD/mad* heterozygote suggesting that the effects of the *mad* mutation are not dose dependent and require the homozygote *mad/mad* genetic background to be realised. The effect of *mad* is present in all three of the leaf features assessed in this comparative analysis study. The epidermal pavement cells have a distinctly disordered

appearance compared the other genotypes studied. Area of smaller pavement cells occasionally form clusters, as do area of larger cells (the increased cell size may suggest increased ploidy. This is limited because, although there is a relationship between cell size and endoreduplication, it is possible for small cells to have undergone endoreduplication and for large cells not to (Sugimoto-Shirasu, K. and Roberts, K. (2003))). This arrangement of cells was not noted in other genotypes where cells have a more uniform organisation. Another notable feature is the occasional clustering of trichomes and stomata, it is tempting to suggest that these clusters of stomata, found here in numbers more consistent with that of the lower leaf surface, are areas of abaxialised cells. An overabundance of adaxial stomata is a characteristic feature of *mad* leaves, being found on all leaves assessed. Far from being uniform in appearance and alignment as in Col and *MAD/mad*, *mad* trichomes have no particular directional orientation and are frequently found with the incorrect number of branches. A significant proportion of the trichomes assessed had fewer than three branches, suggesting that the process of trichome development had not been completed, however, some examples were found with four branches so it is probably not as simple as a failure to complete the developmental process.

As with the adaxial leaf epidermis, the wildtype arrangement of pavement cells on the abaxial leaf surface is one of an evenly distributed combination of larger and smaller interlocking cells, with no clusters of larger cells (figure 21). The trichomes found on Col abaxial leaf surfaces were all morphologically normal and asymmetrically aligned with the leaf proximodistal axis. Abaxial stomata were found in much larger numbers than on the adaxial epidermis and were evenly distributed across the leaf surface. The abaxial epidermis of *MAD/mad* leaves was found to be indistinguishable from that of Col with each of the three leaf features studied; pavement cells, trichomes, and stomata, impossible to differentiate from those of Col. This observation, combined with the wildtype appearance of the *MAD/mad* adaxial leaf epidermis, suggests that one copy of *mad* is not sufficient to produce a visible phenotype in the leaf. The fact that the abaxial leaf epidermis of *mad* plants is severely affected comes as no surprise following the results on the adaxial surface given above. Most striking is the number of trichomes, both morphologically normal and otherwise, found on the abaxial leaf surface. A predominantly adaxial feature found in such abundance on an abaxial surface again supports the theory that a polarity defect has partially adaxialised the lower leaf surfaces. Abaxial stomata are, like their adaxial counterparts, found in clusters and, along with trichomes, are also found over the leaf mid-vein, something not noted in the other genotypes.

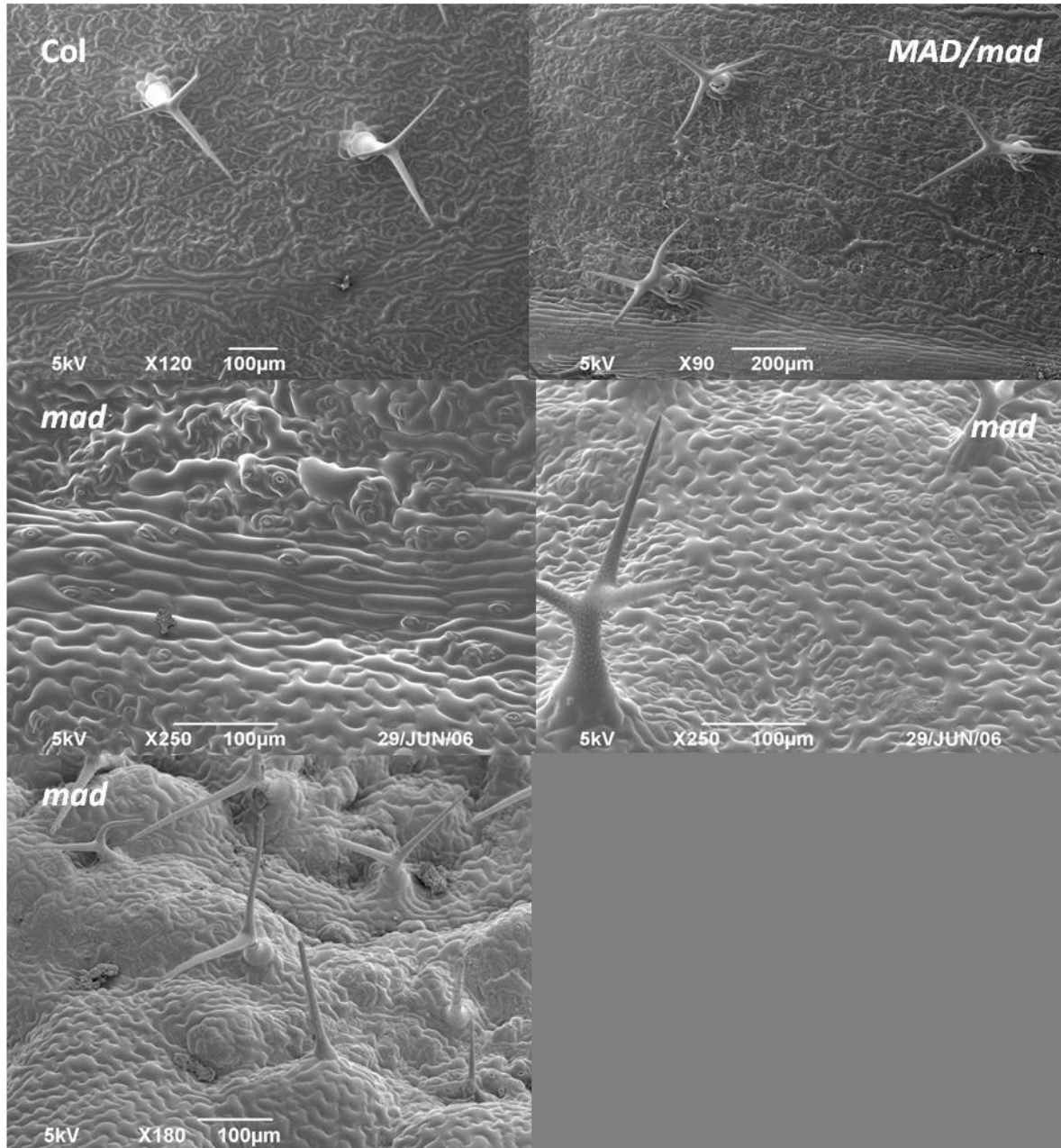


Figure 20. Adaxial rosette leaf surfaces of *Col*, *MAD/mad*, and *mad* plants. The *Col* leaf epidermis is ordered in appearance with regularly spaced stomata and trichomes. All *Col* trichomes had three branches. The *MAD/mad* adaxial epidermis is very similar to that of *Col*. Pavement cells are organised but occasionally encroach upon the mid-vein. The adaxial epidermis of *mad* is comparatively very disorganised: stomata and trichomes are clustered; stomata are too abundant; trichomes do not always have the correct number of branches and are not always in the correct orientation and; the transition of cell types from the midvein to the ordinary epidermis is disrupted.

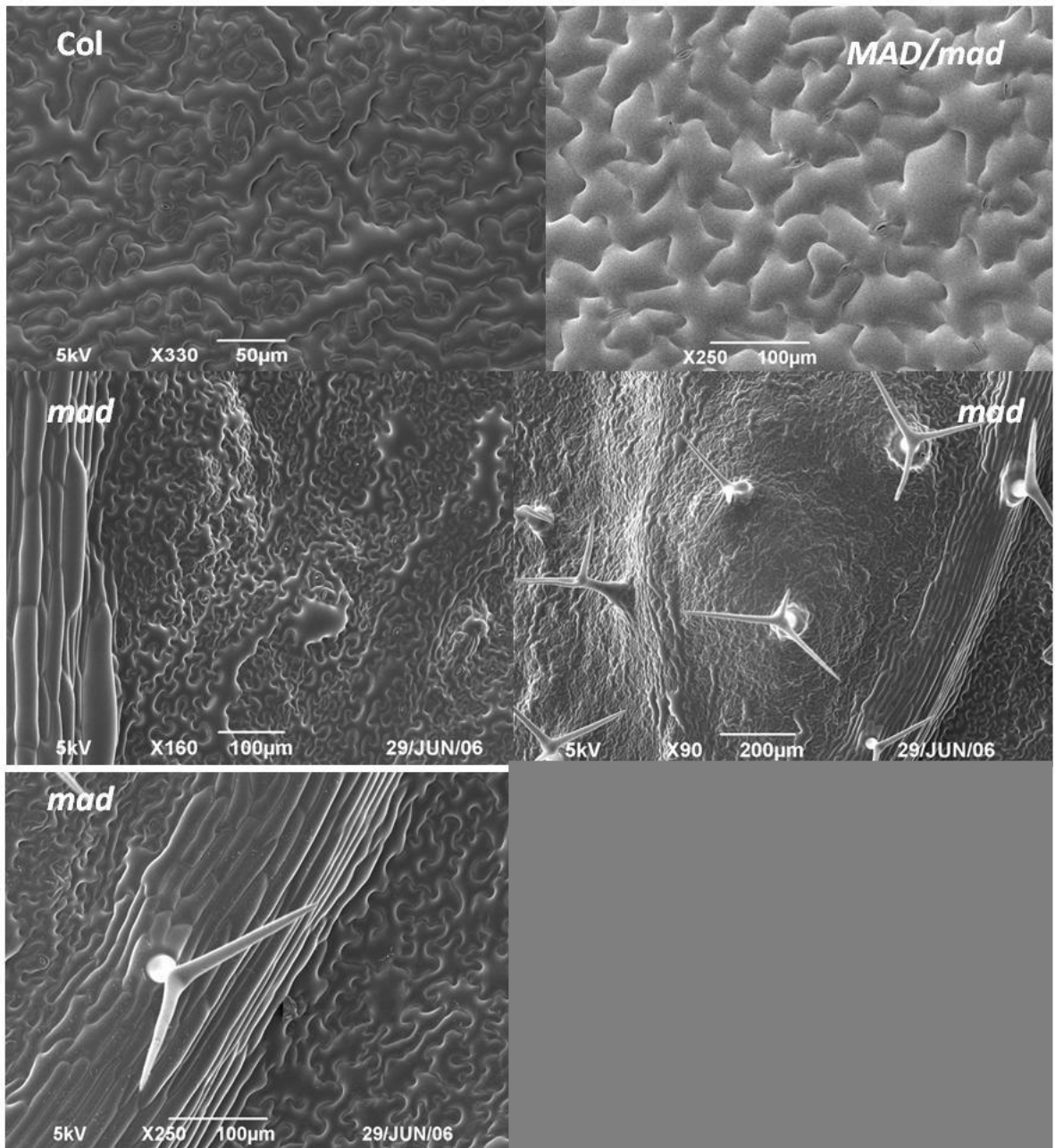
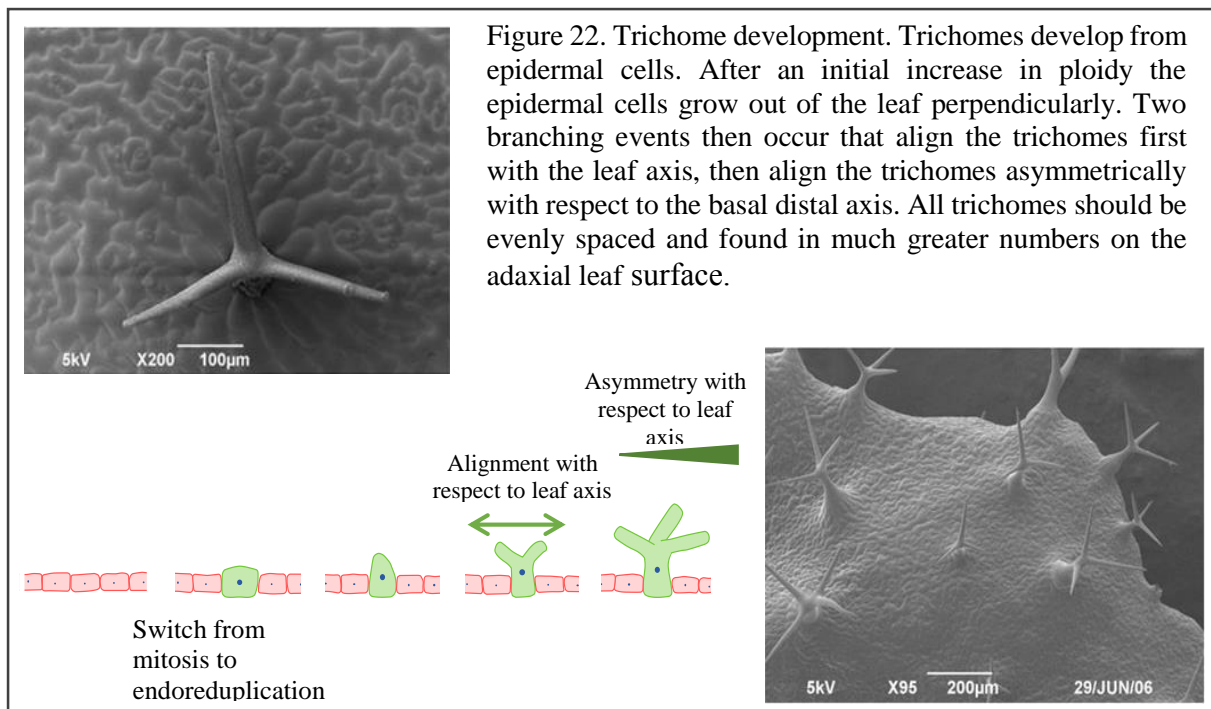


Figure 21. Abaxial rosette leaf surfaces of *Col*, *MAD/mad*, and *mad* plants. The *Col* abaxial epidermis has an organised appearance with regularly spaced stomata. Very few trichomes are found on *Col* abaxial leaf surfaces but those that are present are regularly spaced and morphologically normal. *MAD/mad* abaxial epidermal organisation is indistinguishable from that of *Col*. Abaxial leaf surfaces of *mad* plants have many more trichomes compared to *Col* and *MAD/mad* and, as with the adaxial surfaces, trichomes and stomata tend to be found in clusters. Some of the trichomes also exhibit morphological abnormalities.



Whilst the above data certainly suggest that a polarity defect may be behind the mad leaf appearance it relies purely on the appearance and placement of surface features. Other cell types within the leaf which are associated with either an adaxial or abaxial identity are the palisade and spongy mesophyll respectively (figure 10). SEM cross sections of *Col*, *MAD/mad*, and *mad* leaves were used for visual comparison (figure 23). Both *Col* and *MAD/mad* cross sections exhibit distinct adaxial palisade layers with an abaxial spongy mesophyll layer. The *mad* cross sections are more variable. In over half of the sample sections viewed an adaxial palisade layer was distinguishable. Morphological abnormalities were present in some of the palisade cells giving them a more amorphous shape as opposed to the more regular block shape seen in *Col* and *MAD/mad*. In some sections of *mad* leaves there was no apparent palisade layer, either adaxially or abaxially. This could be because the regular shape of the palisade cells had become even more amorphous than seen in other *mad* cross sections, or that the palisade layer is absent. The latter would suggest abaxialisation of particular leaf sections. No sections were found in which palisade cells were found abaxially and, since the observed polarity defect in the epidermis affects both surfaces, it would seem like the former suggestion of abnormal palisade cells is the most likely.

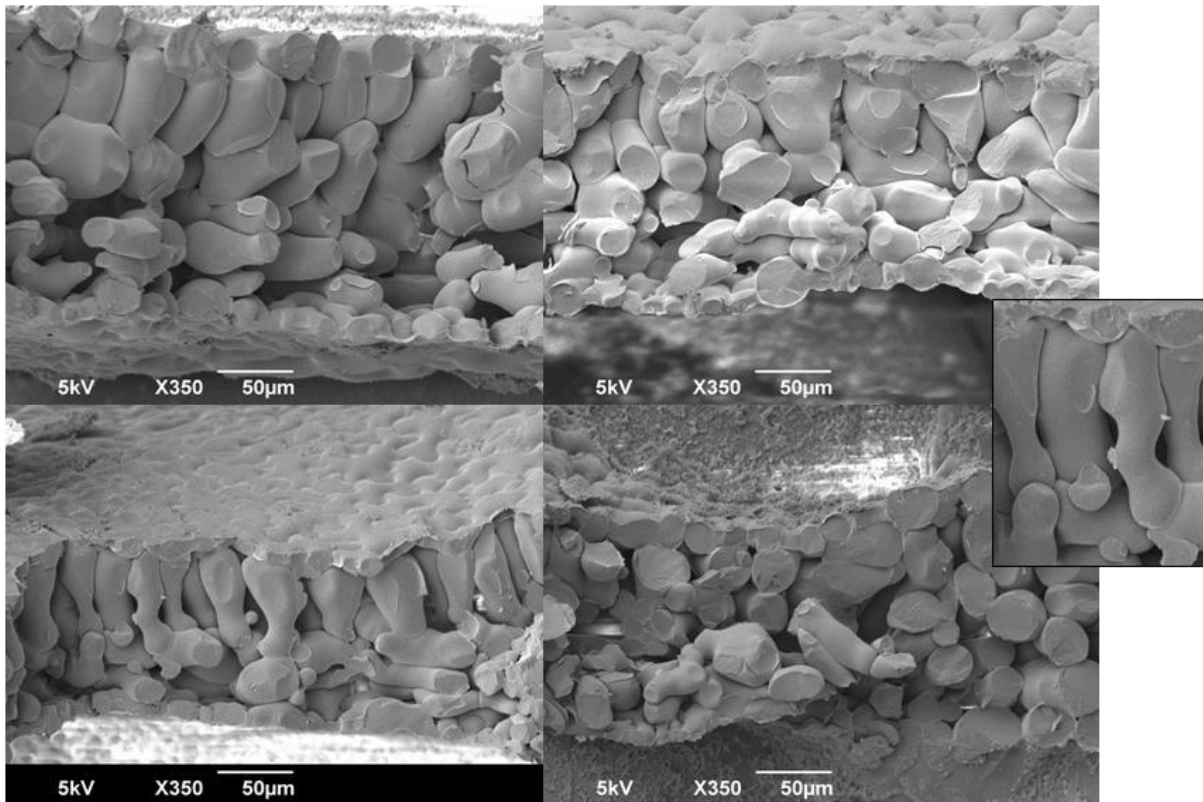


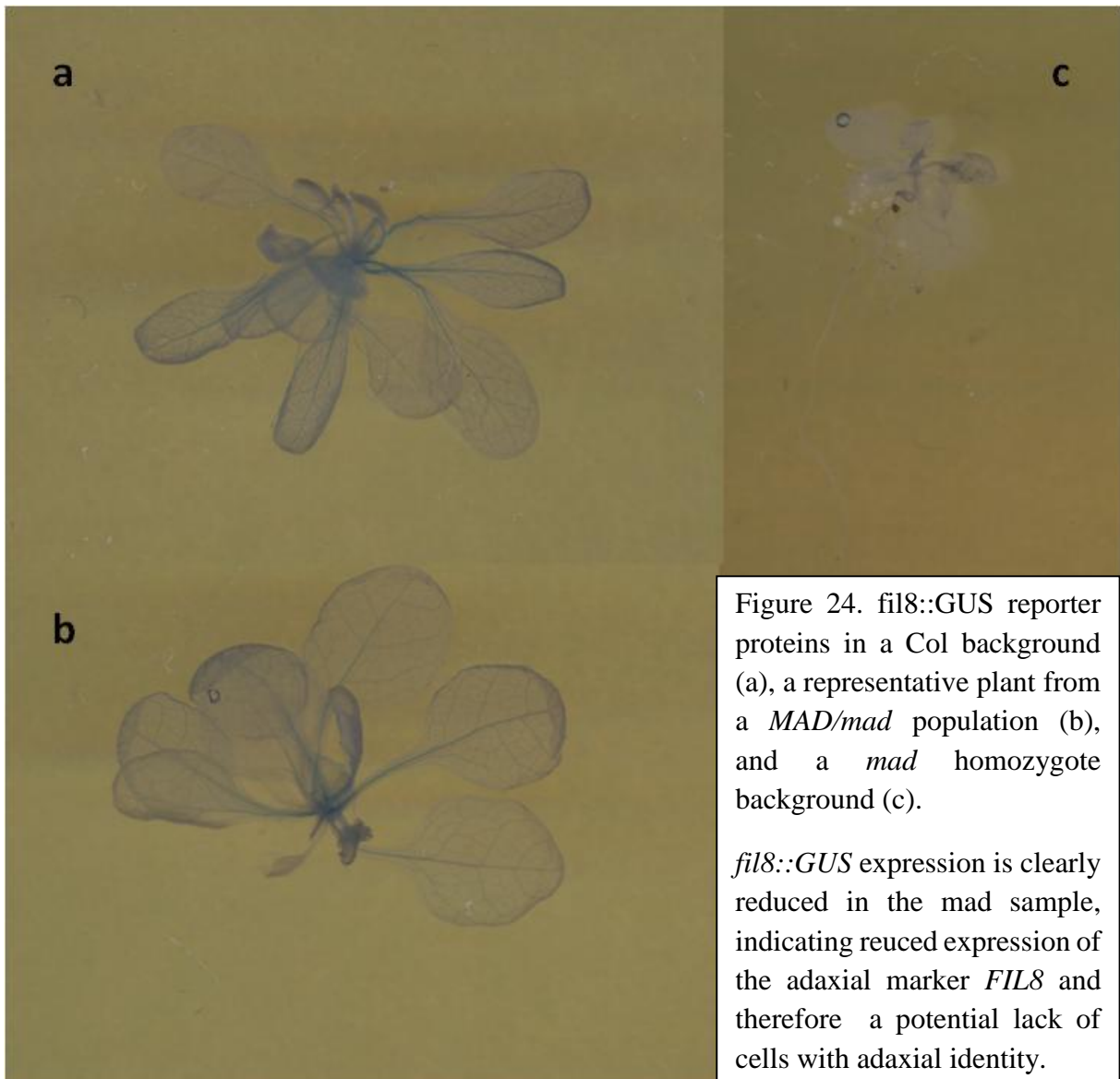
Figure 23. Cross sections of rosette leaves. Clockwise from top left: Col, *MAD/mad*, *mad*, *mad*. Both Col and *MAD/mad* exhibit normal leaf morphology with distinct layers of palisade and mesophyll cells. The majority of *mad* leaves visually assessed in this way exhibited no distinct layer of palisade cells

mad palisade cells are frequently morphologically abnormal (see inset).

In an attempt to clarify whether or not the morphological abnormalities seen in *mad* leaves are in fact a result of a polarity defect *MAD/mad*, and Col were crossed with the abaxial marker construct *fil8::GUS*. If GUS expression was lower than that seen in wildtype plants it may suggest that genes necessary for abaxial identity are not being expressed at the correct level. The Col,*fil8::GUS*, *MAD/mad,fil8::GUS*, and *mad,fil8::GUS* plants were grown anexically on ATS media and at 12 days post-germination they underwent the GUS staining procedure in the materials and methods section. The results can be seen in figure 24. It should be noted that, because plants were stained at the rosette stage in this experiment it was impossible to differentiate *MAD/mad* heterozygotes and wildtype segregants. The staining in the plants of the *MAD/mad* population was uniform and no visible difference between any of the plants was present. It was therefore concluded that staining levels in *MAD/mad* and Col were essentially the same. The level of GUS expression in *mad* does seem to be lower than in Col and

MAD/mad. The degree of the reduction cannot be gauged as this is only a qualitative analysis. The results below suggest lower than normal expression of *fil8*. As *fil8* is expressed abaxially this suggests partial abaxialisation of *mad* leaves.

Experiments were carried out using *rev9::GUS* but the stain did not take well and GUS expression was not detectable.



3.4 Fertility in *MAD/mad* and *mad*

Germination rates of *mad* genotype seeds are apparently lower than those of wildtype plants. To follow up this initial observation, seeds of the Col, *MAD/mad*, and *mad* genotypes were grown under standard conditions (see page 45), and the germination rate of each measured. 400 seeds of each genotype were sown and, at the end of a 21 day period, germinated plant numbers were counted. These numbers were converted to percentages and can be seen in figure 25. Of 400 seeds sown for each genotype, 397 Col seeds, 356, *MAD/mad* seeds, and 197 *mad* seeds germinated. At 49.3%, the germination rate of *mad* seeds is considerably lower than that of the other genotypes assessed. All seeds assessed in this way were collected at the same time and store for the same time before use. What was initially less obvious was the, much smaller, but still marked reduction in fertility seen in *MAD/mad* (89% compared to 99.3% Col germination). Seeds (stored dry for 6 months) to the weight of 0.2g of each of the Col, *max1*, *MAD/mad* and *mad* genotypes were counted to ascertain the number of seeds in 0.2g and, from there, the approximate seed weight. All seed was of the same age. The idea behind this was that lighter seeds may indicate a defect in seed development that could contribute to germination differences. The number of seeds of each genotype in 0.2g are as follows; Col: 11308 seeds, *max1*: 11648, *MAD/mad*: 12028, *mad*: 11924. These numbers are all very similar and differences in seed weight negligible.

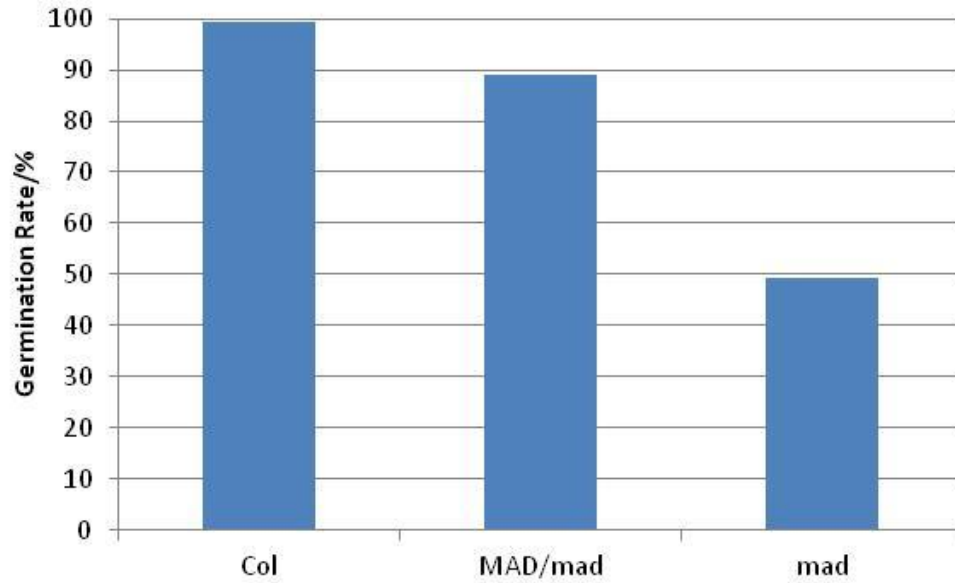


Figure 25. Germination rates of Col, *MAD/mad*, and *mad*. Germination rate stands at 99.25% for Col, 89% for *MAD/mad* and 49.25% for *mad*.

Seeds were sown at a density of 1 seed per p40 pot and 10 trays of each were measured.

Plants were soil grown under standard glasshouse conditions.

Germination rates were assessed at 21 days from the time of sowing.

Polarity defects are rarely limited to one organ, for example, in the case of *filamentous flower* and *crabsclaw* polarity defects are also present in the floral organs as well as the leaves (Siegfried, K.R. *et al.* (1999)) (Kerstetter, R.A. *et al.* (2001)). The possibility that the postulated polarity defect in *mad* leaves discussed above may also affect the floral organs and therefore have an eventual bearing on seed development in *mad*, and to a lesser extent *MAD/mad*, was investigated using SEM imaging of the floral organs.

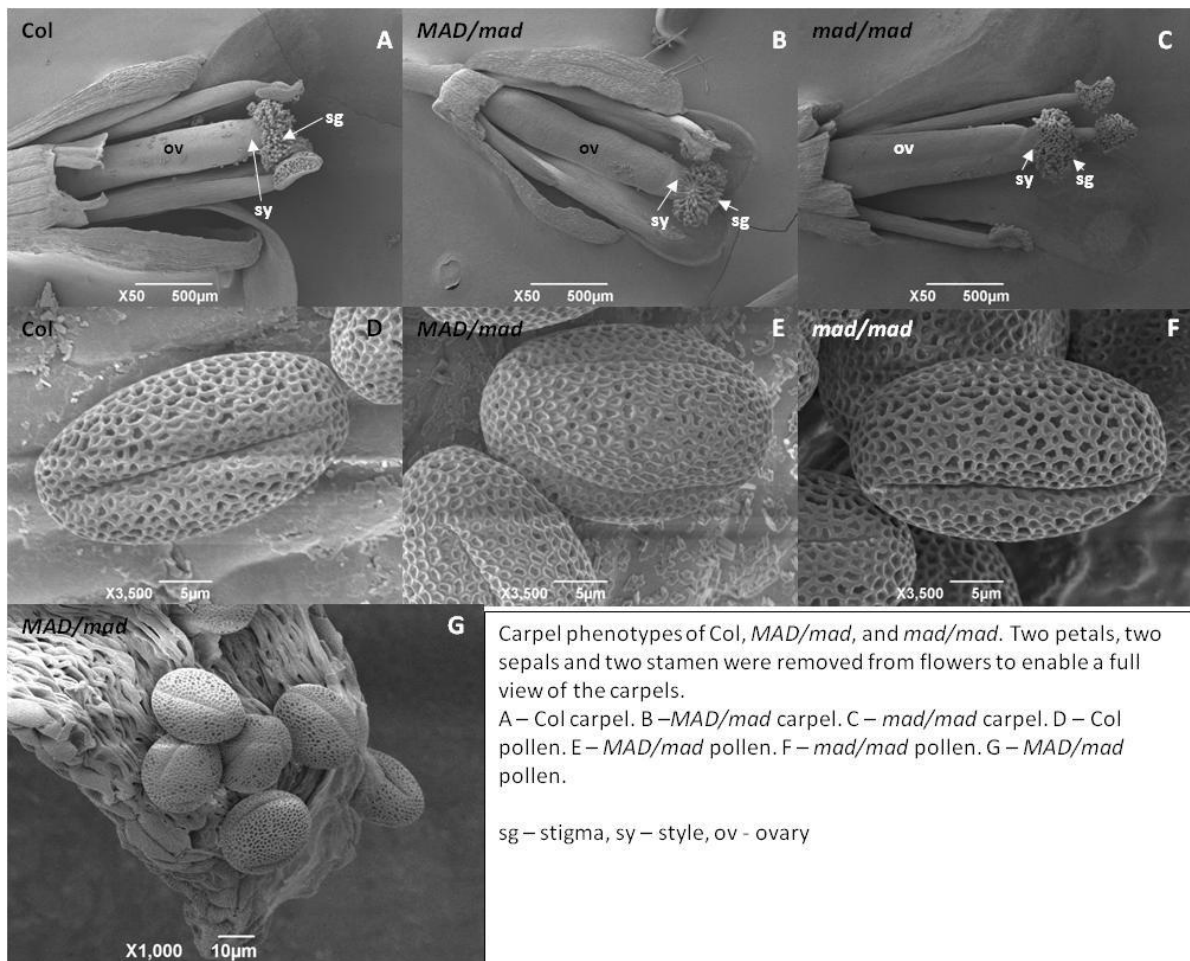


Figure 26. Carpel and pollen phenotypes of Col, *MAD/mad* and *mad*. There are no morphological differences between Col and *MAD/mad* samples and *mad*, suggesting that the potential partial abaxialisation of *mad* leaves is not present in the floral organs.

Figure 26 shows SEM images of Col, *MAD/mad* and *mad* floral organs. No physical differences are apparent between the three genotypes assessed. In all three examples the carpels are properly fused and appear morphologically normal. There is no evidence of a polarity defect in *MAD/mad* or *mad/mad* floral organs.

3.5 Auxin Status of *MAD/mad*

Auxin transport assays accurately measure the levels of auxin flux through a stem section. The protocol for this procedure is detailed on page 49. This assay was used to compare the levels of polar auxin transport in Col, *max1*, and *max1,MAD/mad* plants. Unfortunately *mad* plants are too small for use in this, or the following, experiment. As *max1,MAD/mad* is not reliably distinguishable from Col, especially at an early stage of development, stem segments were

taken above the first node (the same was done for all genotypes). The remainder of the plants were allowed to grow, seed was collected and sown to check for the presence of the *mad* homozygote and thereby confirm the genotype. Stem segments remained frozen during this time so only *max1, MAD/mad* was selected for the assay. The increased level of auxin transport in *max1* is well documented (Bennett, T. *et al* (2006)). The assay results for *MAD/mad* show a level of auxin transport that is not significantly different to that of *max1* (figure 27). This suggests that *MAD/mad* does not inhibit bud outgrowth in *max1* by decreasing auxin transport.

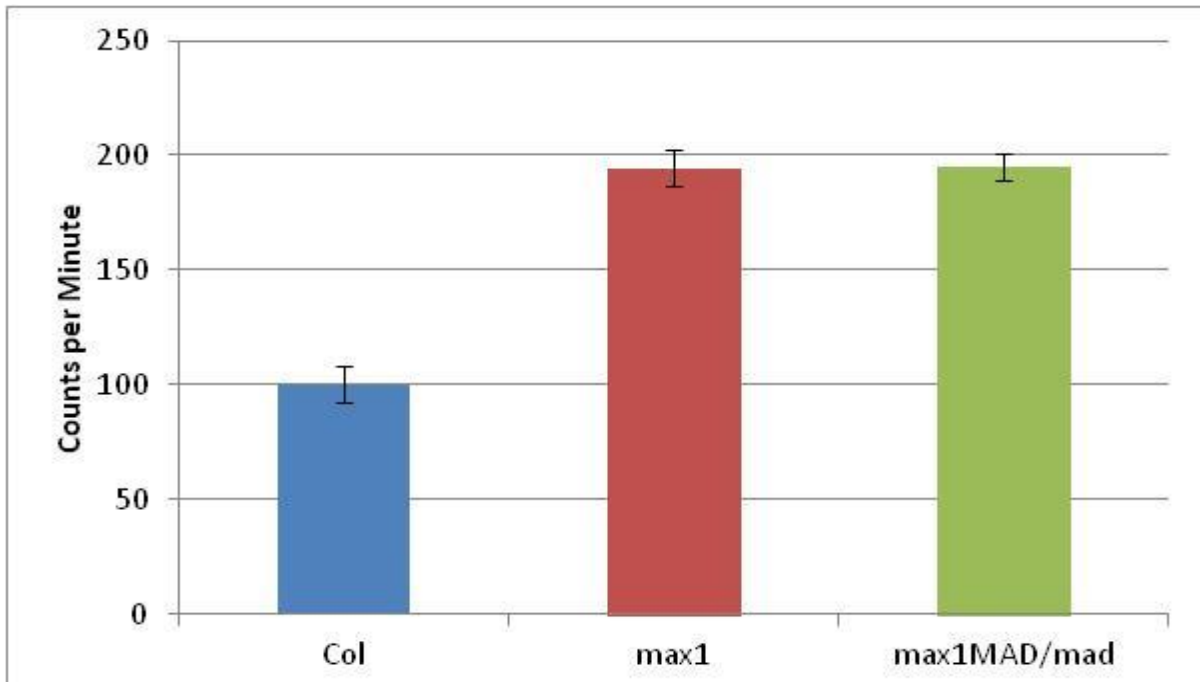


Figure 27. Auxin transport in Col, *max1*, and *max1MAD/mad*. Wildtype auxin transport is significantly lower than that of both *max1* and *max1MAD/mad*. There is no significant difference between auxin transport in *max1* and *max1MAD/mad* which both display elevated levels compared to wildtype.

Stem segments were taken from glasshouse grown, 6 week old plants. 30 plants of each were used for each experiment with 3 replicates completed.

Error bars indicate standard error. ANOVA Col, *max1* sig. = 0.017. Col, *MAD/mad, max1* sig. = 0.020. *MAD/mad, max1, max1* sig. = 0.272.

In order to further investigate the similarity in auxin transport between *max1* and *max1MAD/mad* a RT-PCR experiment was carried out (method detailed on page 55) to assess the expression levels of the auxin efflux gene *PIN1* in *max1MAD/mad*. The higher levels of *PIN1* expression in *max1* contribute directly to the increased auxin transport seen in *max1*. *PIN1* expression in *MAD/mad* was not qualitatively different from that of *max1* in a preliminary

experiment (data not available). They were both noticeably higher than Col. These results are not surprising as increased amounts of PIN1 protein would facilitate the increased auxin transport levels seen for both *max1* and *max1MAD/mad* in figure 27. These results could be further confirmed with a *PIN1::GFP*, *MAD/mad* double mutant undergoing confocal analysis to visualise the level of PIN1 protein localised at the basal cell membranes in the plant vascular-associated cells.

The responsiveness of buds to the presence of exogenous auxin has a large impact on the overall aerial morphology of the entire plant. Using the split plate assay (see pg.50) auxin moving in the stem has been demonstrated to have a strong inhibitory effect on bud outgrowth. This auxin-mediated repression of bud outgrowth is attenuated in the *max* mutants. The split plate assay was applied to *max1MAD/mad* mutants, along with Col and *max1* as controls. The results indicate that the *max1MAD/mad* genotype has a bud auxin response that is more similar to that of Col than that of *max1* (figure 28). Indeed, up to the 144hr/6 day mark the Col and *max1MAD/mad* bud growth trajectories are almost identical. The deviation of *max1MAD/mad* from Col seen after 144hr was noted in each of the four separate assays carried out and suggests that this late onset low level of resistance to auxin is a feature of *max1MAD/mad* auxin response. The last point notwithstanding, *max1MAD/mad* plants do not exhibit auxin resistance to anything like the degree seen in *max1*. The disparity in bud outgrowth between *max1MAD/mad* and *max1* implies that the ability of *MAD/mad* to lower *max1* branching levels lies in the restoration of sensitivity to *max1* buds by an auxin transport-independent mechanism.

To ensure that only *max1MAD/mad* plants were measured only sections including the second node were used. The remainder was allowed to grow, transferred to soil and seed collected to check genotype using the same method mentioned above.

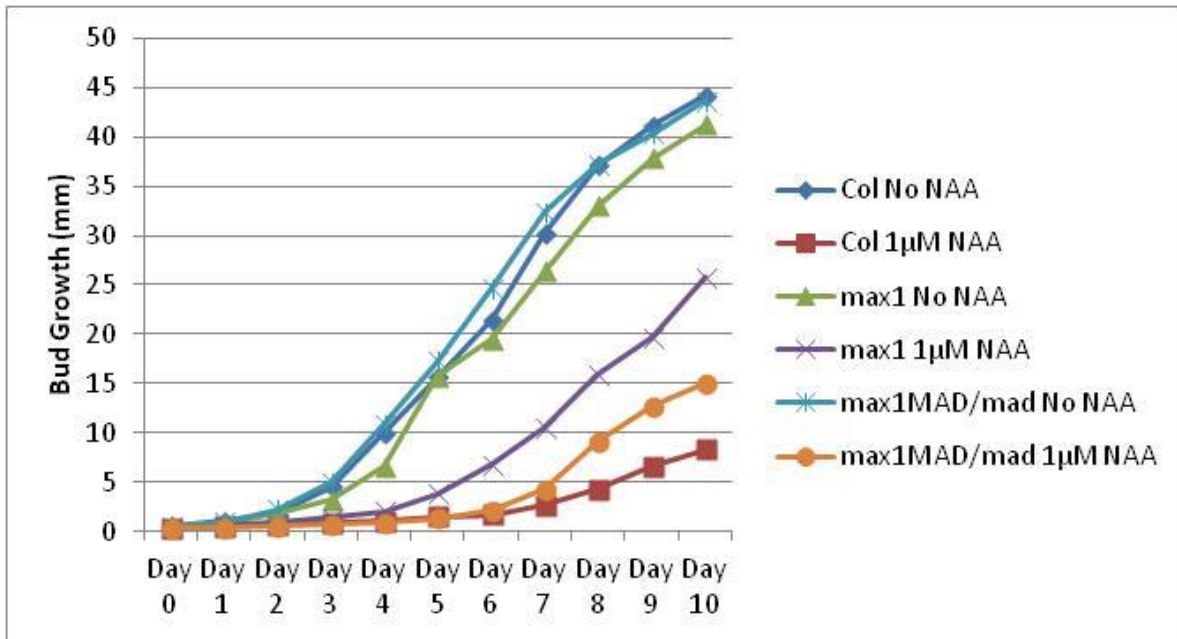


Figure 28. Bud auxin response in *Col*, *max1*, and *max1MAD/mad*. All three genotypes exhibit a similar growth curve in the absence of apically applied auxin. When a simulated apex is added, in the form of 1µM of the synthetic auxin NAA, bud outgrowth levels drop severely in *Col*. The response in both *max1MAD/mad* is less pronounced than in *max1* but is not as extreme as in *Col*.

Plants used were grown anexically in weck jars under standard growth room conditions. Stem segments were transferred to split plates when the plants had produced between one and two buds.

Approximately 30 plants of each genotype were used for each experiment, of which there were 3 replicates. The results shown above are pooled from the 3 replicates.

3.6 The effect of crowding on the *MAD/mad* mutant phenotype

Growing plants in higher densities places them under certain stresses. Competition for resources is heightened and this affects plant growth. When faced with these conditions, it is of vital importance to maximise intake of nutrients and access to sunlight. Access to sunlight when in crowded conditions is monopolised by taller plants. The response of plants that are below the 'canopy layer' is to allocate more of its resources to growth to achieve maximum height. This is characteristic of the shade avoidance response which is triggered by red:far red ratio and includes stem elongation (Casal, J. (2013), Pierik, R and de Wit, M. (2014)). This is not the same as phototropism, which is triggered by blue light and is just about growth toward a light source. This results in tall plants with few secondary branches, typical of the shade avoidance response which occurs when the light perceived by a plant has a low ratio of red to far red light (caused by light passing through chlorophyll rich leaves of nearby plants) (Casal, J. (2013), Pierik, R and de Wit, M. (2014)). Access to light is, of course, not the only important factor influencing plant physiology in crowded conditions. As well as having to forego growth of secondary, less vital, aerial features, plants must also make a heavier investment in root growth. Low levels of nutrients in the soil make it necessary to increase root:soil contact. This is manifested in a distinct change in shoot to root ratio with lowering levels of nutrients resulting in more biomass being allocated to root growth (Postma, J.A. *et al* (2014)). Previous experimentation has shown *max1* to have a slight resistance to this change. The *BRANCHED1* (*BRC1*) gene in *Arabidopsis* promotes bud dormancy in response to shade (González-Grandío, E. *et al.* (2013)) allowing vertical growth to predominate. These responses have a measurable effect on shoot and root architecture with crowding conditions favouring the simplification of the former and increased complexity of the latter. The experiments described in this section investigate the shift in shoot to root biomass seen at different levels of crowding and nitrate availability in Col, *max1* and *MAD/mad* genotypes as well as investigating the effects that these conditions confer upon shoot and root architecture. The resistance demonstrated by *max1* is an interesting feature which may confer a disadvantage when grown in competition with another *Arabidopsis* genotype. To test this hypothesis, in addition to the monoculture experiments outlined above, Col, *max1* and Col,*MAD/mad* polycultures were also analysed to see if such a disadvantage is evident.

Plants for this experiment were grown on the NO₃⁻ limiting mix of 50% vermiculite sand and 50% Terragreen supplemented with either 9mM or 1.8mM NO₃⁻. Adding the sufficient and

limiting NO₃⁻ treatment to the experiment highlighted whether or not there was a nutrient independent component to the results seen in the basic crowding experiment, ie. Higher plant density with adequate NO₃⁻ present. The combination of genotype, NO₃⁻ treatment and density are detailed in table 3. All measurements were taken at 7 weeks. For the *MAD/mad* plants it is necessary to check the genotype as it cannot be accurately determined visually. Once measurements were taken the plants were dried. Seeds were then taken from putative *MAD/mad* plants and sown to check for the presence of the *mad* homozygote. As all plants were logged individually it was possible to eliminate any *MAD/MAD* plants from the *MAD/mad* data pool. The experiment was carried out using three separate blocks of plants providing three replicates.

		Low Density (2 per p40)		Medium Density (4 per p40)		High Density (16 per p40)	
		9mM Nitrate	1.8mM Nitrate	9mM Nitrate	1.8mM Nitrate	9mM Nitrate	1.8mM Nitrate
Genotype	Col	Col	Col	Col	Col	Col	Col
	<i>max1</i>	<i>max1</i>	<i>max1</i>	<i>max1</i>	<i>max1</i>	<i>max1</i>	<i>max1</i>
	<i>MAD/mad</i>	<i>MAD/mad</i>	<i>MAD/mad</i>	<i>MAD/mad</i>	<i>MAD/mad</i>	<i>MAD/mad</i>	<i>MAD/mad</i>
	Col + <i>max1</i>	Col + <i>max1</i>	Col + <i>max1</i>	Col + <i>max1</i>	Col + <i>max1</i>	Col + <i>max1</i>	Col + <i>max1</i>
	Col + <i>MAD/mad</i>	Col + <i>MAD/mad</i>	Col + <i>MAD/mad</i>	Col + <i>MAD/mad</i>	Col + <i>MAD/mad</i>	Col + <i>MAD/mad</i>	Col + <i>MAD/mad</i>

Table 5. Treatments applied to each genotype/ genotype combination in the investigation into the effects of crowding in *Arabidopsis*.

Polycultures are designated as genotype+genotype. For example, Col and *max1* grown in the same culture is referred to as Col +*max1*

Shoot:Root ratio (fresh weight)

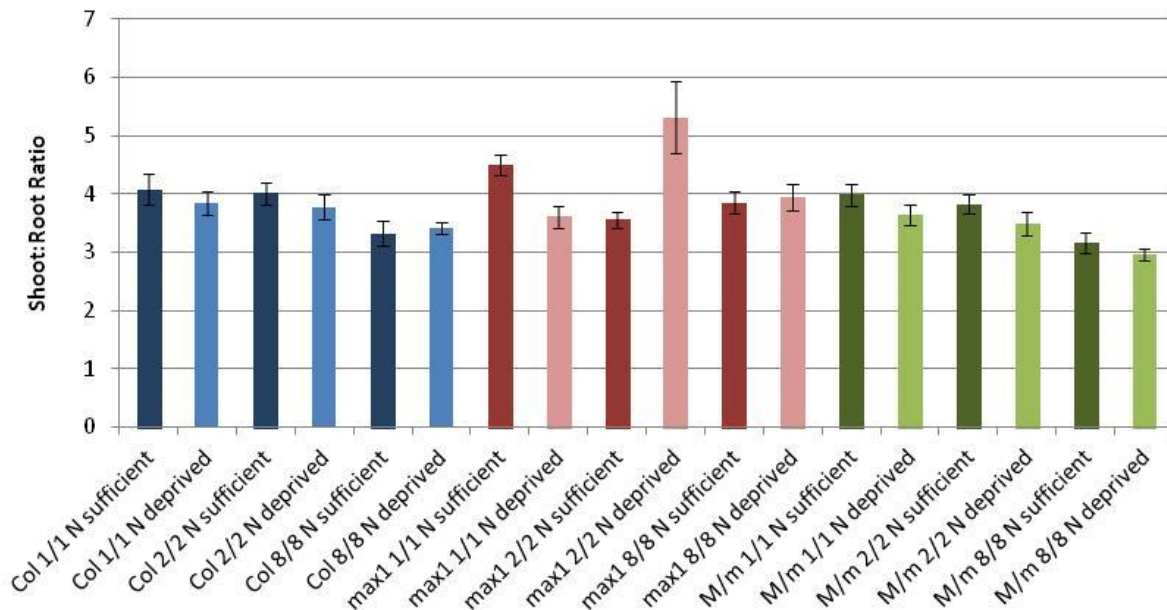


Figure 29. Shoot to Root ratios of 7 week old *Arabidopsis thaliana* plants according to genotype and Nitrate availability. Plants of each genotype (Col, *max1*, and *MAD/mad*) were grown in nutrient neutral conditions and supplemented with either 9mM NO₃⁻ (sufficient) or 1.8mM NO₃⁻ (limiting). In addition to the nitrate treatments the plants are also subject to low (2 plants per p40), medium (4 plants per p40), or high (16 plants per p40) levels of crowding.

Darker bars indicate sufficient local NO₃⁻, lighter bars indicate insufficient local NO₃⁻.

All plants were grown in monoculture under standard glasshouse conditions (page 43). ATS containing either 9mM NO₃⁻ or 1.8mM NO₃⁻ was supplemented at 0, 3, 4, and 5 weeks.

Error bars indicate standard error

Three-way ANOVA sig = 0.020 for genotype and density, 0.048 for genotype and treatment, and 0.547 for treatment and density.

Figure 29 shows the effect of crowding on shoot to root ratio in monocultures of Col, *max1*, and *MAD/mad*. Col shows no significant reduction in shoot to root ratio (S:R) between the low and medium density treatments, nor does a low NO₃⁻ availability affect the S:R at low and medium densities. An effect is only seen at high densities which result in significantly lower S:R ratios in Col. Subjecting high density Col to low NO₃⁻ conditions has no additive effect and it would therefore seem that the change in S:R seen in high density Col populations is independent of NO₃⁻ availability. The S:Rs seen in *max1* are far more variable, with NO₃⁻ availability seeming to be an important factor in *max1* S:R ratio at low density. This feature is not carried over into the medium density results and NO₃⁻ availability has no effect in high density. These results are too variable to be reliable. Looking at the high density results the S:R

ratio for max1 is significantly higher than that of Col, demonstrating the resistance to shoot to root shifts in biomass previously demonstrated. Results for *MAD/mad* are very similar to those of Col with NO_3^- availability having no effect on S:Rs at any density. The slight resistance to biomass reallocation seen in max1 is certainly not present in *MAD/mad*.

A straightforward measurement of the weight of shoot and root does not give a full enough picture of the effects that crowding has on the overall structure of a plant. In times of crowding a plant sacrifices any non vital growth and reroutes the resources into essential growth. The hypothesis is that higher levels of crowding will result in plants with fewer lateral branches and more developed root systems. The following experiments give a fuller picture of the shoot and root architecture of plants at different growth densities.

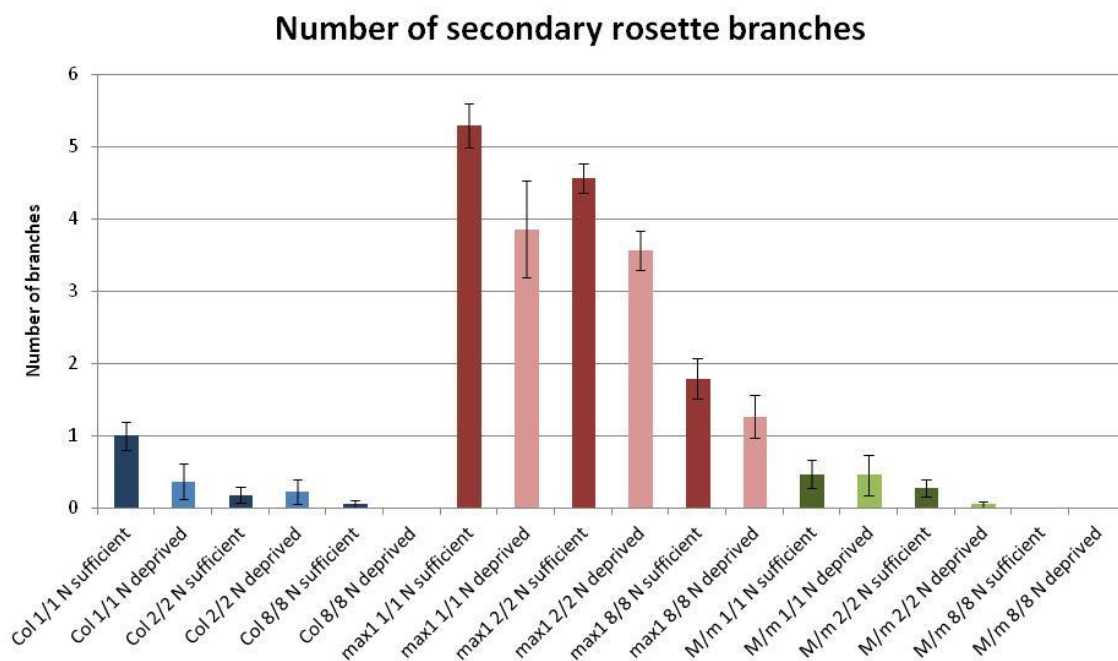


Figure 30. Secondary branches in 7 week old *Arabidopsis thaliana* plants according to genotype and Nitrate availability.

Col1/1 indicates that there are 2 Col plants per p40, 2/2 = 4 plants per p40 and 8/8 = 16 per p40

Darker bars indicate sufficient local NO_3^- , lighter bars indicate insufficient local NO_3^- .

All plants were grown in monoculture under standard glasshouse conditions (page 45). ATS containing either 9mM NO_3^- or 1.8mM NO_3^- was supplemented at 0, 3, 4, and 5 weeks.

Three-way ANOVA sig = 0.003 for genotype and density, 0.065 for genotype and treatment, and 0.087 for treatment and density.

Comparative branching is difficult to analyse in a meaningful way in Col plants as the number of rosette branches even in ideal conditions is usually between 0 and 2. This means that differences in branching levels over a population of plants are very small and this in turn limits the analysis that can take place. In figure 30 the mean number of rosette branches in Col is approximately 1. This drops significantly in NO_3^- limiting conditions. At medium density mead branch numbers are near zero in N sufficient conditions, and so any further reduction caused by N limitation cannot be detected. The same result cannot be seen at medium density. The numbers are so low that comparative analysis would be meaningless. There is no significant difference between the nitrate treatments at this density. At high density the branching levels seen in Col are extremely low and no rosette branching is seen at all in the high density, low NO_3^- treatment. More obvious results are seen with *max1*. A higher level of branching in N sufficient conditions makes differences between the treatments that much easier to see. As with Col at low density, the effects of low NO_3^- treatment are translated into a significant reduction in rosette branching, an effect which is also seen in the medium density treatments. The effect is reduced when *max1* are grown at high density with the difference in branching between sufficient and low NO_3^- treatments being less significant than at lower densities. The evidence here suggests that, in *max1*, lowering NO_3^- levels results in fewer rosette branches. This effect is present regardless of plant density. Also, increasing the density reduces branching, independent of nutrient supply. *MAD/mad* data suffers from the same analytical problems as Col with regards rosette branching. The numbers are so low (lower than Col) that the effects of NO_3^- limiting conditions on *MAD/mad* populations cannot be stated with any certainty. The number of *MAD/mad* rosette branches has a definite downward trend between low and medium density and no branches are recorded at high density regardless of NO_3^- treatment.

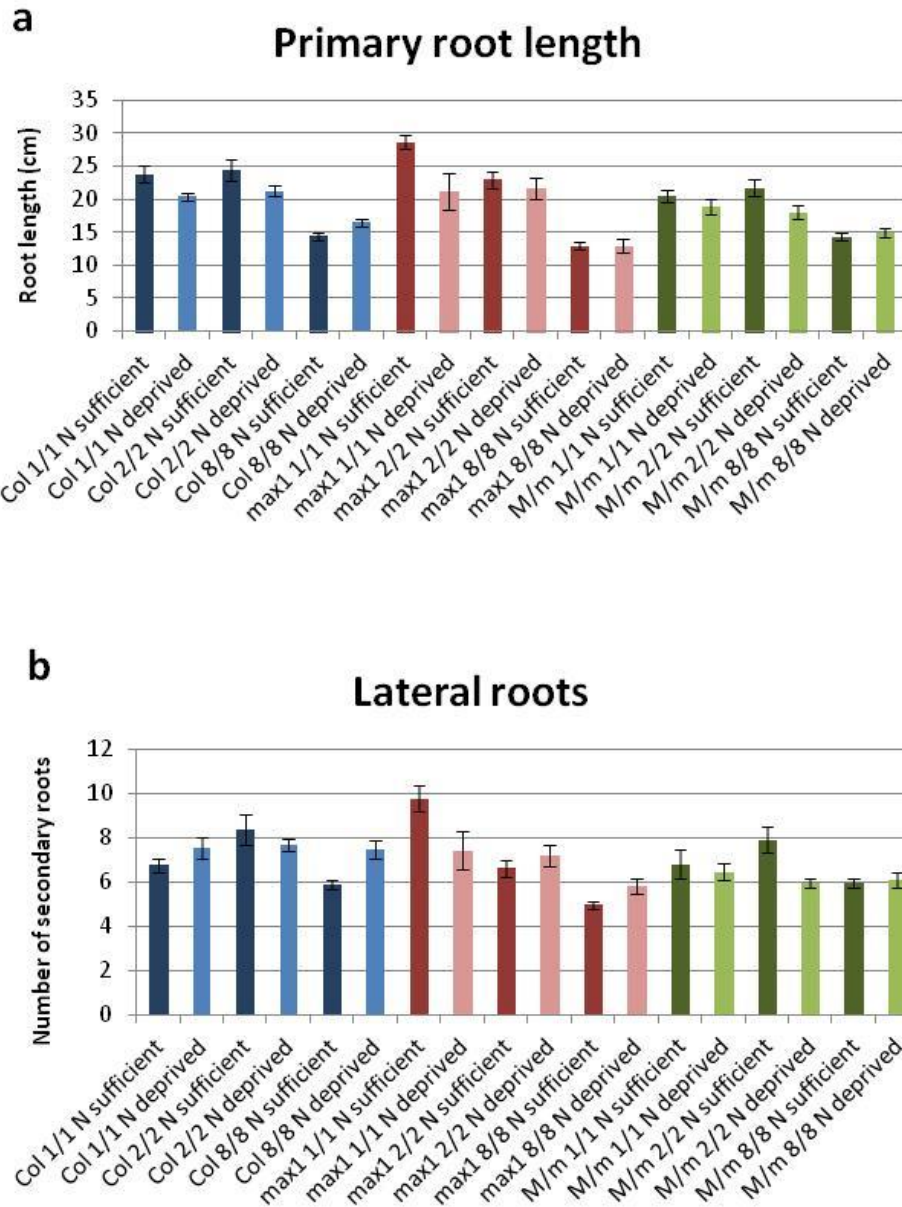


Figure 31. Primary root length (a) and number of lateral roots (b) in 7 week old *Arabidopsis thaliana* plants according to genotype and Nitrate availability.

Darker bars indicate sufficient NO_3^- , lighter bars indicate insufficient NO_3^- .

All plants were grown in monoculture under standard glasshouse conditions (page 45). ATS containing either 9mM NO_3^- or 1.8mM NO_3^- was supplemented at 0, 3, 4, and 5 weeks.

Error bars indicate standard error

Three-way ANOVA primary root sig = 0.160 for genotype and density, 0.421 for genotype and treatment, and 0.161 for treatment and density. Lateral roots sig= 0.001 for genotype and density, 0.047 for genotype and treatment, and 0.002 for treatment and density.

Looking at both the primary root length and the number of secondary roots allows a reasonable assessment of root architecture. An interesting relationship between root length, N supply and crowding density can be seen in figure 31(a). N limited plants grown at higher densities tend to have shorter roots than those grown with sufficient N. This is not the case at lower densities, where N supply had relatively little effect, or even slightly increased primary root length. Plants at higher densities will be smaller as a result of living in a competitive environment, so it seems obvious that the roots will be shorter in smaller plants. What is of interest is how the root architecture of the *max1* plants, which have a degree of resistance to shifts in S:R with low N availability, compares to genotypes which typically increase root growth on low N. NO_3^- limitation at low and medium densities has the effect of lowering the average root length in all genotypes, an effect not seen in plants at higher densities. There appears to be no correlation between lateral root number and either crowding or NO_3^- levels in either Col or *MAD/mad* (figure 31(b)). An overall downward trend can be seen in *max1*(figure 31(b)). These data suggest that the increase in root biomass witnessed in limited NO_3^- conditions, either as a result of increased competition for resources or limited local availability, is not found in lower level roots but is found in tertiary roots and higher. This makes sense as increasing the number of tertiary roots will have a far greater impact on the surface area to volume ratio of the root than an increase in larger volume components would have. Further investigation of the higher order root branching of these genotypes under similar conditions may provide the evidence needed.

The second phase of this experiment involved exactly the same crowding and NO_3^- treatments as for the monocultures above but combined Col with either *max1* or *MAD/mad*. The purpose of this experiment was to determine whether a genotype reacts differently when in a polyculture as opposed to a monoculture and if the reaction of one genotype gives it any advantage over another. The results above suggest that *MAD/mad* responds to both crowding and NO_3^- limitation in a very similar way to Col whereas *max1* exhibits a slightly different response in both resistance to shoot to root biomass reallocation and the maintenance of increased shoot branching levels with the characteristic resistance in shoot to root biomass allocation and maintains a higher level of shoot branching than either Col or *MAD/mad*.

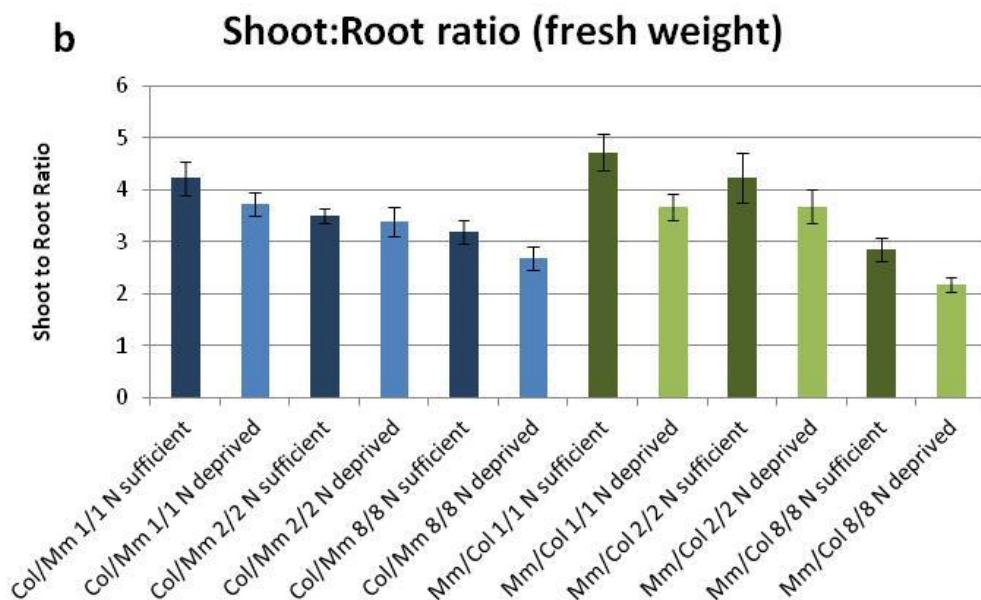
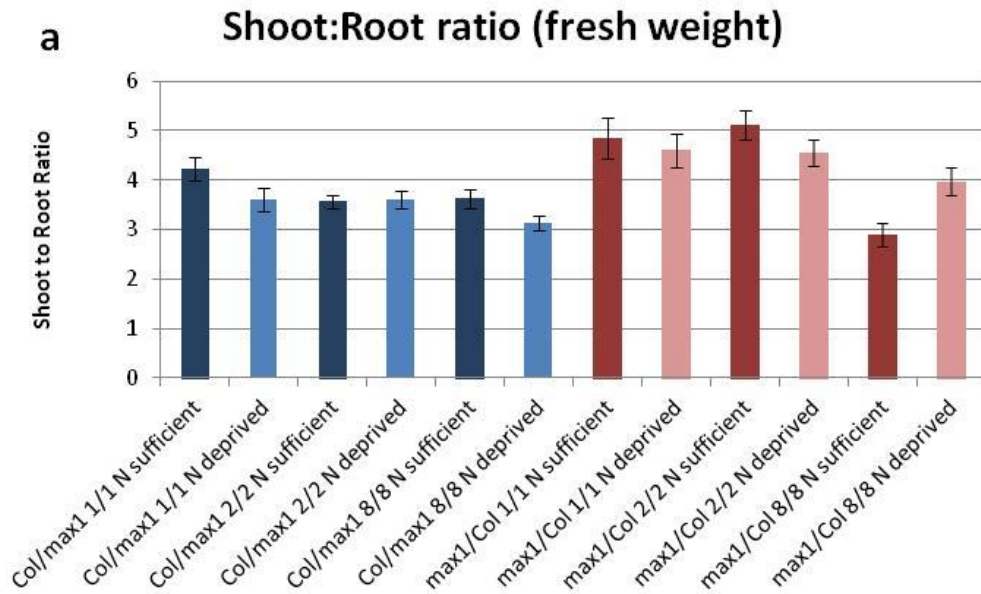


Figure 32. Shoot to Root ratios of; Col and *max1* in a Col,*max1* polyculture (a), and Col and *MAD/mad* in a Col,*MAD/mad* polyculture.

The first genotype in the label is the one plotted.

Plants were 7 weeks old at time of measurement.

Darker bars indicate sufficient local NO_3^- , lighter bars indicate insufficient local NO_3^- .

All plants were grown in monoculture under standard glasshouse conditions (page 45). ATS containing either 9mM NO_3^- or 1.8mM NO_3^- was supplemented at 0, 3, 4, and 5 weeks.

Three-way ANOVA Col/*max1* sig = 0.141 for genotype and density, 0.008 for genotype and treatment, and 0.114 for treatment and density. Col *MAD/mad* sig = 0.090 for genotype and density, 0.291 for genotype and treatment, and 0.173 for treatment and density

The results for the Col,*max1* polyculture (figure 32(b)) show similar results to the Col and *max1* monocultures (figure 32 (a)). Col S:Rs are consistently lower than those of *max1* when subjected to the same treatments with the exception of *max1* at high density in NO₃⁻ sufficient conditions. This result is very low and does not follow the overall *max1* trend. The anomalous result notwithstanding, *max1* demonstrates the same resistance to change in S:R as it does when in a monoculture. The results for Col seem to indicate a slight increase in resistance to a shoot to root shift in biomass. It is tempting to speculate that because the *max1* plants allocate less of their biomass to roots the competition for nutrients in the soil is not what it would be in Col monoculture of the same density thereby reducing the need for Col plants to concentrate so many resources on root growth. Another striking result is the much bigger difference between *max1* and WT than in the monocultures, suggesting that *max1* shoots outcompete Col Shoots, and/or Col roots outcompete *max1* roots.

In a Col,*MAD/mad* polyculture Col exhibits a much more familiar reduction in S:R as crowding increases, with NO₃⁻ limitation effecting a slight reduction in S:R as in the Col monoculture. S:Rs of *MAD/mad* also demonstrate the same downward trend seen in the *MAD/mad* monoculture. These results are much more like the monoculture results seen in the previous experiments. This fits with the above observation that *max1* doesn't provide as much subterranean competition as a genotype with the typical response to crowding and low NO₃⁻ availability. Because *MAD/mad* has a similar response to Col and allocates more biomass to its roots, Col faces more competition for soil based nutrients and responds appropriately by doing the same. Hence the similar looking results in figure 32(b).

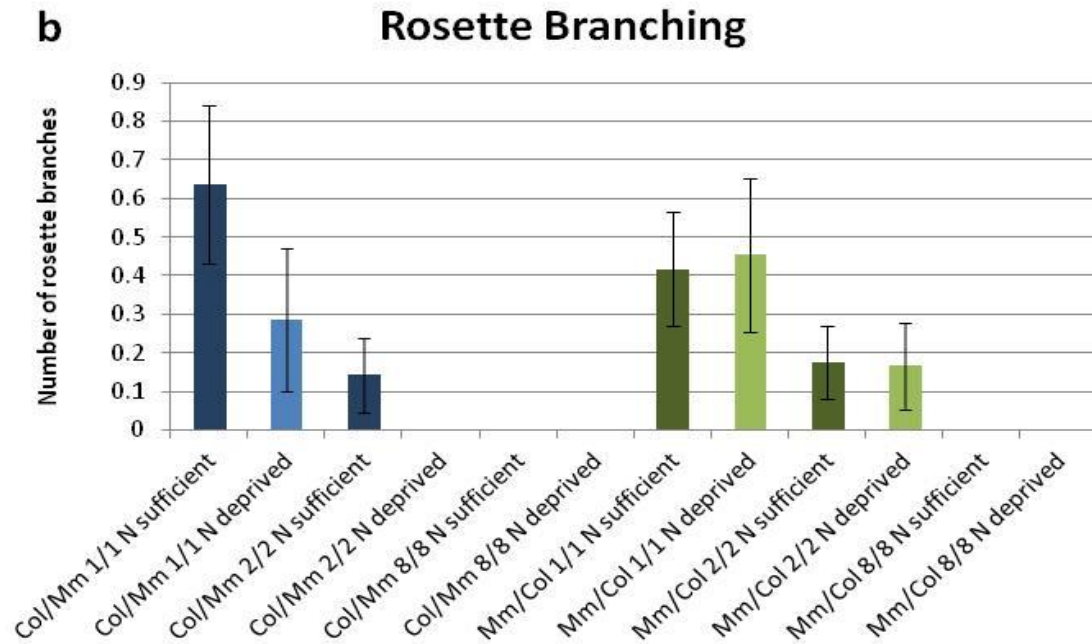
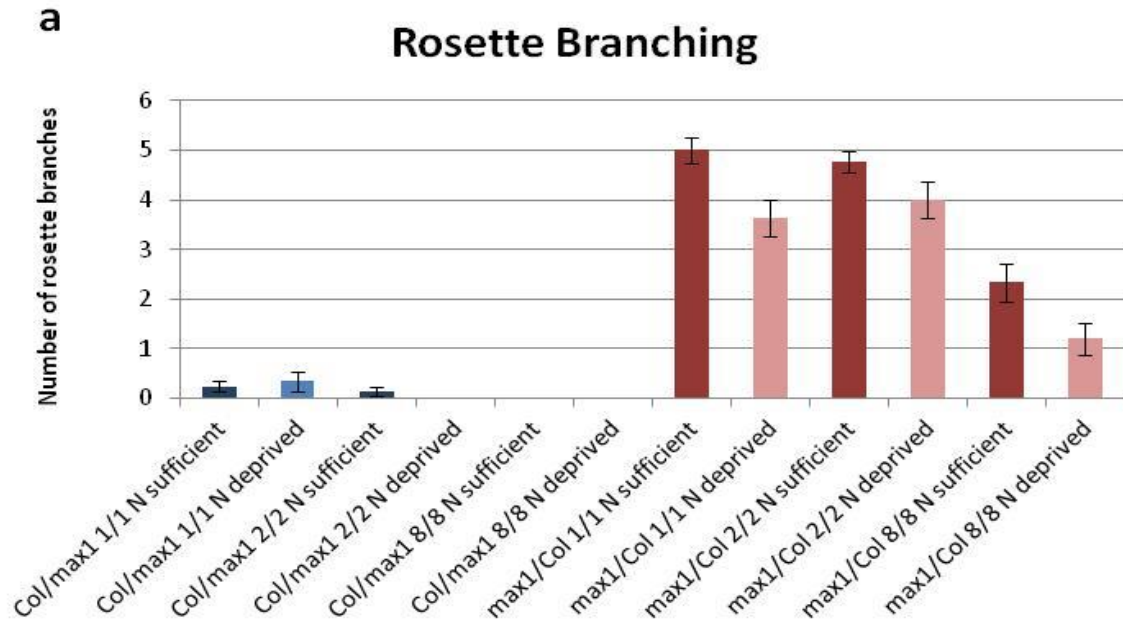


Figure 33. Rosette branching in; Col and *max1* in a Col,*max1* polyculture (a), and Col and *MAD/mad* in a Col,*MAD/mad* polyculture.

Plants were 7 weeks old at time of measurement.

Darker bars indicate sufficient local NO_3^- , lighter bars indicate insufficient local NO_3^- .

All plants were grown in monoculture under standard glasshouse conditions (page 45). ATS containing either 9mM NO_3^- or 1.8mM NO_3^- was supplemented at 0, 3, 4, and 5 weeks.

Error bars indicate standard error

Three-way ANOVA Col, *max1* sig = 0.174 for genotype and density, 0.076 for genotype and treatment, and 0.453 for treatment and density. Col, *MAD/mad* sig = 0.648 for genotype and density, 0.216 for genotype and treatment, and 0.560 for treatment and density

When grown in direct competition with *max1*, Col rosette branching levels are exceptionally low. As shown in figure 33(a), the average number of Col rosette branches in a low density, NO₃⁻ sufficient environment is approximately 0.2, lower than Col in a monoculture. This low number may be explained by the presence of *max1*. The branching levels in *max1* follow the same trend as in a monoculture; high levels of branching compared to Col in every possible treatment combination. Higher branching levels will reduce the red to far-red light ratio reaching Col and thereby induce a shade avoidance response, stimulating Col to grow upwards and suppress branching.

In a Col,*MAD/mad* polyculture Col is not under as much pressure to grow upwards as the much less branchy *MAD/mad* does not cast as much shade Col as *max1*. With this in mind it is easy to understand why both Col and *MAD/mad* behave as they do in a monoculture with branching levels in both genotypes reducing significantly according to crowding levels. As with the monoculture NO₃⁻ availability has a variable effect on branching levels.

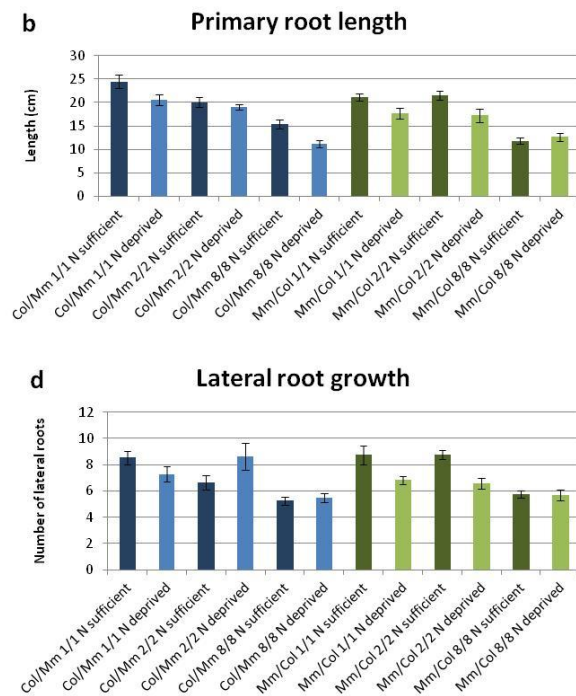
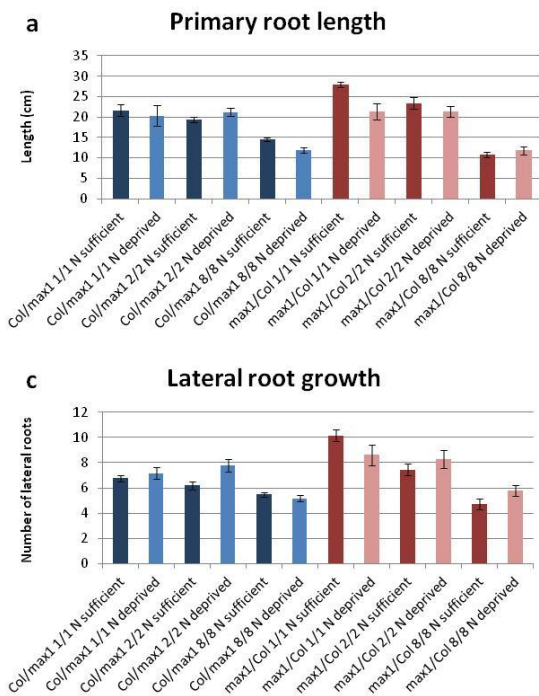


Figure 34 (previous page). Primary root length and lateral root growth in; Col and *max1* in a Col,*max1* polyculture (a and c), and Col and *MAD/mad* in a Col,*MAD/mad* polyculture (b and d).

Plants were 7 weeks old at time of measurement.

Darker bars indicate sufficient local NO_3^- , lighter bars indicate insufficient local NO_3^- .

All plants were grown in monoculture under standard glasshouse conditions (page 45). ATS containing either 9mM NO_3^- or 1.8mM NO_3^- was supplemented at 0, 3, 4, and 5 weeks.

Error bars indicate standard error.

Three-way ANOVA Col, *max1* Primary root length sig = 0.002 for genotype and density, 0.160 for genotype and treatment, and 0.050 for treatment and density. Col, *max1* Lateral roots sig = 0.034 for genotype and density, 0.397 for genotype and treatment, and 0.030 for treatment and density. Col, *MAD/mad* Primary root length sig = 0.122 for genotype and density, 0.547 for genotype and treatment, and 0.379 for treatment and density. Col, *MAD/mad* Lateral roots sig = 0.297 for genotype and density, 0.063 for genotype and treatment, and 0.054 for treatment and density

Primary root length of Col plants in a Col,*max1* polyculture are similar than those of *max1* at low and medium densities, with the exception of *max1* at low density and with sufficient NO_3^- (figure 34 (a)). Root lengths of both genotypes are significantly reduced at high densities. Limiting NO_3^- availability seems to have very little effect on root length. This is also the case in both Col and *MAD/mad* plants in a Col,*MAD/mad* polyculture (figure 34 (b)). Root lengths are similar in both the low and medium density treatments with NO_3^- limitation having little effect on root length.

The number of lateral roots seem to be the same for any of the three genotypes, despite the NO_3^- treatment, when at high densities. *max1* exhibits higher lateral root growth at lower densities (figure 34 (c)). Aside from these observations there appears little correlation between treatment and lateral root growth. The NO_3^- level has a very variable effect. As suggested before, these results are very limited as the main area of root growth is most probably at a tertiary level or higher and is therefore not represented by the above results.

In conclusion, *max1* appears to benefit from being in a polyculture with Col, at least at the lower densities. At medium density in monoculture, *max1* and Col root parameters are similar, but in competition, *max1* has longer primary and more secondary roots than Col. It would be interesting to find out whether *max1* has an abnormal requirement for Nitrogen, or whether it is used more efficiently, or whether the roots are more efficient at nutrient absorption.

3.7 Mapping the *MAD* locus

Initial Mapping

A mapping population of 500 *mad* plants was obtained using the method cited on page 31. This population underwent linkage analysis with a set of markers at known locations in the *Arabidopsis* genome (table 6). Linkage was determined between *MAD* and the marker GAPC, found on the p arm of At. Chromosome 3, at a position of 1.1 million base pairs (figure 35). The lack of linkage between *MAD* and the chromosome marker AFC1 is not surprising given the remote location of AFC1, at 19.8 million base pairs it is found in the distal section of the q arm, at the other end of the chromosome. To further narrow this potential search area two additional chromosome 3 p arm markers (CA1 at ~196,500bp and NGA126 at 3.48 million bp) were tested. The resulting recombination frequencies were higher than those seen using the GAPC marker, suggesting that the *MAD* locus was closer to GAPC than either of the above markers and so this marker was chosen as the starting point for the subsequent chromosome walk.

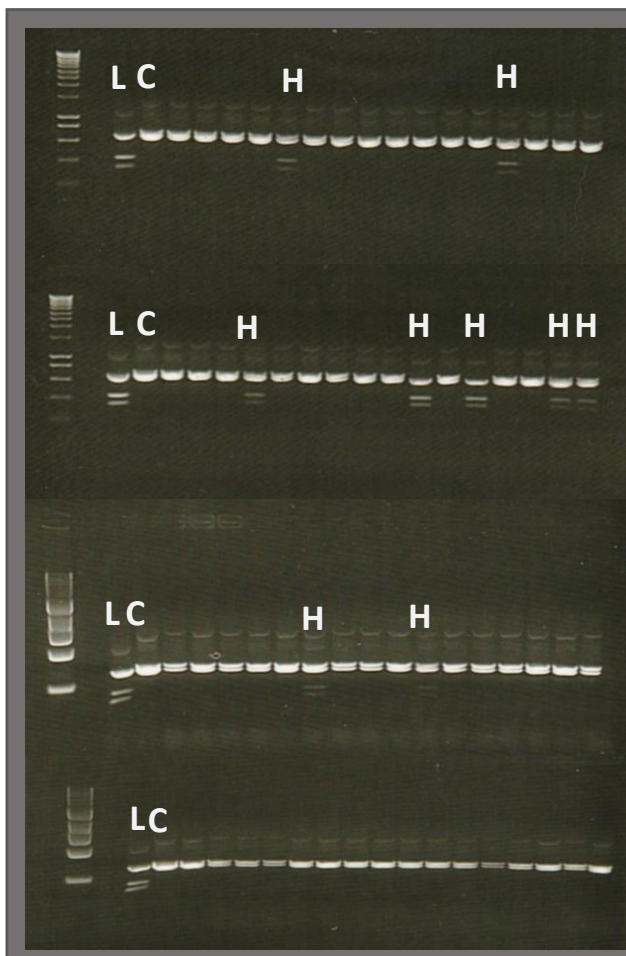


Figure 35. *MAD*, GAPC linkage.

L denotes *Landsberg erecta* control, C denotes Columbia control. H indicates a heterozygote.

The initial 72 samples of *mad* DNA tested with the GAPC marker, located at 1.1 million bp on the p arm of At chromosome 3 indicate only 9 heterozygotes. This means that, not only is the *MAD* locus linked to GAPC, it is fairly close. The fewer the heterozygotes, the closer the target gene is to the genetic marker.

Ladder used is Hyper ladder 1 (Bioline), samples were run on a 1% agarose gel

Chromosome walking, as well as the initial mapping process, takes advantage of the many natural differences in sequence between *Arabidopsis* ecotypes. In this case *MAD* is in the Col genetic background but has been crossed with *Landsberg erecta* (Ler). There are therefore both Col and Ler alleles in the mapping population. Unlinked markers segregate independently from the gene of interest and there will be an approximate Col:Ler ratio of 1:1. If the marker is linked to the gene of interest then more Col alleles will be present as the gene is the Col background. The markers are either Cleaved Amplified Polymorphic Sequence (CAPS) (Konieczny, A. and Ausubel, F.M. (1993)) markers or Simple Sequence Length Polymorphisms (SSLPs) (Bell, C.J. and Ecker, J.R. (1994)). CAPS markers amplify a DNA segment that includes a restriction enzyme site in one of the ecotypes but not the other, or a different number of restriction sites according to ecotype. SSLPs are a result of insertion-deletion events (INDELS) resulting in a specific sequence being longer in one ecotype than in the other. These both allow a section of DNA to be identified as Col or Ler.

Chromosome	Position (bp)	Marker Name	Type
1	7.1 million	CAT3	CAPS
1	23.8 million	NPR1	CAPS
3	1.1 million	GAPC	CAPS
3	19.8 million	AFC1	CAPS
4	6.4 million	DET1.1	CAPS
5	17.6 million	KLPNHC	CAPS
5	24.8 million	LFY3	CAPS
Additional Chromosome 3 markers			
3	196,488	CA1	CAPS
3	3.48 million	NGA126	SSLP

Table 6. Markers used in the initial mapping phase of the *MAD* gene. A range of markers across the genome were used. Linkage between *MAD* and the GAPC marker located *MAD* on the p arm of chromosome 3. Two further chromosome 3 markers were used to give a better idea of the general area containing the *MAD* locus

Fine Structure Mapping

Narrowing down the region containing *MAD* involved designing markers at specific genetic locations. This was achieved by using the Cereon database to indentify appropriately sited polymorphisms and designing primers to amplify the required section of DNA. The products were then run out on an agarose gel to allow visualisation of the results of the polymorphisms. If a CAPS marker was used, then the appropriate enzyme was used in an intermediary digest step. The markers used for the close structure mapping of *MAD* are detailed in table 7.

Name	Position (bp)	BAC	Type
CER469977	1.95 million	F24P17	SSLP
CER470642	2.7 million	T16O11	SSLP
CER457855	2.77 million	MZB10	SSLP
CER470384	3 million	F11F8	SSLP
CER464602	3.05 million	T22K18	CAPS
CER464949	3.08 million	T22K18	SSLP
CER464953	3.13 million	T22K18	SSLP
CER463987	3.17 million	F14P13	CAPS
CER464213	3.2 million	F14P13	CAPS
CER464660	3.22 million	F14P13	SSLP
CER464637	3.24 million	F13M14	SSLP
CER464637	3.31 million	F13M14	SSLP
CER464922	3.68 million	T19F11	SSLP

Table 7. Markers used for the fine structure mapping of *MAD*. Once the approximate area had been identified the above markers were designed to delineate the potential area containing the *MAD* locus. The Cereon database has listed polymorphisms which are located on specific BACs according to their position in the *Arabidopsis* genome. The markers used were either cleaved amplified polymorphic sequence (CAPS) markers or simple sequence length polymorphisms (SSLPs).

Finding suitable markers in the region containing *MAD* proved to be challenging. Reliable markers are of course not evenly distributed across the genome and they are not present in a great number in the area in which the search was focussed. Enough successful markers were produced to allow the isolation of the *MAD* locus to a 370kb region (figure 36). This is still too large an area to determine which gene is *MAD*, ideally the chromosome walk should narrow the region to approximately 50kb which equates to roughly 0.25cM, with recombinants left on either side of the gene. A further problem arises here as only one downstream recombinant remains. Further work should include continuation of the chromosome walk and, possibly the generation of another mapping population if recombinants run out. Once a narrow enough region has been isolated it can be sequenced and compared to wildtype, thereby identifying the mutated gene and the nature of the mutation.

A Bacterial Artificial Chromosome (BAC) library is available for the entire *Arabidopsis* genome. The *MAD* mutation has been delineated to an area that is covered by 5 BACs; F13M14, T7M13, F9F8, F11B9, and F24K9.

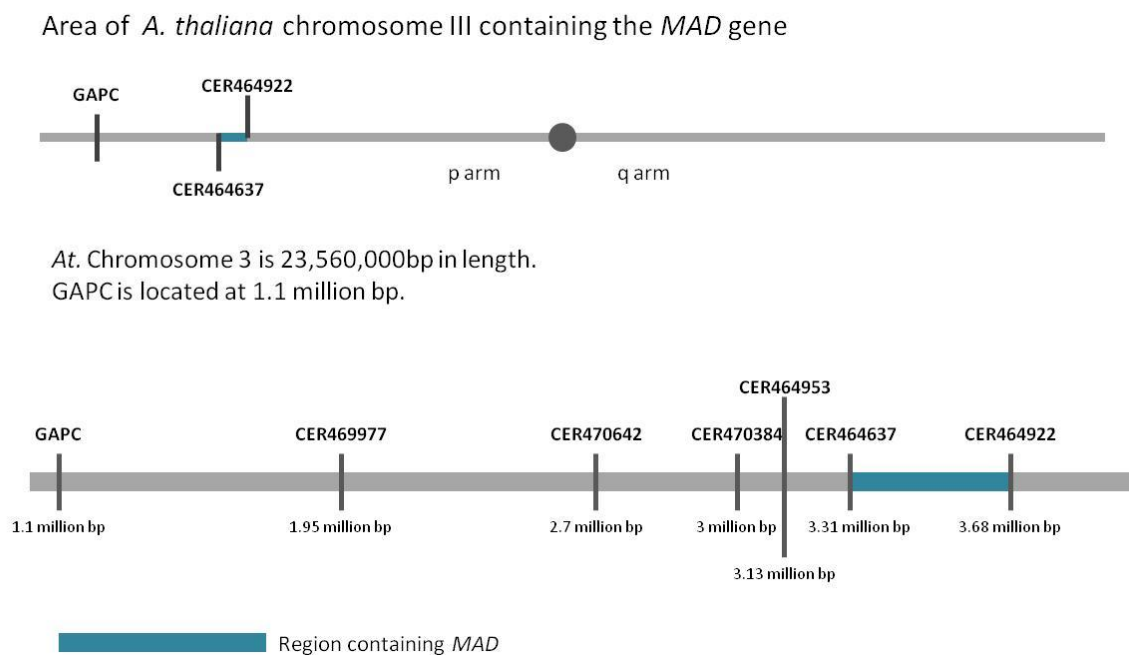


Figure 36. The location of the *MAD* locus. The exact gene identification of *MAD* is not yet known but the area in which it lies has been delineated to a 370kb regions between the genetic markers CER464637 and CER464922. This places it at between 3.31 and 3.68 million bp along At. Chromosome 3. There are five recombinant left upstream of the region containing *MAD* and one downstream.

3. 8 Discussion

The *MAD* mutation is a semi-dominant suppressor of several *Arabidopsis* increased branching mutants. The term semi-dominance in this instance refers to the phenotypic effect of the *mad* mutation on the *MAD* allele with respect to height. *MAD/MAD* (or wildtype) individuals are, of course, of an average wildtype height (approximately 350 mm (figure 14)). *MAD/mad* individuals are shorter than wildtype plants at approximately 250mm (figure 14) but plants homozygous for the *mad* mutation are much shorter with an average height of only 60mm (figure 14). This difference in phenotype severity between the *mad* hetero- and homozygote indicates the semi-dominant nature of *mad*. Further assessment of this aspect of the *mad* mutation is made extremely difficult because of the severe phenotype of the *mad* homozygote (figure 13). Many physiological tests, such as those that would have determined the auxin status of *mad* plants have not been possible to conduct. With this in mind it cannot be asserted with confidence that the *mad* mutation has a semi-dominant effect on other traits seen in the *mad* heterozygote. It does however, seem unlikely that *mad* would have a dose dependent effect on one trait and not others. In all probability the extreme height phenotype seen in *mad* is a result of other, as yet unknown, effects of the *mad* mutation, resulting in a stunted, weakened plant. Because it is a semi-dominant mutation it is likely that it is not loss of function and therefore it is difficult to infer the wild-type function of *MAD*.

Mad/mad only affects the *max1* branching phenotype and not other *max1* effects therefore it is not a general downstream mediator of SL signalling. *MAD/mad* partially restores *max1* branching levels at the auxin signalling level, leaving auxin transport unaffected. The similar levels of *PIN1* transcription in *MAD/madmax1* and *max1* are further proof of this. That fact that *MAD/mad* partially restores wildtype branching levels to all the *max* mutants suggests that it acts downstream of, or in parallel to *MAX2*. A primary target for the SL pathway, which can account for the branching phenotypes, is auxin transport. The fact that *MAD/mad* does not restore auxin transport to wild-type suggests that it does not work via SL-independent activation of the signalling pathway.

MAD/mad can suppress the activation of *axr1* buds, which is postulated to be primarily the result of an over-production of auxin in the bud, due to reduced feedback inhibition on auxin synthesis. This would make *axr1* buds a strong auxin source which, according to the auxin canalisation hypothesis (page 16) would result in an increased flow of auxin to the stem

vasculature, resulting in bud outgrowth. These data could suggest a more general role for *MAD* in bud activation, it could for example be involved in the regulation of cytokinin biosynthesis. This could be tested by crossing *MAD/mad* to relevant cytokinin biosynthesis gene::reporter fusions such as *ISOPENTYNYLTRANSFERASE::GFP*, to determine whether transcription levels are affected. This seems unlikely as *mad* does not appear to suppress branching in otherwise wildtype plants. The repression may be there, but with the already low levels of branching in wildtype *Arabidopsis* it may be impossible to see. Further physiological work should be carried out in the *MAD/mad* genotype. The hormone response experiments in this study were carried out using *MAD/madmax1* plants and, whilst they showed the effect that the *mad* mutation had on *max1*, they did not show the effect of the *mad* mutation on its own.

The *mad* mutation also seems to confer partial adaxialisation on *mad/mad* leaves. This effect is not seen in *MAD/mad* leaves and therefore requires a higher dose of the *mad* allele. Auxin is involved in many developmental processes including the establishment of the ab-adaxial axis in leaves (Scarpella, E. *et al.* (2006)). The SAM is responsible for the production of new organs, including leaves. Leaf adaxial-abaxial polarity also depends on the SAM (Sussex, I.M. (1951) (Reinhardt, D. (2005)). A signal that passes from the SAM to the adaxial domain of a leaf primordium to promote adaxial identity had long been considered (Sussex, I.M. (1951)). Several potential candidates were proposed as the signal molecule including Small RNAs (Yao, X. *et al.* (2009) (Chitwood, D.H. *et al.* (2009)) and a γ -aminobutyric acid (GABA) shunt metabolite (Toykura, K. *et al.* (2011)). Very little was known about this signal molecule, including how it was transported and its precise involvement in leaf polarity. It is now thought that an auxin signal in the opposite direction is responsible for the maintenance of leaf cell polar identity in leaf primordia (Qi, J. *et al.* (2014)). It has been shown that, in early leaf primordia there are transient zones on the adaxial side that have low auxin levels and that this low auxin level contributes to ad-abaxial patterning (Qi, J. *et al.* (2014)). Establishment of the low auxin zone is facilitated by auxin efflux from the leaf primordium to the SAM. The ARF MONOPTEROS (MP) is activated in the presence of auxin and promotes abaxial cell fate (or discourages adaxial cell fate) (Qi, J. *et al.* (2014)). ETTIN (ARF3) and ARF4 are also involved in establishing adaxial/abaxial polarity (Pekker, I. *et al.* (2005) (Garcia, D. *et al.* (2006)). MP acts as a transcriptional activator and ETTIN ARF4 act as transcriptional repressors (Boer, D.R. *et al.* (2014)). All three of the above transcription factors bind DNA motifs found in auxin inducible genes. Disrupting any of these transcription factors or altering their relative activity could have the potential to alter cell fate. This is perhaps the case in *mad* plants. *MAD/mad*

respond more to exogenous auxin in bud assay experiments than wildtype plants (figure 28) so *MAD* may very well be involved in auxin signalling. If so, it is not unreasonable to state that *MAD* may be involved in leaf cell polarity via activation or repression of genes via ARFs. The adaxial marker *REVOLUTA* is also involved in leaf polarity, identifying cells with an adaxial fate (Tageshime, T. *et.al.* (2013)). *REVOLUTA* acts in parallel with auxin in determining leaf cell fate and not in the same pathway. This is demonstrated by the additive phenotypes seen in *pid rev* and *pin1-1 rev* (Qi, J. *et.al.* (2014)). It is not likely that the *mad* mutation has an effect on *REVOLUTA*. The altered auxin signalling of *MAD/mad* makes the previous suggestion much more likely. Decreasing the activity of *ETTIN* or *ARF4*, or increasing the activity of *MP* would result in an increase in adaxial cell fate.

The region of chromosome 3 containing *MAD* is too large to be able to indentify the gene conclusively. Among the 230 genes in the region, spanning 5 BACs (F13M14, T7M13, F9F8, F11B9, and F24K9), three stood out as potential candidates for *MAD*. Further mapping work is required to give a conclusive answer as to the identity of *MAD* and, given the small number of recombinants left, a fresh mapping population may be a good idea. Alternatively a whole genome sequencing approach may be tried.

From a speculative point of view all three of the genes posited could have a role in the regulation of bud outgrowth. *SPY* (*SPINDLY/AT3G11540.1*) is located at 3631887-3637955 AtCh3 and is found on the annotation unit F24K9. *SPY* could have a direct, positive impact on bud simply by increasing the cytokinin levels the bud. This could be enough for the bud to escape the effects of apical dominance (Müller, D. *et.al.* (2015)). Although the *spy* morphological phenotype does not resemble that of *mad* mutants it is possible that it is a dominant, or semi-dominant allele, but this is unlikely. The idea that it may be a semi-dominant allele is an attractive prospect given the semi-dominant nature of the *mad* mutation.

The *AT3G11130.1* clathrin encoding gene, located at 3482149-3491908 AtCh3 and is found on the F9F8 annotation unit, could be involved in *PIN1* recycling. It is expressed in both the plasma membrane and the golgi body, suggesting a role in endocytosis (Ito, J. *et.al.* (2010)). Any disruption to this would result in reduced auxin efflux from the cell and would have a direct effect of levels of auxin transport. The *MAD* heterozygote reduces *max1* levels of auxin transport levels, although not to that of wildtype plants (figure 27), lending support to this theory. *AT3G1130.1* has yet to be characterised so nothing is known about any morphological phenotype a mutation may confer.

MES17 (*METHYL ETHERASE 17*) is a third candidate, found on the T7M13 annotation unit and at 3401078-3402672 AtCh3. It encodes a methyl IAA esterase and can therefore convert inactive MeIAA to biologically active IAA. A *mes17* plant would have reduced levels of active auxin, and therefore reduced inhibition. This would of course result in an increase in branching which would not fit with the *MAD* heterozygous phenotype. A mutation in the promoter region of *MES17* may have the effect of *MES17* constitutive or increased expression, which would result in the availability of more bioactive auxin. *MES17* has a wide range of expression (Yang, Y. *et.al.* (2008)). *MES17* is also posited to act upstream of *AXR1* (Yang, Y. *et.al.* (2008)). This is also a potential place for *MAD*. The possibility of an auxin-related explanation for the *mad* phenotype makes *MES17* a more attractive candidate but there are severe reservations given the need for *MES17* production to be increased rather than reduced.

Figure 37 illustrates where the above genes could be involved in the regulation of bud outgrowth.

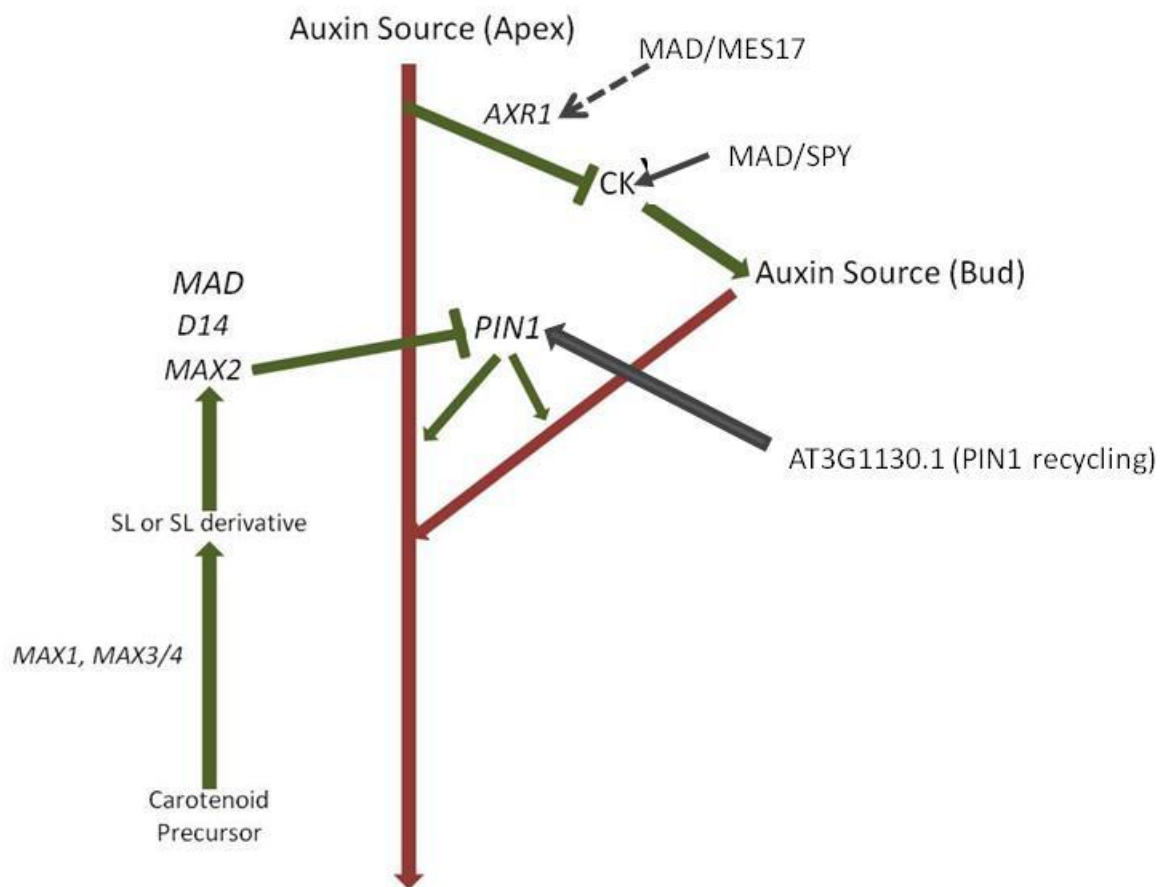


Figure 37. (previous page) Postulated mechanistic model of the regulation of bud outgrowth including MAD candidate genes detailed on page 102-103. Auxin transport (red arrows) is limited by the amount of the PIN1 auxin efflux proteins present. Limiting auxin transport down the stem reduces its strength as an auxin sink. This results in reduced auxin export from the bud resulting in repression of bud outgrowth.

Cytokinins (CKs) promote bud outgrowth. *AXR1* controls bud outgrowth by reducing transcription of CK biosynthetic genes.

MAD may act downstream of the *MAX* pathway in the transduction of the SL signal. *MAD* action may be more general; it may affect cytokinin biosynthesis directly, or indirectly, by repressing *AXR1*

It is also a possibility that *MAD* is directly regulating bud activity independently of these processes.

Black arrows indicated possible *MAD* involvement and dashed lines indicate uncertainty as to the effect of *MAD* action

Targeted knock-out of these genes via homologous recombination (Endo, M. and Toki, S. (2014)) followed by complementation testing would be a sensible approach to verifying or ruling out *MES17*, *SPY* or *AT3G1130.1* as the *MAD* gene. A more targeted approach could be taken in the form of CRISPR (Clustered Regularly Interspaced Short Palindromic Repeats), a gene editing technique that relies on the Cas9 enzyme. Cas9 uses a guide RNA molecule to edit targeted DNA by either disrupting the gene or inserting further sequences. The targeted nature of CRISPR makes precise editing possible.

The crowding experiments with Col, *max1*, and the *mad* heterozygotes produced some interesting, although not always conclusive results. The most interesting results came from the polyculture tests. Columbia plants seemed to experience greater competition in a Col/*max1* polyculture than in a Col/*mad* heterozygote polyculture. The traits exhibited in *max1* when in a low nutrient environment ie. a slight resistance to the shift in shoot to root biomass allocation seen in wildtype plants and the maintenance of higher levels of shoot branching when compared to wildtype plants. Col secondary branching is very low when in a *max1* polyculture, lower than in a Col monoculture. This is likely to be because Col plants are undergoing a shade avoidance response (see figure 33 and page 42) as a result of the higher branching levels of *max1*. Allocating more biomass to the shoot is a strategy that will not necessarily pay off and is not seen in a Col/*mad* heterozygote polyculture, most likely as a result of the Col levels of shoot branching exhibited by *mad* heterozygotes. The *mad* heterozygotes have not shown the

slight resistance in shoot to root biomass allocation seen in *max1*, especially at medium densities. Given that the *mad* mutation does not restore wildtype levels of auxin transport to *max1* plants (figure 27) it can be stated that the capacity to transport auxin is not a factor, in this particular instant, in the response of *max1* plants to low available nitrate. The crowding experiments could be improved upon, if repeated, to yield much more illuminating results: measuring the relative weights of shoots and roots directly is perhaps not the best way to analyse biomass allocation. These measurements would be far more accurate if carbon content was to be measured directly, for example, using a simple sugars assay. Testing the levels of nitrate in the different samples would also provide information as to whether one type was more efficient at absorbing nitrates. These experiments could certainly build upon the groundwork laid by the basic crowding experiments.

4. Characterisation of the *17-4* mutant phenotype

4.1 Isolation of the *17-4* mutation

One of the defining characteristics of *max1* plants is a dampened response to low levels of available nitrates. Wildtype plants undergo a shift in shoot:root biomass as relatively more resources are allocated to root growth, supporting NO₃⁻ uptake. Relatively less biomass is allocated to the shoots, most notably there are fewer rosette branches. The alteration in shoot:root biomass is less pronounced in *max1* with a higher fraction of biomass allocated to the shoot, *max1* plants retain an increased branching phenotype in low NO₃⁻ conditions to such a degree that they are easily identified in a mixed population. There are two important points here; 1. More branches does not necessarily mean more biomass. A small number of thick-stemmed vigorous branches can have the same biomass as a large number of thin stemmed branches. 2. The reduced shift in root fraction in the *max* mutants probably results from inability to suppress branching, not the other way round. This premise formed the basis of the following mutant screen design.

A screen was designed to look for plants which exhibited a higher than average level of shoot branching in low (1.8mM) NO₃⁻ conditions. To begin, wildtype (Col) seeds were treated using an EMS mutagenesis protocol. Seed was collected from the M1 population and was used throughout the screen. M1 seed was sown onto a mixture of sand and terragreen, to give a nutrient free starting point, which was then supplemented with ATS with an NO₃⁻ concentration of 1.8mM. This concentration is limiting for growth, but it does not result in extreme deprivation. The plants were assessed at 6 weeks old. Any plants with 2 or more rosette branches were selected for further investigation. Further investigation involved two primary stages. The first involved collecting seeds from the plant of interest and regrowth in the same, low nitrate, conditions to check that the phenotype was still present in the next generation. Should the first test be passed the plant underwent complementation testing with *max1-max4* to determine whether the isolated mutant was one of the currently recognised *max* mutants. A complementation test is used to identify recessive mutations in the same gene. If the two

mutants affect the same gene, then when the two plants are crossed, the progeny will exhibit the mutant phenotype associated with that gene. If the mutations are in different genes then the progeny will all be heterozygous for each mutation so no mutant phenotype will be visually evident. Complementation testing revealed 2 *max3* mutants which were then removed from the test group.

4.2 Mutants Isolated using the NO₃⁻ deprivation screen

The screen was designed specifically to isolate mutants with higher than normal levels of branching in a NO₃⁻ limited environment. Any mutants found may be used to further study the control of shoot branching. It is an established fact that *max1* retains higher than normal levels of branching in low NO₃⁻ conditions.

All plants in the screen were assessed at 6 weeks old. If the plant had two or more rosette branches, seed was collected. After the collected seed had dried, it was sown onto the same low NO₃⁻ media used for the screen. The purpose of this was to see if the increased branching phenotype persisted into the F2. For most of the plants selected this was not the case. Two of the selected plants proved to be infertile, *11-1* and *40-17* produced very few seeds that did not germinate. The remaining plants underwent complementation tests with *max1*, *max2*, *max3* and *max4*. Unfortunately, both *5-27* and *30-1* did not complement *max3* and in doing so identified themselves as both being *max3*. The results are summarised in table 8.

This left only one remaining mutant; *17-4*.

Tray/Plant	No of Rosette Branches	Persistence of Phenotype	Complementation Tests			
			<i>max1</i>	<i>max2</i>	<i>max3</i>	<i>max4</i>
1 31	3	NO				
4 2	2	NO				
5 27	3	YES	COMP	COMP	NO COMP	COMP
8 10	2	NO				
8 12	2	NO				
11 1	5	INFERTILE				
11 17	2	NO				
11 29	2	NO				
12 4	3	NO				
14 6	2	NO				
17 4	6	YES	COMP	COMP	COMP	COMP
17 28	2	NO				
22 11	2	NO				
29 38	2	NO				
30 1	3	YES	COMP	COMP	NO COMP	COMP
31 3	2	NO				
38 2	2	NO				
40 17	3	INFERTILE				
41 4	2	NO				

Table 8. Mutants isolated in the NO₃⁻ deprivation screen. Seed collected from each mutant were collected and sewn to check for fertility and persistence of the increased branching phenotype. The plants that were both fertile and retained the increased branching phenotype underwent complementation testing with the *max* mutants to check for *max* identity. 5-27 and 30-1 complemented with *max3*. 17-4 however did not complement with any of the *max* mutants.

Once all of the initial testing mentioned above was complete, *17-4* was backcrossed 4 times into Col to ensure the removal of other mutations (although it is not possible to say whether all other mutations have been removed) which could affect the outcome of further tests. The results of the basic phenotypic analysis are shown below. *17-4* has been measured alongside both *max1* and *max2*, as representative strigolactone synthesis and signalling mutants (figures 38-40).

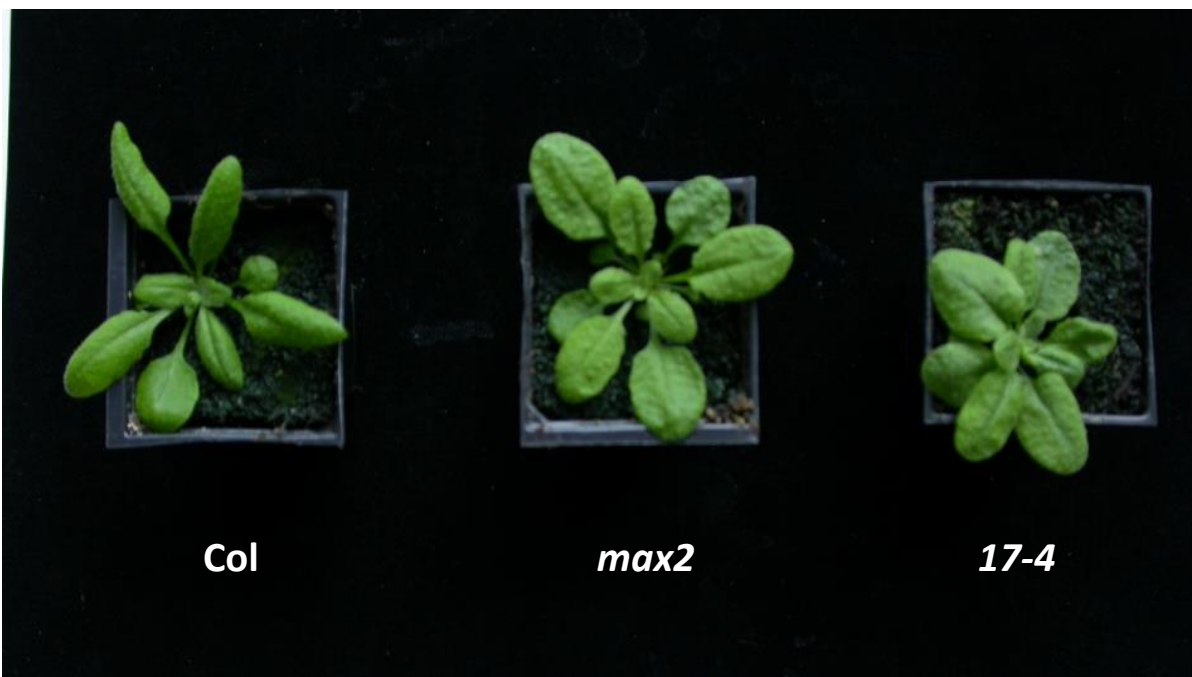


Figure 38. 28 day old Col, *max2*, and *17-4* plants. The morphological similarities between *max2* and *17-4* rosette leaves during the vegetative growth phase can be seen in this image. The *17-4* rosette is more compact than that of either Col or *max2* and the rosette leaves seen in Col appear narrower than in *max2* or *17-4*.



Figure 39. 6 week old examples of Col, *max2* and *17-4* plants. The similarities between *max2* and *17-4* are evident. Both *max2* and *17-4* exhibit reduced height, increased rosette branching, and a fuller rosette when compared to wildtype plants.

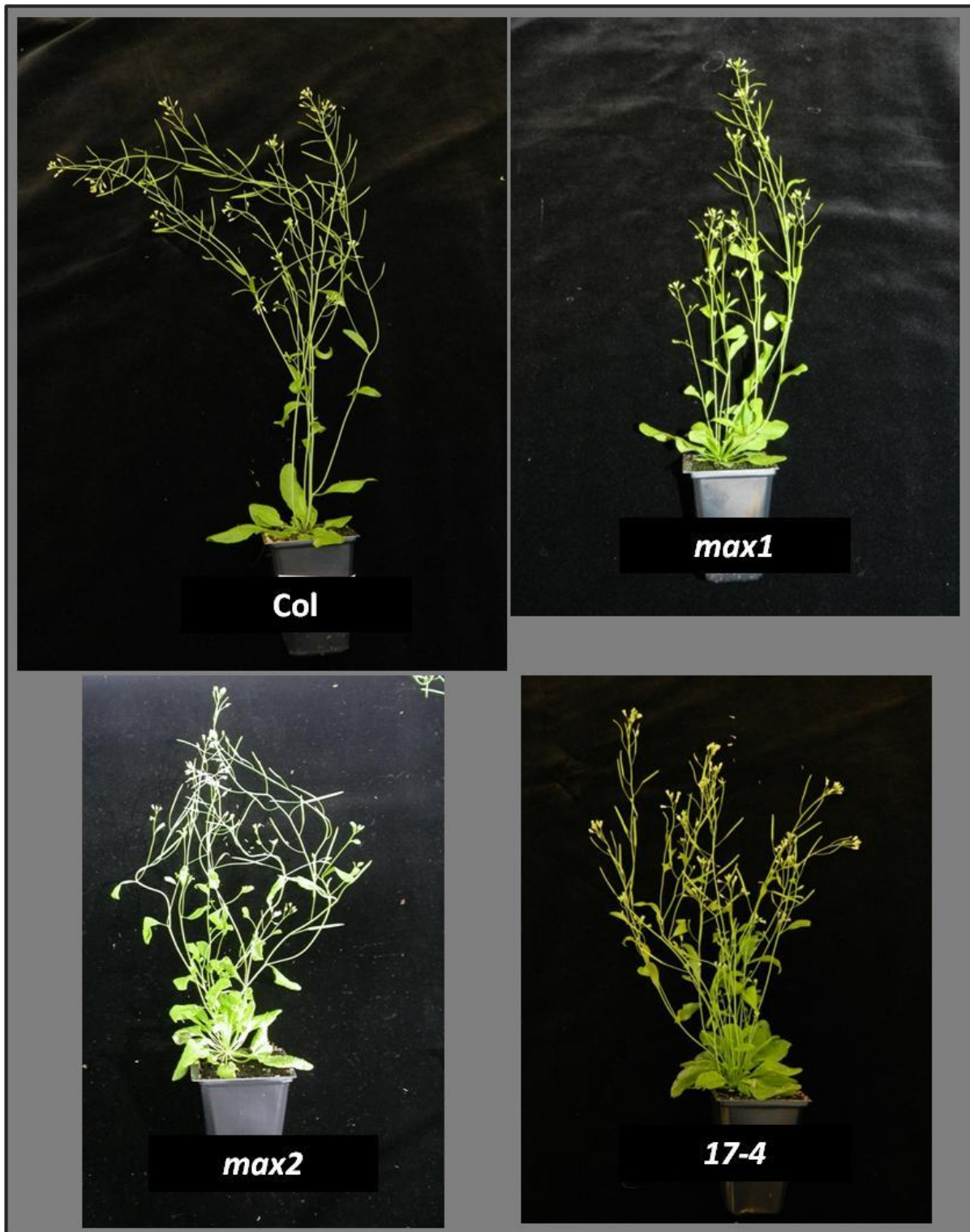


Figure 40. Comparative aerial morphology of 6 week old Col (here serving as a wildtype example), *max1*, *max2* and 17-4. The *max1* and *max2* mutants exhibit increased branching levels and decreased height, when compared to Col, established phenotypes conferred by mutation in *max1* and *max2*. The 17-4 plant exhibits a similar height to *max1* and *max2* but apparently higher levels of rosette branching than either of the *max* mutants.

Plants shown are 6 weeks old.

As seen above, *17-4* and both *max1* and *max2* have certain traits in common. As a first example, all three of these mutants have a shortened stature compared to wildtype plants. The reduction in height seen in *max1* plants is less pronounced than in *max2* and *17-4*. Of the two shorter phenotypes, *17-4* is the taller but is unlikely to be significantly different (figure 41).

It has previously been noted that *max1* plants have shorter cauline leaf internodes along the bolting stem than wildtype plants (see figure 42). This characteristic is again evident in this dataset and distinguishes *max1* from both *max2* and *17-4*. *17-4* and *max2* bolting stem internodes were both found to be longer than those of *max1*, with the exception of the most basal internode which was comparable in length in all three genotypes. A fourth internode is not present in approximately 35% of 6 week old *17-4* plants. This could be because of a slightly slower rate of growth (noted but not quantified) seen in *17-4* compared to other genotypes studied.

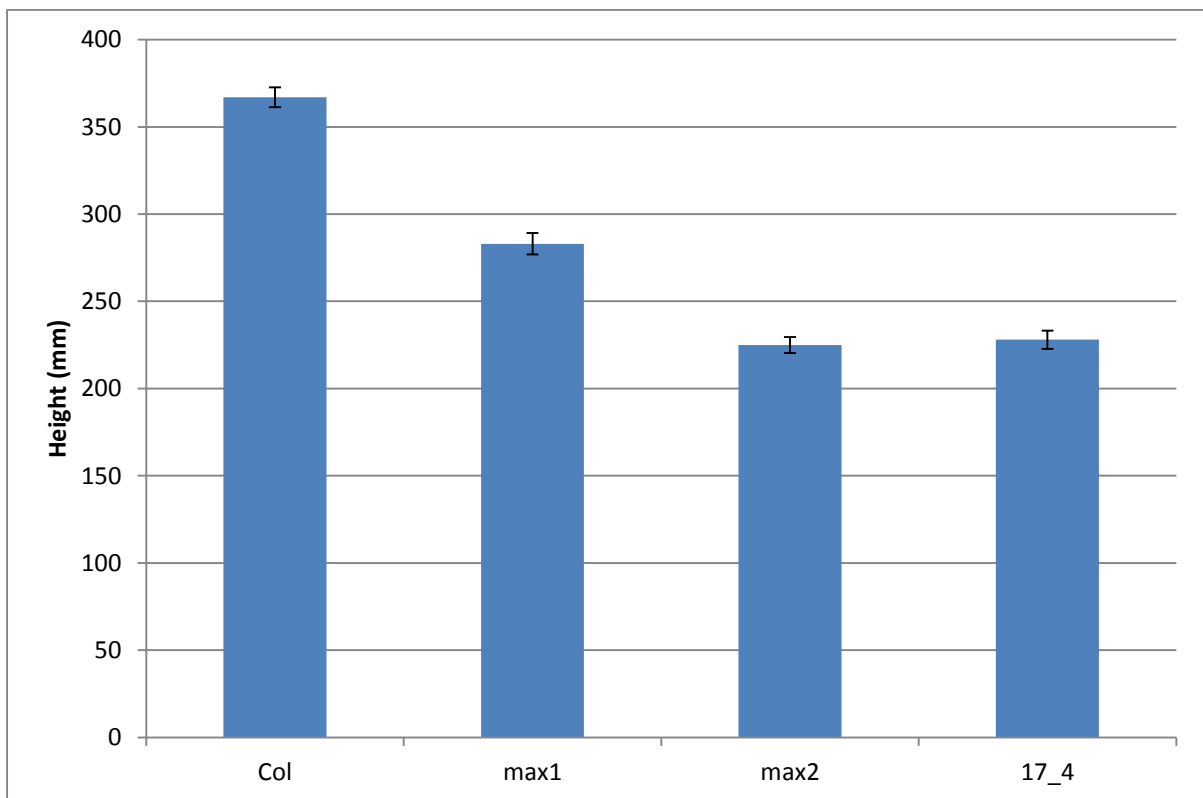


Figure 41. Average heights of 6 week old Col, *max1*, *max2* and *17-4* plants. *max1* is shorter in stature than Col, with *max2* and *17-4* exhibiting a further reduction in height.

Error bars indicate standard error N =30 ANOVA Col, *17-4* sig. = 0.008. *max1*, *17-4* sig. = 0.021. *max2*, *17-4* sig. = 0.137.

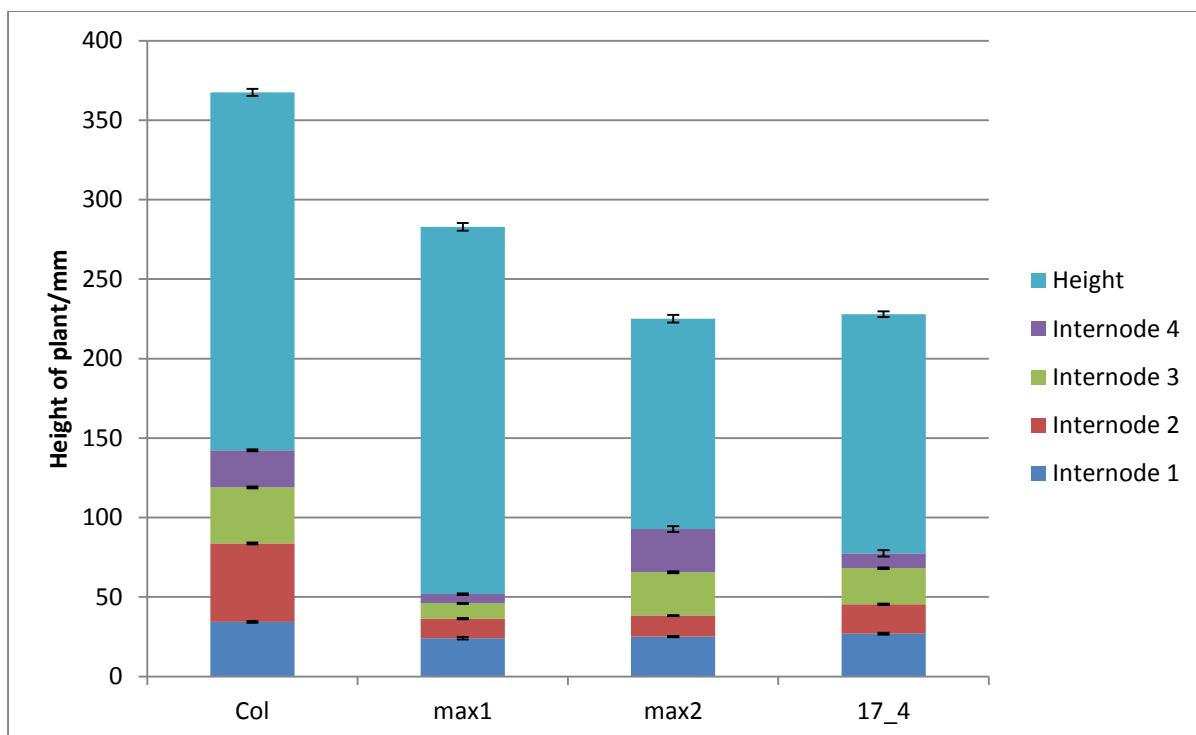


Figure 42. Average cauline internode lengths and total heights of 6 week old Col, *max1*, *max2* and *17-4* plants.

Error bars indicate standard error N =30. ANOVA (height) Col, *max1* sig. = 0.024. Col, *max2* sig. = 0.010. Col, *17-4* sig. = 0.013. *max1*, *max2* sig. = 0.019. *max1*, *17-4* sig. = 0.017. *max2*, *17-4* sig. = 0.092.

The difference in leaf shape between Col and the three mutants is pronounced. Apart from Col leaves being appreciably narrower than those of *max1*, *max2* and *17-4*, there is also a considerable difference in length. Col rosette leaves have longer leaves (average 33.5mm) and petioles (average 17.2mm) are longer than those of the other genotypes. The shortest leaf length is found in *max1* plants at an average of 22.5mm. This is shortly followed by *max2* (average 25.3mm) and *17-4* (average 27.5mm). Rosette leaves of *17-4* are significantly different in length from those of *max1*, but not those of *max2*. As expected the petioles of *max1* and *max2* are shorter than those of Col plants. The compact rosette of *17-4* plants (see figures 38-40 and 43) suggests that petiole length is reduced to a greater degree than either of the *max* mutants and this is indeed the case. The average petiole length in *17-4* is 9.3mm. Because the leaf blade lengths are similar between the mutants, it is this shortened petiole length that gives *17-4* its characteristic compact rosette compared to *max1* and *max2*. The leaf blade length to petiole length ratios are significantly lower for Col (1:1.95), *max1* (1:2.03), and *max2* (1:1.91) than for *17-4* (1:2.95).

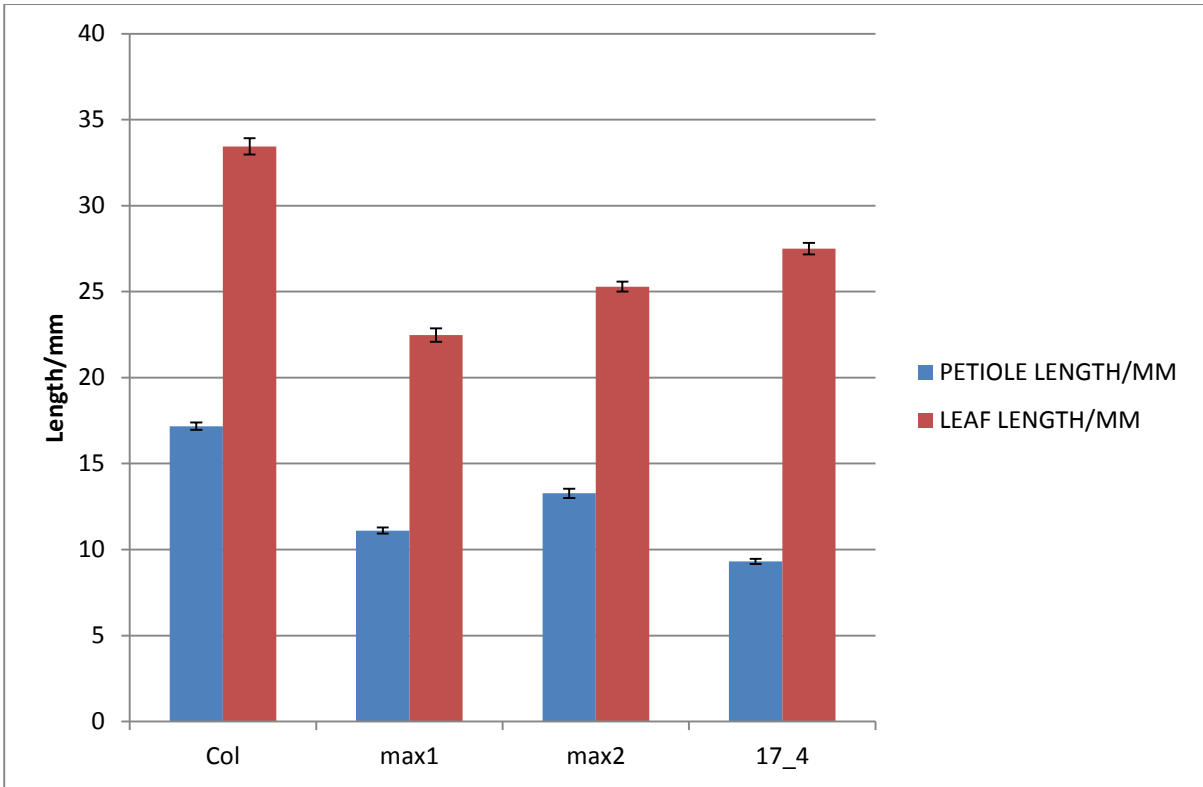


Figure 43. Average leaf length and petiole length of 6 week old Col, *max1*, *max2* and *17-4* plants.

Error bars indicate standard error N =30 ANOVA (leaf length) Col, *max1* sig. = 0.014. Col, *max2* sig. = 0.012. Col, *17-4* sig. = 0.022. *max1*, *max2* sig. = 0.067. *max1*, *17-4* sig. = 0.057. *max2*, *17-4* sig. = 0.048. ANOVA (petiole length) Col, *max1* sig. = 0.031. Col, *max2* sig. = 0.036. Col, *17-4* sig. = 0.040. *max1*, *max2* sig. = 0.062. *max1*, *17-4* sig. = 0.051. *max2*, *17-4* sig. = 0.043.

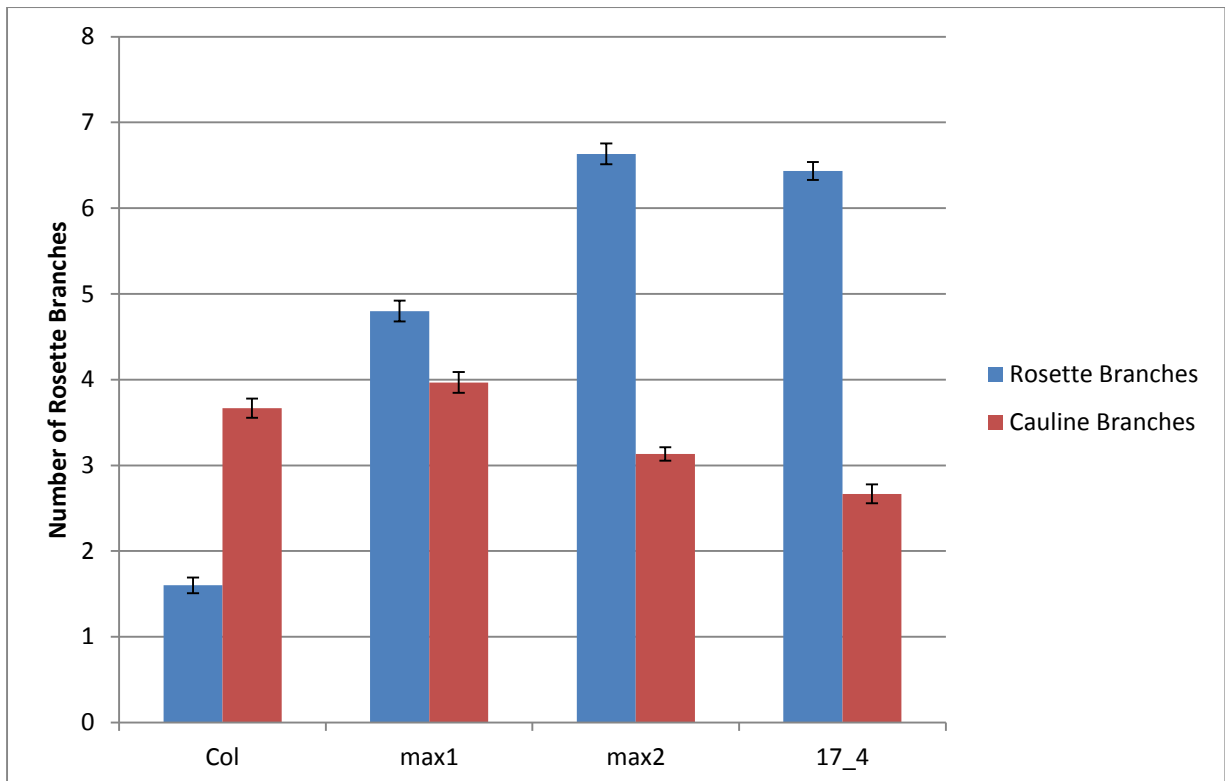


Figure 44. Average number of rosette branches of 6 week old Col, *max1*, *max2* and *17-4* plants.

Error bars indicate standard error N =30. ANOVA (rosette branches) Col, *max1* sig. = 0.008. Col, *max2* sig. = <0.001. Col, *17-4* sig. = <0.001. *max1*, *max2* sig. = 0.017. *max1*, *17-4* sig. = 0.019. *max2*, *17-4* sig. = 0.056. ANOVA (cauline branches) Col, *max1* sig. = 0.276. Col, *max2* sig. = 0.071. Col, *17-4* sig. = 0.041. *max1*, *max2* sig. = 0.044. *max1*, *17-4* sig. = 0.037. *max2*, *17-4* sig. = 0.046.

The final area of phenotypic comparison concerns branching levels. Both Rosette and cauline branches were counted, giving a complete analysis of primary shoot branching. In *Arabidopsis* buds activate in a basipetal gradient and thus when there are rosette branches, this indicates that all cauline nodes have produced a branch. Variation in cauline branch numbers is therefore caused by variation in cauline node numbers. As noted above, *17-4* has on average fewer cauline nodes than WT. Because all cauline nodes produce a branch, variation in branching is most clearly reflected in the number of rosette branches. Here, the analysis agrees with results obtained previously with regards comparative branching levels of Col, *max1*, and *max2*. Col, with an average of 1.6 rosette branches has significantly fewer than either *max1* (average 4.8 rosette branches), or *max2* (average 6.6 rosette branches) (figure 44). *17-4* plants have an average of 6.4 rosette branches (figure 43). This is a very similar number to *max2* but significantly higher than either *max1* or Col.

4.3 Auxin Status of *17-4*

Both auxin transport levels and auxin-mediated repression of bud outgrowth in *max1* plants are unlike those seen in wildtype plants. Increased auxin transport and resistance to auxin-mediated apical dominance are characteristic features of *max1*. As *17-4* was isolated in a screen designed to identify mutants behaving like *max1* in a low nutrient environment, establishing the auxin status of *17-4* and comparing it to that of *max1* will give a very good insight into the aspects of branching control that are affected in *17-4*.

The first phase of the investigation concerned polar auxin transport (PAT) levels. It is well established that *max1* consistently demonstrates higher levels of PAT than wildtype *Arabidopsis* plants. Standard auxin transport assays were carried out using; wildtype plants (Col), *max1* plants, and *17-4* plants. The method for the auxin transport assay used is detailed on page 49. The results show a level of auxin transport in *17-4* that is similar to that of *max1* (figure 45). Auxin transport in *17-4* is therefore higher than that of wildtype. This can be seen as a definite contributing factor to the increased branching phenotype of *17-4*.

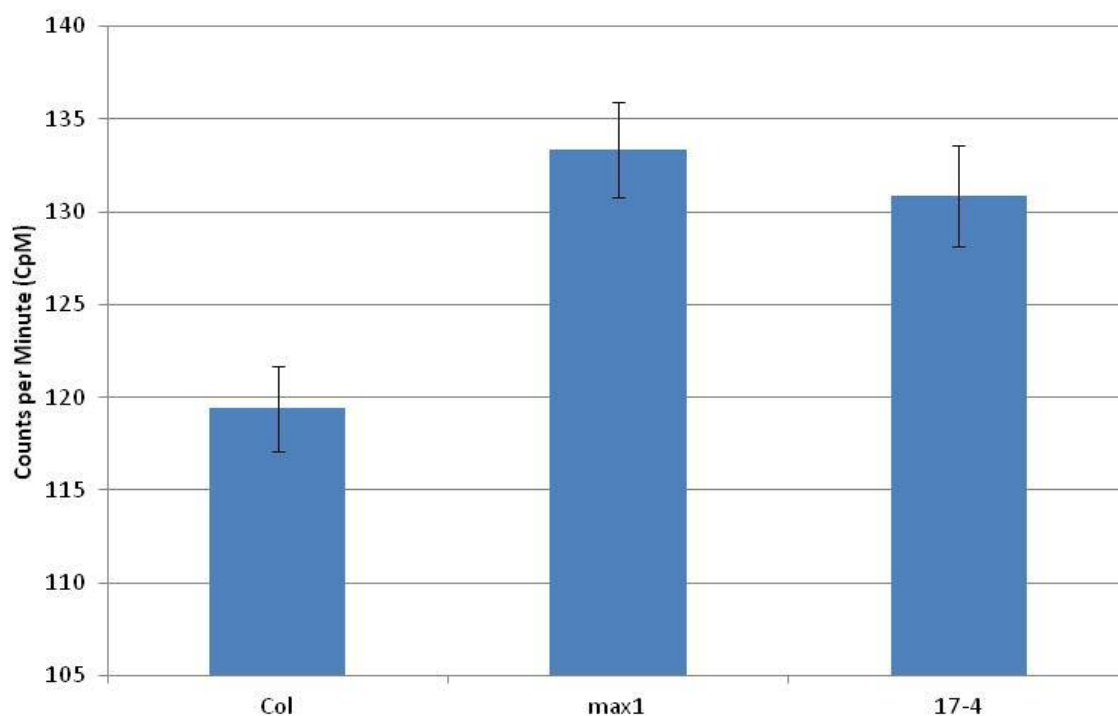


Figure 45. Auxin transport levels in Col, *max1*, and *17-4*. Auxin transport in *17-4* is significantly higher than that in Col and not dissimilar to that of *max1*.

Stem segments were taken from glasshouse grown, 6 week old plants. 30 plants of each were used for each experiment with 3 replicates completed.

Error bars indicate standard error N=30. ANOVA (leaf length) Col, *max1* sig. = 0.029. Col, *17-4* sig. = 0.032. *max1*, *17-4* sig. = 0.241.

Auxin transport is not the only factor that can affect the auxin-mediated repression of bud outgrowth. As mentioned above, a level of resistance to apical dominance is characteristic of *max1* mutants and they exhibit bud outgrowth even in the presence of apically applied auxin. The split plate assay detailed on page 50 was used to demonstrate the relative levels of auxin resistance of Col, *max1*, and *17-4* plants. The results can be seen in figure 46. In the absence of apically applied auxin all three genotypes has very similar bud growth trajectories. When 1 μ M auxin is applied to the apical end of the stem segment, simulating an actual plant apex, the growth curves are altered. Strong repression of bud outgrowth is seen in Col. The auxin resistance of *max1* can clearly be seen in the increased bud outgrowth compared to Col. A similar level of resistance can also be seen in *17-4*. These results suggest that the auxin status of *17-4* is very much like that of *max1*. It can be inferred from these results that the increased branching phenotype of *17-4* has an increased level of auxin transport and a partial resistance to apical auxin, as contributory factors.

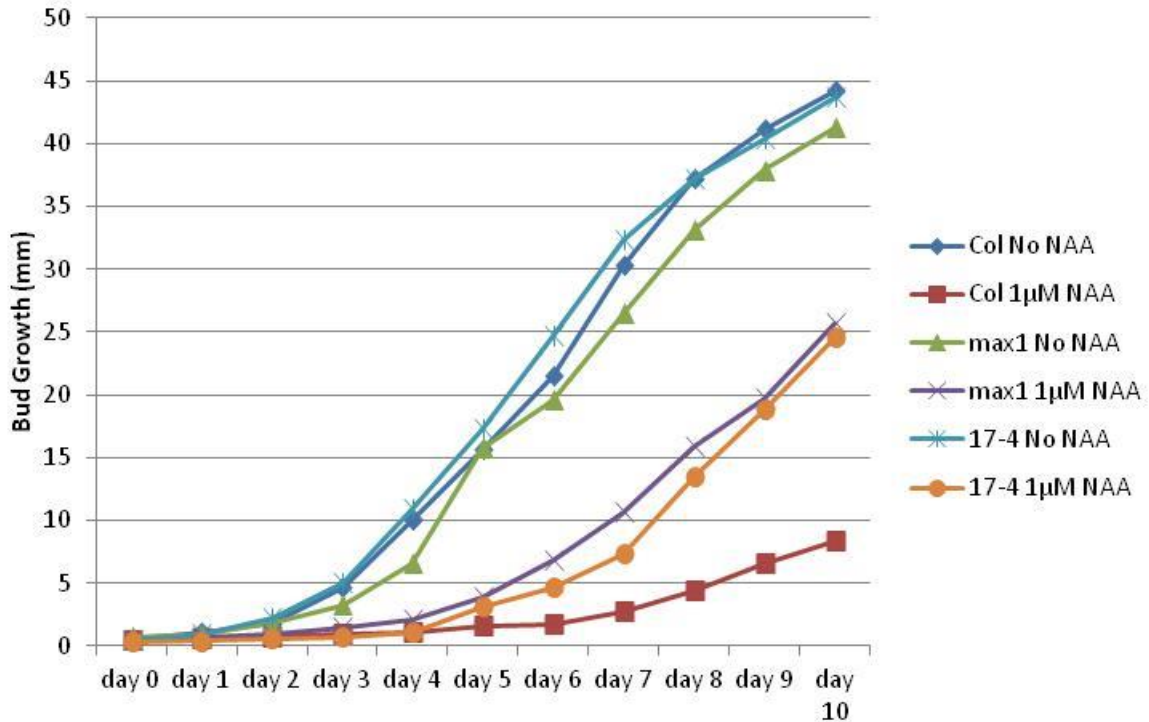


Figure 46. Bud auxin response in Col, *max1*, and *17-4*. All three genotypes exhibit a similar growth curve in the absence of apically applied auxin. When a simulated apex is added, in the form of 1µM of the synthetic auxin NAA, bud outgrowth levels drop severely in Col. The response in both *max1* and *17-4* is far less pronounced suggesting a degree of resistance to apical auxin.

Plants used were grown anexically in weck jars under standard growth room conditions. Stem segments were transferred to split plates when the plants had produced between one and two buds.

Approximately 30 plants of each genotype were used for each experiment, of which there were 3 replicates.

N=30

4.4 The effect of exogenous GR24 on the *17-4* branching phenotype

The *17-4* genotype has so far been shown to produce plants which behave very much like *max1* insofar as they have similar auxin transport levels and similar bud growth trajectories in the presence of apically applied auxin. Recently, strigolactones (SL) have been shown to play an important role in the control of shoot branching with a SL, or SL derivative being identified as the mobile product of the *MAX* biosynthetic gene pathway (figure 8). This means that, as *MAX1*, *MAX3*, and *MAX4* are involved in the biosynthesis of the strigolactone compound their mutants are deficient in specific SL production and branching is not suppressed. *MAX2* and

D14 have been shown to be necessary for SL responses (Soundapanna, I. *et.al.* (2015)) (Chevaliera, F. *et.al.* (2014)). Growing plants on media containing the synthetic SL GR24 has previously been carried out and demonstrated the ability of GR24 to reduce branching levels in Col, the biosynthetic *max* mutants, but not *max2* (Stirnberg, P. personal communication). The reduction seen in *max2* was far less pronounced than in other genotypes tested. This is because strigolactone production is not affected in *max2*, only its perception. The following experiment was carried out to determine the effect of GR24 on *17-4*, the results are shown in figure 47.

Col and *max1,3* and *4* behave as expected with a low concentration (0.1 μ M) of GR24 being sufficient to reduce branching levels significantly. Higher concentrations have a greater effect resulting in considerable repression across all genotypes tested with almost complete repression of Col at 10 μ M GR24. The response of *max2* to 0.1 μ M GR24 is a dramatic (over 50%) reduction in branching levels but this is where the similarity between *max2* and the other genotypes tested ends. The presence of greater concentrations of GR24 do not result in any further decrease in branching levels. As mentioned above, usually there is no effect on *max2*, and it would be surprising for a resistant mutant to respond to a low concentration of something but then not to a higher concentration. These results still demonstrate that *17-4* is a response mutant but the results are not entirely as expected. The dose dependent result seen in the other genotypes is not seen here. The *17-4* reaction is very much like that of *max2*. A small amount of GR24 is sufficient to restore partially wildtype branching levels but they cannot be further restored by more GR24. The mutants that experienced a greater response to exogenous GR24 are all involved in SL biosynthesis (*max1*, *max3*, and *max4*), the response seen in *max2* was unexpected and this experiment should be repeated, to rule out other conditions that may have affected branching number. These data suggest that *17-4* is either involved in a SL-independent bud repression system or takes part in a process that is downstream of *MAX1* in the bud growth regulation pathway.

With this in mind PCR and sequencing was used to see if *17-4* was *D14*. This is a possibility as *D14* acts downstream of *MAX1* and is involved in the SL response. The preliminary results were negative, with no sequence differences detected (data not shown). *17-4* is therefore unlikely to be *D14* but this does not rule out another role in the *MAX* pathway.

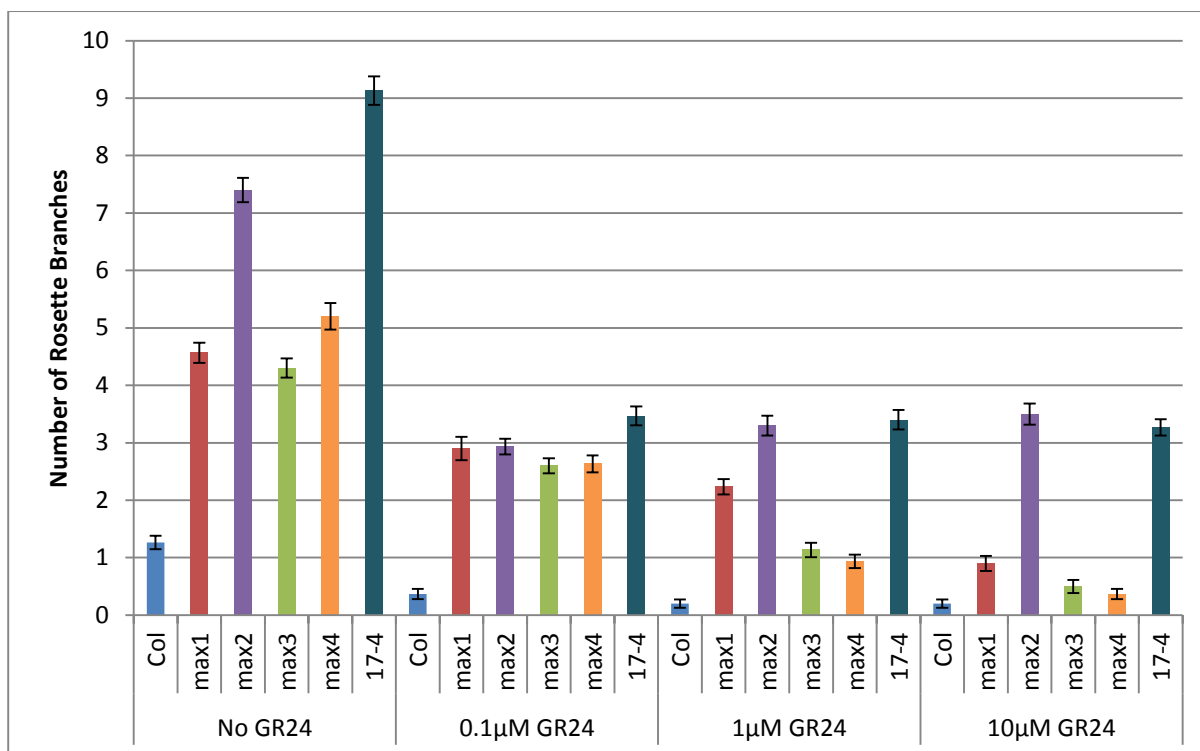


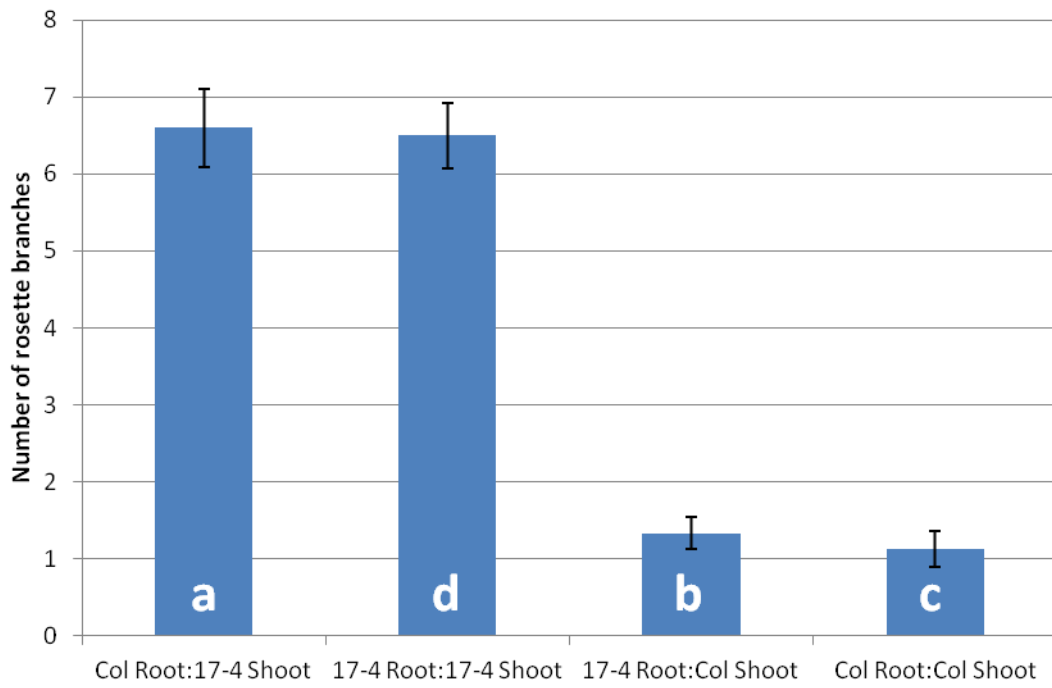
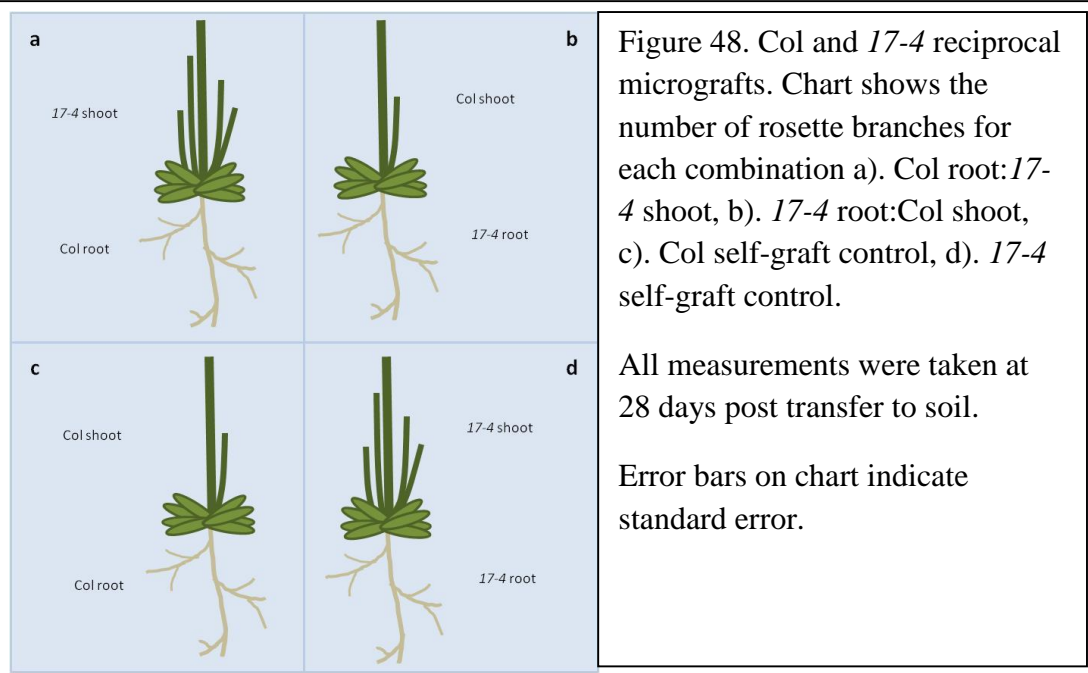
Figure 47. Rosette branching in plants grown in Weck jars on media supplemented with different concentrations of the synthetic SL GR24.

Plants were grown anexically under standard glasshouse conditions on ATS media and measured at 4 weeks post germination.

4.5 Reciprocal Micrografting of Col and 17-4

Micrografting techniques (see page 51) were used to join the root and shoot stocks of both Col and 17-4 in all possible combinations. The purpose of this experiment was to see whether a wildtype root stock could restore normal branching levels 17-4 shoots, which show high levels of branching. Restoration of wildtype branching using this method would indicate that bud outgrowth was controlled remotely by a signal molecule synthesised in the roots (not necessarily exclusively). The signal would travel acropetally, across the graft union, to its point of action in the shoot. Several other highly branched mutants, *max1*, *max3*, and *max4*, behave in this way, being involved in a biosynthetic pathway which produces a strigolactone or strigolactone-derivative which inhibits branching indirectly at the node (Bennett, T. *et al* (2006)) (Stirnberg, P. *et al* (2002)) (Brewer, P.B. *et al* (2009)). Determination of shoot phenotype was based on the number of rosette branches, 2 branches or less being the cut off

point for Col and 3 or more indicating *17-4* (it should be noted that *17-4* rarely has fewer than 5 rosette branches). Measurements were taken at 28 days after the grafted plants were transferred from ATS media to soil. Figure 48 shows the results of the reciprocal grafts. Figure 48(a) shows the shoot branching levels of a *17-4* shoot grafted onto a wildtype rootstock. Branching levels remain significantly higher than wildtype with an average of 6.6 rosette branches per plant which is not significantly different from the *17-4* self-graft control. These results show that the *17-4* branching phenotype is not graft rescuable. That is not to say that it is not involved in the *MAX* branching control pathway. The genes involved in producing the strigolactone-based signal are only one part of the pathway with downstream processes involving the perception and transduction of the signal, for example, the *MAX2* gene is required for strigolactone response and, like *17-4*, *max2* mutants shoots are not graft rescuable by wildtype roots. It is here that a possible role for *17-4* should not be ruled out. The reciprocal graft: Col shoot onto a *17-4* rootstock, resulted in wildtype shoot branching, not significantly different from the Col self graft control, showing the inability of a *17-4* root to confer its branching phenotype on a wildtype shoot.



4.6 Discussion

As an initial comment, the low nitrate screen which isolated *17-4* cannot be described as particularly successful. To produce a single viable mutant, along with two *max3* mutants was a disappointing result. The *max3* plants could have been the result of contamination but every effort was made to ensure strict protocol was followed making this unlikely. The lack of highly branched mutant isolated in this screen can be seen as a result in itself, suggesting a strong link between local nitrate availability and shoot branching levels. The fact that the only viable mutants produced were either part of the SL biosynthesis pathway, i.e. the *max3* mutants, or potentially involved in SL signalling also suggests a connection between SLs and nitrate availability. With this in mind the low nitrate screen would not necessarily have been useful for isolating mutants which would allow an insight into elements of branching control that are independent of SLs. A larger scale screen may well have produced more mutants in downstream SL signalling but given the low-throughput outcome it seems unlikely.

Despite the similarities between *17-4* and *max2*, both morphological and physiological, complementation testing has ruled out the possibility that *17-4* is a current recognised allele of *max2*. There remains the possibility that *17-4* is a novel allele of *max2* capable of intra-allelic complementation. The most common mechanisms for intra-allelic complementation are either (1) The protein works as a dimer and a functional dimer can be constituted from the two mutant alleles e.g. if you had a transcription factor that worked as a dimer and one allele was mutant in the nuclear localisation sequence and the other in the transcriptional activation domain, the heterodimer might be able to get into the nucleus and activate transcription. (2) The protein has two distinct activities that can function independently. For MAX2 maybe there are two targets that need to be degraded and one allele can recruit one to the SCF, and the other can recruit the other. For shoot branching suppression, both targets would need to be degraded.

Initial mapping work by the Leyser lab has since discovered that *17-4* is on AtCh2, the same chromosome as *MAX2*. This makes the prediction that *17-4* is a novel allele of *max2* even more likely. *MAX2* has yet to be sequenced in *17-4*. This seems like a logical next step.

The *17-4* increased branching phenotype is probably a result of both its increased auxin transport capacity and a resistance to the inhibitory effects of auxin on bud outgrowth. *17-4* is not graft rescuable and is therefore not involved in SL biosynthesis. This is not to say that *17-4* is not involved in the *MAX* pathway. Downstream perception and transduction of the SL signal apparently requires *17-4*.

Growing *17-4* on media containing GR24 does not fully restore branching levels. This suggests that *17-4* takes part in a process that is downstream of *MAX1* in the bud growth regulation pathway. The reaction of *17-4* to GR24 is strikingly similar to that of *max2* adding further weight to the argument that *17-4* is a novel allele of *MAX2*. The initial response to GR24 is a marked reduction in branching. *MAX2* is involved in SL perception. Without *MAX2*, SL cannot inhibit branching via this pathway. There are thought to be *MAX2*-independent SL signalling pathways (Waldie, T. *et.al.* (2014)) which would allow some repression of branching to occur, even in the absence of *MAX2*. These *MAX2* independent pathways exist only in theory for the present and in no amount of detail.

As *17-4* seems to function in the same part of the *MAX* pathway as *D14* (figure 48) it was postulated that *17-4* may be the *Arabidopsis D14*. Results were negative so this probably isn't the case, but a role for *17-4* in this stage of SL signal processing should not be ruled out. *17-4* may be neither *MAX2*, or *D14* but still be involved in SL signalling. There are several candidates downstream of *MAX2*. There is much unknown about SL signalling. *MAX2*-mediated protein degradation is an essential element of SL signalling. Like *max2*, mutations in *17-4* produce a highly branched phenotype that is not graft rescuable (Stirnberg, P. *et.al.* (2002)). This is explained by cell autonomous nature of *MAX2* function (Stirnberg, P. *et.al.* (2007)). Supporting the suggestion that *17-4* is not *D14* is the nature of the *d14* mutant which does not demonstrate additional phenotypes which are seen in *max2/rms4/d3* mutants such as a lower than wildtype germination rate and elongated hypocotyls. It has been suggested that these phenotypes are a result of the involvement of *MAX2/RMS4/D3* in KAI-2-dependent signalling. (Stirnberg, P. *et.al.* (2002) (Waters, M.T. *et.al.* (2012b) (Nelson, D.C. *et.al.* (2011) (Scaffidi, A. *et.al.* (2013))). Little is known about KAI-2 signalling other than it is thought to involve KAI-2 as a receptor for an SL-related compound and has been co-opted as the receptor for the smoke-derived signal molecule karrikin which is important in species that grow after fires. (reviewed in Flematti, G.R. *et.al.* (2015))). The reduction in branching seen in *17-4* plants treated with GR24 was unexpected and may be the result of *MAX2*-independent signalling. As so little is known about these potential signalling pathways it would be highly speculative to suggest a link.

As mentioned above, it is possible that *17-4* is one of the downstream signalling targets of *MAX2* and/or *D14*. This list of candidates starts with the direct interactors of *MAX2* and *D14*. The first possibility is that *17-4* encodes an *Arabidopsis* DELLA protein. The rice DELLA protein SLR1 interacts with SL, in vitro (Nakamura, H. *et.al.* (2013)) and *della* mutants have

increased branching phenotypes (Bassel, G.W. *et.al.* (2008)). Data from experiments in pea suggest that SL and DELLAs act independently in the shoot, making their role in shoot branching more questionable (de Saint Germain, A. *et.al.* (2013)) but this does not necessarily rule DELLA proteins out as candidates for 17-4. BES1 (BRASSINOSTEROID INSENSITIVE1 EMS SUPPRESSOR) has been shown to interact with MAX2 in several assays, albeit in an SL-independent manner. Despite the SL-independent nature of SL BES1 interaction, GR24 can reduce BES1 stability in a process which requires MAX2. BES1 stability appears to be enhanced in *d14* mutants although no interaction between BES1 and D14 has been identified. It may be the case that SL signalling results in degradation of BES1 via MAX2/D14. Hyperstable gain of function mutations of *BES1* also result in an increased branching phenotype (de Saint Germain, A. *et.al.* (2013)).

Another possibility is that *17-4* is a second site suppressor of *max2/d14*. Phenotypes of SL mutants are likely a result of a build-up of proteins that would ordinarily be targeted for degradation via SCF^{MAX2}. The *SUPPRESSOR OF MAX2 1 (SMAX1)* suppressor of *max2* seedling phenotypes (Stanga, J.P. *et.al.* (2013)). The *smax1* mutation does not rescue the *max2* branching phenotype. There are eight *SMAX1-LIKE (SMAXL)* genes in *Arabidopsis* and *SMAXL7* is highly expressed in the shoot making it possible that it is involved in SL signalling downstream of MAX2 (Stanga, J.P. *et.al.* (2013)) and therefore a potential candidate for *17-4*.

A dominant mutation in *D53* in rice results in short, high tillering plant, characteristic of SL mutants (Jiang, L. *et.al.* (2013) (Zhou, F. *et.al.* (2013)). *D53* encodes a rice SMAXL. *D53* interacts with D14 in a SL-dependent manner. It is a possibility that *17-4* is an *Arabidopsis D53* orthologue. This could be tested by sequencing the *D53*-like proteins SMAXL6, SMAXL7 and SMAXL8 (Wang, L. *et.al.* (2015)) in *17-4*.

SL acts systemically by initiating the recycling of the PIN1 auxin efflux proteins from the cell membrane (Bennet, T. *et.al.* (2006) (Crawford, S. *et.al.* (2010) (Shinohara, N. *et.al.* (2013)). The mechanism of SL action involves triggering rapid depletion of PIN1 from the plasma membrane. This process is clathrin-dependent and is in all probability endocytosis (Shinohara, N. *et.al.* (2013)). *17-4* could be a part of this mechanism. A logical first step in assessing this possibility would be to use a GFP:PIN1 based analysis to checked both PIN1 levels and localisation in *17-4* individuals.

As well as acting systemically via PIN1, SLs also transcriptionally upregulate several genes in the *TCP* family in bud (Braun, N. *et.al.* (2012) (Dun, E. *et.al.* (2012)). Analysing comparative

transcription levels of *TCP* genes in *max2*, Col, and *17-4* would assess any effect that *17-4* has in this particular mechanism.

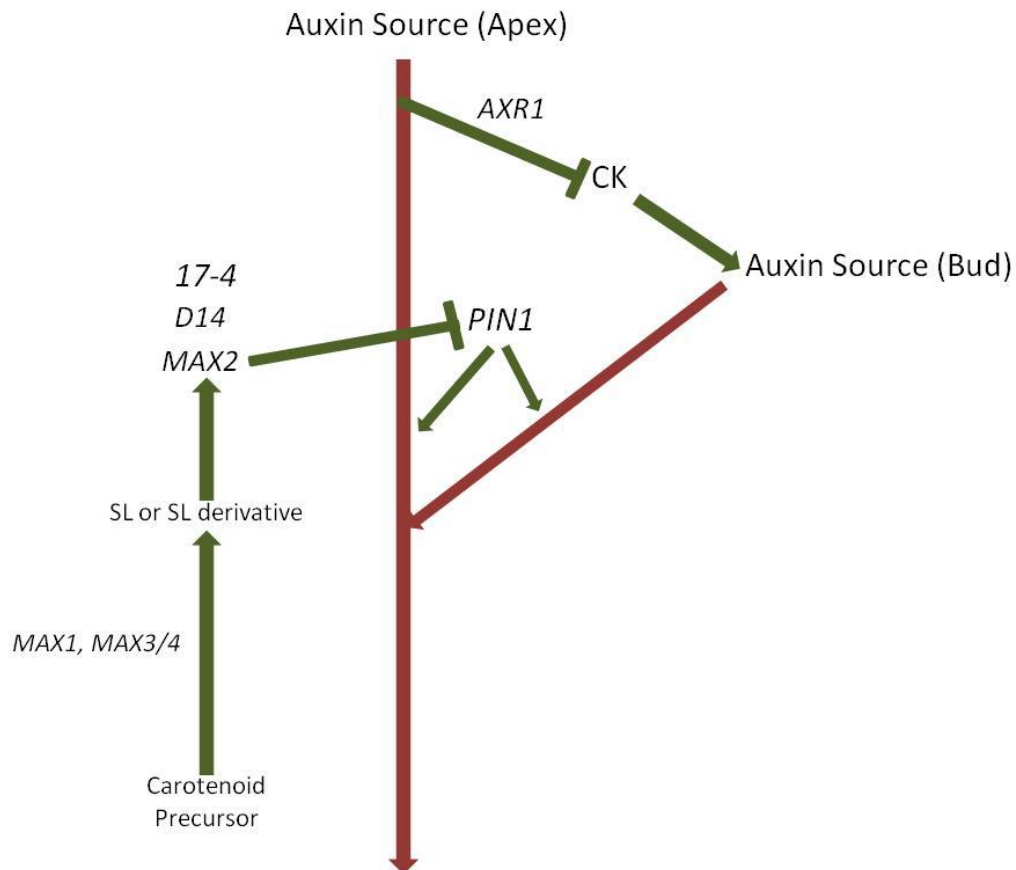


Figure 49. Postulated mechanistic model of the regulation of bud outgrowth. Auxin transport (red arrows) is affected by the amount of the PIN1 auxin efflux proteins present. Reduced auxin transport down the stem reduces its strength as an auxin sink. This results in reduced auxin export from the bud resulting in repression of bud outgrowth.

Cytokinins (CKs) promote bud outgrowth. *AXR1* controls bud outgrowth by several mechanisms, likely to include reducing transcription of CK biosynthetic genes.

17-4 could be involved downstream of the *MAX* pathway, in the transduction of the SL signal.

5. Conclusion

This project has focused on mutations in two genes and their putative involvement in shoot branching in *Arabidopsis*. This work contributes to an ever expanding body of work on the understanding of the mechanisms of shoot branching carried out across the world and in different species.

By characterising the phenotypes generated by the *mad* mutation and delineating the *MAD* locus to an area from which candidate genes can be highlighted and assessed, it has been possible to assign several putative roles for *MAD* in the regulation of shoot branching. Detailed in figure 50 are areas in the proposed mechanism of bud outgrowth control in which *MAD* may act. What is most obvious is that the potential roles for *MAD* are not limited to one area figure 50. Whilst *MAD* may be involved in SL signalling, the results from the candidate gene search did not produce any obvious gene that would suggest this. *MAD* may be more involved, directly (*SPY*), or indirectly (*MES17*) in cytokinin-related bud growth, or may be involved in auxin export from the bud, via PIN1 recycling (*AT3G11130.1*). *17-4* by contrast, appears far more likely to have a role in SL signalling, either at the *MAX2/D14* stage, or further downstream (figure 50). Little is known and even less is certain about the downstream signalling events following SL perception which limits what can be speculated about the role of *17-4*. Further work in this field is continuing rapidly and it may not be long before *17-4* finds a definite role in the regulation of bud outgrowth.

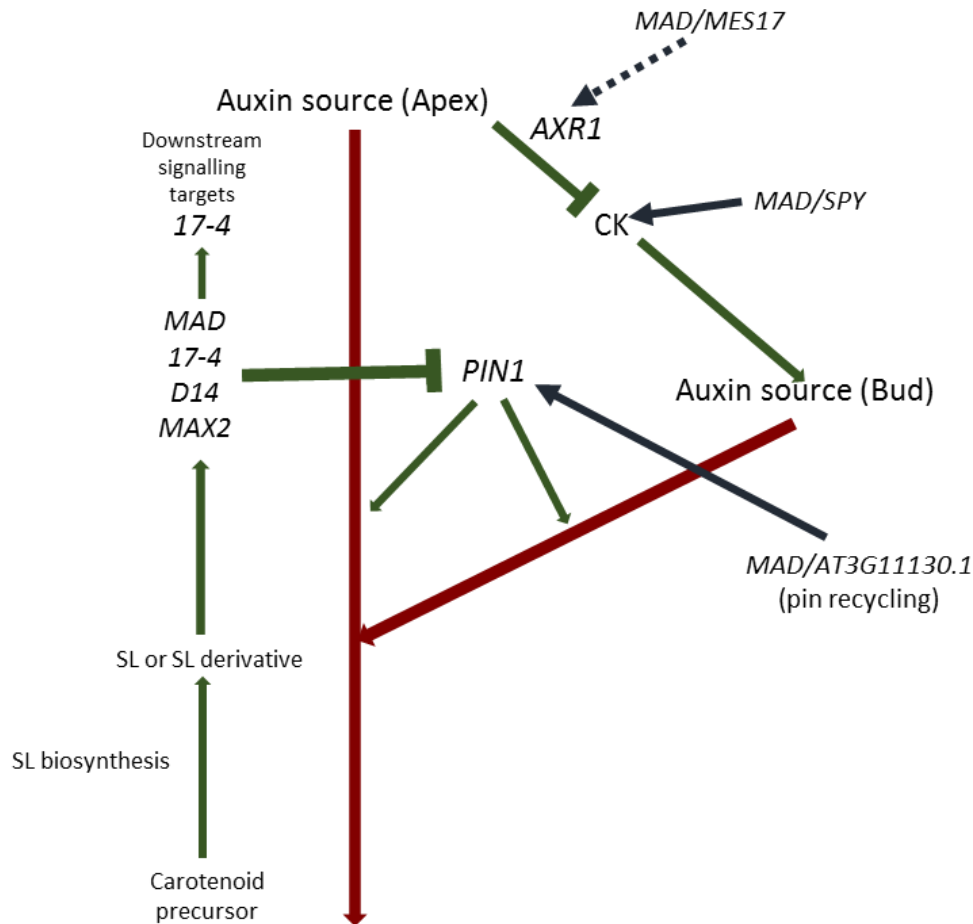


Figure 50. Postulated mechanistic model of the regulation of bud outgrowth incorporation potential roles for both *MAD* and *17-4*.

Auxin transport (red arrows) is limited by the amount of the PIN1 auxin efflux proteins present. Limiting auxin transport down the stem reduces its strength as an auxin sink. This results in reduced auxin export from the bud resulting in repression of bud outgrowth.

Cytokinins (CKs) promote bud outgrowth. *AXR1* controls bud outgrowth by reducing transcription of CK biosynthetic genes. *MES17* is posited to act upstream of *AXR1* (Yang, Y. *et.al.* (2008)).

MAD may act downstream of the *MAX* pathway in the transduction of the SL signal. *MAD* action may be more general; it may affect cytokinin biosynthesis directly, or indirectly, by repressing *AXR1*

MAD could also be involved in PIN1 recycling. The candidate gene *AT3G1130.1* encodes a clathrin protein which hints at a role in endocytosis.

It seems very likely that *17-4* acts either at the *MAX2/D14* stage of SL signalling, or further downstream. The potential candidates are detailed in chapter 4.6.

Black arrows indicated possible *MAD* involvement and dashed lines indicate uncertainty as to the effect of *MAD* action.

weed killers can remove unwanted plants leaving the crop plants behind. Selective weed killers contain an artificial version of auxin or gibberellins which cause rapid unsustainable growth in target plants. Auxin is also used in rooting powders to stimulate root development of cuttings, this is extremely important for plants that do not produce viable seeds or are not self fertile.

The ability to control branching in a species is not only limited to food crops. Extensive work is being done in willow (*Salix spp.*) which can be used as a carbon neutral biofuel. The importance of any alternative energy source to fossil fuels should not be overlooked. Information from *Arabidopsis* sources has been successfully extrapolated to willow with QTL mapping confirming *SxMAX4* as a coppicing response gene (Ward, S.P. *et.al.* (2013), Salmon, J. *et.al.* (2014)).

Arabidopsis has proved invaluable as a model genetic organism, especially since its genome sequencing project ended in 2000 (*A. thaliana* genome (2000)). It has a small genome of only 135Mbp, smaller than expected, its generation time is only six weeks. It is both self-compatible and easily transformable and it is even closely related to Canola, a generic named applied to oil produced from a cultivar of either *Brassica napus* or *Brassica rapa*, both major crop species. *Arabidopsis* is not however of any real agronomic significance. Most of the worlds staple foods are monocots, for example rice and maize, whereas *Arabidopsis* is not only a dicot but it doesn't produce fruit. Seed research is also difficult in *Arabidopsis* as a result of the seeds being too small to work with practically. These aspects of *Arabidopsis* biology place limits on the amount of information that can be extrapolated to cereals and fruit bearing plants. As would be expected from such distantly related species there is very little conservation of gene order exists between *Arabidopsis* and the cereal plant maize, despite approximately 90% of maize proteins having a homolog in *Arabidopsis* (Brendel, V. *et.al.* 2002). This makes the sequencing of more plant genomes a necessity.

Although gene order is hardly conserved between *Arabidopsis* and other species, many gene functions are conserved, for example; developmental pathways, stress responses, nutrient and light responses. Information gathered in *Arabidopsis* can therefore be used to predict the developmental biology of another species, where fewer resources are available, although the limits to extent of synteny between *Arabidopsis* and other species should be considered.

A more targeted mode of action in *Arabidopsis*, or any species with a sequenced genome such as rice, than the reverse genetics approach taken during this study involves selecting a gene

directly from the database, induce a mutation in that gene and observing the phenotypic outcome. To increase levels of shoot branching, for example, the target gene could be involved in branching inhibition like those involved in strigolactone biosynthesis or signalling, or expression levels of a branching stimulant like cytokinin. Precision modification of plant genomes is a very useful tool which can aid in understanding gene function. Through the application of this advance in molecular biology, molecular plant breeding is producing more accurate results. One of the best methods available at the moment for inducing specific DNA sequence changes into genomes is gene targeting via homologous recombination (Endo, M. and Toki, S. (2014)). Another option is CRISPR (Clustered Regularly Interspaced Short Palindromic Repeats), a gene editing technique that relies on the Cas9 enzyme. Cas9 uses a guide RNA molecule to edit targeted DNA by either disrupting the gene or inserting further sequences (Jiang, W. *et.al.* (2014)). The targeted nature of CRISPR makes precise editing possible. Another option is CRISPR (Clustered Regularly Interspaced Short Palindromic Repeats), a gene editing technique that relies on the Cas9 enzyme. Cas9 uses a guide RNA molecule to edit targeted DNA by either disrupting the gene or inserting further sequences (Jiang, W. *et.al.* (2014)). The targeted nature of CRISPR makes precise editing possible.

Microarrays are also being used to identify genes which response to specific stimuli, for example in a recent study, the addition of cytokinin, which elicited responses from genes which turned out to be involved in cytokinin degradation and bud dormancy (Müller, D. *et.al.* (2015)). The pathways involved in cold tolerance in *Arabidopsis* (Fowler, S. and Thomashow, M.F. (2002)), and the identification of an acyl transferase enzyme which is involved in flavour development in strawberries (Aharoni, A. *et.al.* (2000)), are just a couple of examples of discoveries made using microarray data.

Plants cannot always acquire an adventitious trait without another aspect of their development suffering as a consequence. As an example, the *max1* mutant in *Arabidopsis* has an increased branching phenotype and therefore produces more seed per plant, however, in low nutrient conditions *max1* does not allocate as much of its resources to root growth and development as a wildtype (Columbia ecotype) plant. This limits its nutrient uptake as there is reduced root surface area. This phenomenon is known as evolutionary trade-off. Another example is the trade-off between growth rate and defence against herbivory, exemplified in Mooney, K.A. (2010)). These experiments are not always carried out *in vivo*. Virtual plants can have specific traits and be subjected to various conditions in a computational model. These conducted

simulations assess the potential effects of different scenarios with advances in accuracy being made all the time (Bornhofen, S. and Lattaud, C. (2006)).

Comparative genomics is another area to be exploited. A comparative genomics approach is important in allowing theories to be put to the test where reliance on one species would have failed. The impact of comparative genomics on the study of natural variation is substantial. It allows discovery of the molecular basis of complex traits, and genetic pathways by combining cross species data. This is proving especially relevant in cereal crops which have a high degree of orthology. The potential for crop improvement and the exploitation of natural diversity will prove to be important for future developments in this field.

Crop design is a natural follow on from humans taking advantage of natural variants of crops which are generated from wild progenitor plants. Crop improvements are mediated via diverse crops that can adapt to a variety of prevailing conditions to enable food security for the future. With sequencing of genomes such as that of rice, and the development of high-throughput sequencing technology, a large number of genomes from the same species can be collated to detect the genetic basis of phenotypic variations plants. Maps of these genome variations allow genome-wide association studies of both complex traits and evolutionary changes within a species. The GWAS approach has the potential to improve crop studies via genomics-assisted breeding (Huang, X. and Han, B. (2014))

All of the above techniques integrate together as systems biology: combining DNA sequencing, gene expression analyses, metabolite function, genotype and phenotype, to produce a comprehensive understanding of biological processes. Genetic approaches must act synergistically with other methods of study to produce the best outcome for the future of plant science.

References

- Aguilar-Martinez, J.A., Poza-Carrión, C., Cubas, P. (2007) *Arabidopsis* BRANCHED1 acts as an integrator of branching signals within axillary buds. *Plant Cell*, **19**, 458-472
- Agusti, J., Herold, S., Schwarz, M. *et al.* (2011) Strigolactone signalling is required for auxin-dependent stimulation of secondary growth in plants. *Proc. Natl Acad. Sci. USA*, **108**, 20242-20247
- Aharoni, A., Keizer, L.C.P., Bouwmeester, H.J., Sun, Z., Alvarez-Huerta, M., Verhoeven, H.A., Blaas, J., *et al.* (2010) Identification of the *SAAT* Gene Involved in Strawberry Flavor Biogenesis by Use of DNA Microarrays. *Plant Cell*, **12(5)**, 647-662
- Akiyama, K., Matsuzaki, K., Hayashi, H. (2005) Plant sesquiterpenes induce hyphal branching in arbuscular mycorrhizal fungi. *Nature*, **435**, 824-827
- Alder, A., Jamil, M., Marzorati, M., Bruno, M., Vermathen, M., Bigler, P., Ghisla, S., Bouwmeester, H., Beyer, P., Al-Babili, S. (2012) The path from β -carotene to carlactone, a strigolactone-like plant hormone. *Science*, **335**, 1348-1351
- Arite, T., Iwata, H., Ohshima, K., Maekawa, M., Nakajima, M., Kojima, M., Sakakibara, H., Kyojuka, J. (2007) *DWARF10*, an *RMS1/MAX4/DAD1* ortholog, controls lateral bud outgrowth in rice. *Plant J.*, **51**, 1019-1029
- Arite, T., Umehara, M., Ishikawa, S., Hanada, A., Maekawa, M., Yamaguchi, S., Kyojuka, J. (2009) *d14*, a strigolactone-insensitive mutant of rice, shows an accelerated outgrowth of tillers. *Plant Cell Physiol.*, **50**, 1416-1424
- Auldridge, M.E., Block, A., Vogel, J.T., Dabney-Smith, C., Mila, I., Bouzayen, M., Magallanes-Lundback, M., DellaPenna, D., McCarty, D.R., Klee, H.J. (2006) Characterisation of three members of the *Arabidopsis* carotenoid cleavage dioxygenase family demonstrates the divergent roles of this multi-functional enzyme family. *Plant J.*, **45**, 982-993
- Awad, A.A., Sato, D., Kusumoto, D., Kamioka, H., Takeuchi, Y., Yoneyama, K. (2006) Characterisation of strigolactones, germination stimulants for the root parasitic plants *Striga* and *Orobanche*, produced by maize, millet and sorghum. *Plant Growth Regul.*, **48**, 221-227
- Baima, S. *et al.* (1995) The expression of the *Athb-8* homeobox gene is restricted to provascular cells in *Arabidopsis thaliana*. *Development*. **121(12)**, 4171-4182
- Bainbridge, K., Sorefan, K., Ward, S., Leyser, O., (2005) Hormonally controlled expression of the *Arabidopsis* *MAX4* shoot branching regulatory gene. *Plant J.*, **44**, 569-580
- Balla, J., Kalousek, P., Reinohl, V., Friml, J., Prochazka, S. (2011) Competitive canalization of PIN-dependent auxin flow from axillary buds controls pea bud outgrowth. *Plant J.*, **65**, 571-577

- Bangerth, F. (1994) Response of cytokinin concentration in the xylem exudates of bean (*Phaseolus vulgaris* L) plants to decapitation and auxin treatment, and relation to apical dominance. *Planta*, **194**, 439-442
- Bassel, G.W., Mullen, R.T. and Bewley, J.D. (2008) *procera* is a putative *DELLA* mutant in tomato (*Solanum lycopersicum*): effects on the seed and vegetative plant. *J. Exp. Bot.* **59**, 585-593
- Bell, C.J. and Ecker, J.R. (1994) Assignment of 30 microsatellite loci to the linkage map of *Arabidopsis*. *Genomics*. **19(1)**, 137-144
- Bell, E.M., Lin, W.C., Husbands, A.Y., Yu, L., Jaganatha, V., Jablonska, B., *et al.* (2012) *Arabidopsis* lateral organ boundaries negatively regulates brassinosteroid accumulation to limit growth in organ boundaries. *Proc. Natl Acad. Sci. USA*, **109**, 21146-21151
- Bennett, T. and Leyser, O. (2006) Something on the side: axillary meristems and plant development. *Plant Mol. Biol.*, **60**, 843-854
- Bennett, T. *et al.* (2006) The *Arabidopsis* MAX pathway controls shoot branching by regulating auxin transport. *Current Biology* **16(6)**, 553-563
- Beveridge, C.A., Ross, J.J., Murfet, I.C. (1996) Branching in pea (Action of genes *RMS3* and *RMS4*). *Plant Physiol.*, **110**, 859-865
- Beveridge, C.A., Symons, G.M., Murfet, I.C., Ross, J.J., Rameau, C. (1997) The *rms1* mutant of pea has elevated indole-3-acetic acid levels and reduced root-sap zeatin riboside content but increased branching controlled by graft-transmissible signal(s). *Plant Physiol.*, **115**, 1251-1258
- Beyer, P. (2010) Golden Rice and 'Golden' crops for human nutrition. *N. Biotechnol.* **27(5)**, 478-481
- Bishopp, A., Lehesranta, S., Vatén, A., Help, H., El-Showk, S., Scheres, B., Helariutta, K., Mähönen, A.P., Sakakibara, H., Helariutta, Y. (2011) Phloem-transported cytokinin regulates polar auxin transport and maintains vascular pattern in the root meristem. *Curr. Biol.*, **21**, 927-932
- Boer, D.R., Freire-Rios, A., van den Berg, W.A., Saaki, T., Manfield, I.W., Kepinski, S., López-Vidriero, I., Franco-Zorrilla, J.M., de Vries, S.C., Solano, R., Weijers, D., Coll, M. (2014) Structural basis for DNA binding specificity by the auxin-dependent ARF transcription factors. *Cell*. **156(3)**, 577-589
- Booker, J., Chatfield, S., Leyser, O. (2003) Auxin acts in xylem-associated or medullary cells to mediate apical dominance. *Plant Cell*, **15**, 495-507
- Booker, J. *et al.* (2004) MAX3/CCD7 is a carotenoid cleavage dioxygenase required for the synthesis of a novel plant signalling molecule. *Current Biology*, **14**, 1232-1238

- Booker, J. *et al.* (2005) *MAX1* encodes a cytochrome P450 family member that acts downstream of MAX3/4 to produce a carotenoid-derived branch-inhibiting hormone. *Developmental Cell* **8**, 443-449
- Bornhofen, S. and Lattaud, C. (2006) Life History Evolution of Virtual Plants: Trading Off Between Growth and Reproduction
Lec. Not. Comp. Sci., **4193**, 808-817
- Boyer, F.D., de Saint Germain, A., Pillot, J.P. *et al.* (2012) Structure-activity relationship studies of strigolactone-related molecules for branching inhibition in garden pea: molecule design for shoot branching. *Plant Physiol.*, **159**, 1524-1544
- Braun, N., de Saint Germain, A., Pillot, J.P., Boutet-Mercey, S., Bouteiller, N. *et al.* (2012) The pea TCP transcription factor PsBRC1 acts downstream of Strigolactones to control shoot branching. *Plant Physiol.* **158**, 225-238
- Brewer, P.B. *et al.* (2009). Strigolactone acts downstream of auxin to regulate bud outgrowth in pea and Arabidopsis. *Plant Physiol.*, **150(1)**, 482-493
- Busch, B.L., Schmitz, G., Rossmann, S., Piron, F., Ding, J., Bendahmane, A. *et al.* (2011) Shoot branching and leaf dissection in tomato are regulated by homologous gene modules. *Plant Cell*, **23**, 3595-3609
- Byrne, M.E. (2006) Shoot meristem function and leaf polarity: the role of class III HD-ZIP genes. *PLoS Genet.* **2(6)**, e89.
- Carrier, D.J. (2008) The binding of auxin to the Arabidopsis auxin influx transporter AUX1. *Plant Physiol.*, **148(1)**, 529-535
- Casal, J.J. (2012). Shade Avoidance. *Arabidopsis Book*.
- Casal, J.J., Sanchez, R.A., Deregibus, V.A. (1986) The effect of plant-density on tillering – the involvement of R/FR ratio and the proportion of radiation intercepted by the plant. *Environ. Exp. Bot.*, **26**, 365-371
- Casal, J.J. (2013) Photoreceptor signalling networks in plant responses to shade. *Annu. Rev. Plant Biol.* **64**, 403-427
- Cheng, Y., Dai, X., Zhao, Y. (2006) Auxin biosynthesis by the YUCCA flavin monooxygenases controls the formation of floral organs and vascular tissues in *Arabidopsis*. *Genes Dev.* **20(13)**, 1790-1799
- Cheng, Y., Dai, X., Zhao, Y. (2007) Auxin synthesized by the YUCCA flavin monooxygenases is essential for embryogenesis and leaf formation in *Arabidopsis*. *Plant Cell.* **19(8)**, 2430-2439
- Chevaliera, F., Nieminen, K., Sánchez-Ferrero, J.C., Rodríguez, M.L., Chagoyen, M., Hardtke, C.S., Cubas, P. (2014) Strigolactone Promotes Degradation of DWARF14, an α/β Hydrolase Essential for Strigolactone Signaling in *Arabidopsis*. *Plant Cell.* **26(3)**, 1134-1150

- Chitwood, D.H., Nogueira, F.T., Howell, M.D., Montgomery, T.A., Carrington, J.C., Timmermans, M.C. (2009) Pattern formation via small RNA mobility. *Genes Dev.* **23(5)**, 549-554
- Cho, M. and Cho, H-Y. (2013) The function of ABCB transporters in auxin transport. *Plant Signal. Behav.* **8(2)**, e22990
- Cline, M.G. (1996) Exogenous auxin effects on lateral bud outgrowth in decapitated shoots. *Annals of Botany.* **78**, 255-266
- Cook, C. E., Whichard, L.P., Turner, B., Wall, M.E and Egley, G.H. (1966) Germination of witchweed (*Striga lutea* Lour.): isolation and properties of a potent stimulant. *Science*, **154**, 1189-1190
- Cope, G.A. and Deshaies, R.J. (2003) COP9 signalosome: a multifunctional regulator of SCF and other cullin-based ubiquitin ligases. *Cell.* **114(6)**, 663-671
- Crawford, S., Shinohara, N., Sieberer, T., Williamson, L., George, G., Hepworth, J., Müller, D., Domagalska, M.A., Leyser, O. (2010) Strigolactones enhance competition between shoot branches by dampening auxin transport. *Development*, **137**, 2905-2913
- D'Agostino, I.B., Deruère, J., Kieber, J.J. (2000) Characterisation of the response of the *Arabidopsis response regulator* gene family to cytokinin. *Plant Physiol.*, **124**, 1706-1717
- De Jong, M., George, G., Ongaro, V., Williamson, L., Willetts, B., Ljung, K., McCulloch, H., Leyser, O. (2014) Auxin and strigolactone signalling are required for modulation of *Arabidopsis* shoot branching by N supply. *Plant Physiol.*, **166**, 384-395
- Delaux, P.M., Xie, X., Timme, R.E., Puech-Pages, V., Dunand, C., Lecompte, E., Delwiche, C.F., Yoneyama, K., Becard, G., Sejalon-Delmas, N. (2012) Origin of strigolactones in the green lineage. *New Phytol.*, **195**, 857-871
- Della Ioio, R., Nakamura, K., Moubayidin, L., Perilli, S., Taniguchi, M., Morita, M.T., Aoyama, T., Costantino, P., Sabatini, S. (2008) A genetic framework for the control of cell division and differentiation in the root meristem. *Science*, **322**, 1380-1384
- DeSmet, I. And Juergens, G. (2007) Patterning the axis in plants-auxin in control. *Curr. Opin. Genet. Dev.* **17**, 337-343
- Ding, Y.F., Huang, P.S., Ling, Q.H. (1995) Relationship between emergence of tiller and nitrogen concentration of leaf blade or leaf sheath on specific node of rice. *J. Nanjing Agric. Univ.*, **18**, 14-18
- Dong, L., Ishak, A., Yu, J., Zhao, R., Zhao, L. (2013) Identification and functional analysis of the three *MAX2* orthologs in chrysanthemum. *J Integr. Plant Biol.*, **55**, 434-442

- Drew, M.C. (1975) Comparison of effects on a localised supply of phosphate, nitrate, ammonium, and potassium on growth on seminal root system, and shoot, in barley. *New Phytol.* **75**, 479-490
- Drummond, R.S., Martinez-Sanchez, N.M., Janssen, B.J., Templeton, K.R., Simons, J.L., Quinn, B.D., Karunairetnam, S., Snowden, K.C. (2009) *Petunia hybrida* *CAROTENOID CLEAVAGE DIOXYGENASE7* is involved in the production of negative and positive branching signals in petunia. *Plant Physiol.* **151**, 1867-1877
- Drummond, R.S., Sheehan, H., Simons, J.L., Martinez-Sanchez, N.M., Turner, R.M., Putterill, J. and Snowden, K.C. (2012) The expression of petunia strigolactone pathway genes is altered as part of the endogenous developmental program. *Front. Plant Sci.* **2**, 115
- Dun, E.A., Hanan, J., Beveridge, C.A. (2009) Computational modelling and molecular physiology experiments reveal new insights into shoot branching in pea. *Plant Cell.*, **21**, 3459-3472
- Dun, E.A., de Saint Germain, A., Rameau, C., Beveridge, C.A. (2012) Antagonistic action of strigolactone and cytokinin in bud outgrowth control. *Plant Physiol.* **158**, 487-498
- Emery, R. J. *et al.* (1998) cis-isomers of cytokinins predominate in chickpea seeds throughout their development. *Plant Physiol.*, **117(4)**, 1515-1523
- Endo, M. and Toki, S. (2014) Toward establishing an efficient and versatile gene targeting system in higher plants. *Biocatal. Agric. Biotechnol.* **3(1)**, 2-6
- Flematti, G.W., Dixon, K.W., Smith, S.M. (2015) What are karrikins and how were they 'discovered' by plants? *BCM. BIOL.* **13**, 108
- Foo, E., Bullier, E., Goussot, M., Foucher, F., Rameau, C., Beveridge, C.A. (2005) The branching gene *RAMOSUS1* mediates interactions among two novel signals and auxin in pea. *Plant Cell*, **17**, 464-474
- Foo, E., Morris, S.E., Parmenter, K., Young, N., Wang, H., Jones, A., Rameau, C., Turnbull, C.G.N., Beveridge, C.A. (2007) Feedback regulation of xylem cytokinin content is conserved in pea and *Arabidopsis*. *Plant Physiol.* **143**, 1418-1428
- Fowler, S. and Thomashow, M.F. (2002) *Arabidopsis* Transcriptome Profiling Indicates That Multiple Regulatory Pathways Are Activated during Cold Acclimation in Addition to the CBF Cold Response Pathway. *Plant Cell*, **14(8)**, 1675-1690
- Fridman, Y. and Savaldi-Goldstein, S. (2013) Brassinosteroids in growth control: how, when and where. *Plant Sci.*, **209**, 24-31
- Fukui, K., Ito, S., Asami, T. (2013) Selective mimics of strigolactone actions and their potential use for controlling damage caused by root parasitic weeds. *Mol. Plant*, **6**, 88-99

- Furutani, M., Vernoux, T., Traas, J., Kato, T., Tasaka, M., Aida, M. (2004) PIN-FORMED1 and PINOID regulate boundary formation and cotyledon development in *Arabidopsis* embryogenesis. *Development*, **131**, 5021-5030
- Gallavotti, A., Zhao, Q., Kyojuka, L., Meeley, R.B., Ritter, M., Doebley, J.F. *et al.* (2004) The role of barren stalk1 in the architecture of maize. *Nature*, **432**, 630-635
- Gälweiler, L. *et al.* (1998) Regulation of polar auxin transport by AtPIN1 in Arabidopsis vascular tissue. *Science*. **282(5397)**, 2226-2230
- Gao, Z.Y., Qian, Q., Liu, X.H., Yan, M.X., Feng, O., Dong, G.J., Liu, J., Han, B. (2009) Dwarf 88, a novel putative esterase gene affecting architecture of rice plant. *Plant Mol. Biol.*, **71**, 265-276
- Garcia, D., Collier, S.A., Byrne, M.E., Martienssen, R.A. (2006) Specification of leaf polarity in *Arabidopsis* via the trans-acting siRNA pathway. *Curr. Biol.* **16(9)**, 933-938
- Geisler, M. *et al.* (2005) Cellular efflux of auxin catalyzed by the Arabidopsis MDR/PGP transporter AtPGP1. *The Plant Journal*. **44(2)**, 179-94
- Geldner, N. *et al.* (2003) The Arabidopsis GNOM ARF-GEF mediates endosomal recycling, auxin transport, and auxin-dependent plant growth. *Cell*. **112(2)**, 219-230
- Gendron, J.M., Liu, J.S., Fan, M., Bai, M.Y., Wenkel, S., Springer, P.S., *et al.* (2012) Brassinosteroids regulate organ boundary formation in the shoot apical meristem of *Arabidopsis*. *Proc. Natl Acad. Sci. USA*. **109**, 21152-21157
- Goldsmith, M.H.M. (1968) The transport of auxin. *Annual review of plant physiology*. **19**, 347-360
- Gomez-Roldan, V., Fermas, S., Brewer, P.B. *et al.* (2008) Strigolactone inhibition of shoot branching. *Nature*, **455**, 189-194
- González-Grandío, E. *et al.* (2013). BRANCHED1 Promotes Axillary Bud Dormancy in Response to Shade in Arabidopsis. *Plant Cell*. **25(3)**, 834-850
- Grbic, V. and Bleecker, A.B. (2000) Axillary meristem development in *Arabidopsis thaliana*. *Plant J*. **21**, 215-223
- Greb, T., Clarenz, O., Schafer, E., Muller, D., Herrero, R., Schmitz, G. *et al.* (2003) Molecular analysis of the *LATERAL SUPPRESSOR* gene in *Arabidopsis* reveals a conserved control mechanism for axillary meristem formation. *Gene Dev*. **17**, 1175-1187
- Greenboim-Wainberg, Y., Maymon, I., Borochoy, R., Alvarez, J., Olszewski, N., Ori, N., Eshed, Y., Weiss, D. (2005) Crosstalk between Gibberellin and Cytokinin: The *Arabidopsis*

- GA response inhibitor SPINDLY plays a positive role in cytokinin signalling. *Plant Cell*, **17**, 92-102
- Grossmann, K. (2007) Auxin herbicide action. Lifting the veil step by step. *Plant Signal Behav.* **2(5)**, 421-423
- Guan, J.C., Koch, K.E., Suzuki, M., Wu, S., Latshaw, S., Petruff, T., Goulet, C., Klee, H.J., McCarty, D.R. (2012) Diverse roles of strigolactone signalling in maize architecture and the uncoupling of a branching-specific subnetwork. *Plant Physiol.*, **160**, 1303-1317
- Guilfoyle, T. and Hagen, G. (2007) Auxin response factors. *Current Opinions in Plant Biology.* **10(5)**, 453-460
- Guo, F-Q. *et al.* (2002) The Arabidopsis dual-affinity nitrate transporter gene AtNRT1.1(CHL1) is regulated by auxin in both shoots and roots. *Journal of Experimental Botany.* **53(370)**, 835-844
- Ha, C.V., Leyva-Gonzalez, M.A., Osakabe, Y. *et al.* (2013) Positive regulatory role of strigolactone in plant responses to drought and salt stress. *Proc. Natl Acad. Sci. USA*, **111**, 851-856
- Hagen, G. and Guilfoyle, T. (2002) Auxin-responsive gene expressions: genes, promoters and regulatory factors. *Plant Molecular Biology.* **49(3-4)**, 373-385
- Hamann, T. *et al.* (1999) The auxin-insensitive bodenlos mutation affects primary root formation and apical-basal patterning in the Arabidopsis embryo. *Development.* **126(7)**, 1387-1395
- Hall, S.M. and Hillman, J.R. (1975) Correlative inhibition of lateral bud growth in *Phaseolus vulgaris* L. Timing of bud growth following decapitation. *Planta*, **123**, 137-143
- Hamiaux, C., Drummond, R.S., Janssen, B.J., Ledger, S.E., Cooney, J.M., Newcomb, R.D., Snowden, K.C. (2012) DAD2 is an α/β hydrolase likely to be involved in the perception of the plant branching hormone strigolactone. *Curr. Biol.*, **22**, 2032-2036
- Hellmann, H. *et al.* (2003) Arabidopsis AXR6 encodes CUL1 implicating SCF E3 ligases in auxin regulation of embryogenesis. *The EMBO journal.* **22(13)**, 3314-3325
- Hilman, J.R., *et al.* (1977). Apical dominance and levels of IAA in *Phaseolus* Lateral buds. *Planta* **134**, 191-193
- Hilton, H.W. (1966) The effects of plant-growth substances on carbohydrate systems. *Adv Carbohydr Chem Biochem.* **21**, 377-430
- Houba-Hérin, N., Pethe, C., d'Alayer, J., Laloue, M. (1999) Cytokinin oxidase from *Zea mays*: purification, cDNA cloning and expression in moss protoplasts. *Plant J.* **17**, 615-626

- Huang, X. and Han, B. (2014) Natural Variations and Genome-Wide Association Studies in Crop Plants. *Ann. Rev. Plant Biol.*, **65**, 531-551
- Hwang, I., Sheen, J., Müller, B. (2012) Cytokinin signalling networks. *Annu. Rev. Plant Biol.* **63**, 353-380
- Ikezaki, M., Kojima, M., Sakakibara, H., Kojima, S., Ueno, Y., Machida, C. *et al.* (2010) Genetic networks regulated by ASYMMETRIC LEAVES1 (AS1) and AS2 in leaf development in *Arabidopsis thaliana*: *KNOX* genes control five morphological events. *Plant J.*, **61**, 70-82
- Ishikawa, S., Maekawa, M., Arite, T., Onishi, K., Takamura, I., Kyojuka, J. (2005) Suppression of tiller bud activity in tillering *dwarf* mutants of rice. *Plant Cell Physiol.* **46**, 79-86
- Ito, J., Batth, T.S., Petzold, C.J., Redding-Johanson, A.M., Mukhopadhyay, A., Verboom, R., Meyer, E.H., Millar, A.H., Heazlewood, J.L. (2011) Analysis of the *Arabidopsis* cytosolic proteome highlights subcellular partitioning of central plant metabolism. *J. Proteome Res.* **10**(4), 1571-1582
- Jacobsen, S.E. and Olszewski, N.E. (1993) Mutations at the *SPINDLY* locus of *Arabidopsis* alter gibberellins signal transduction. *Plant Cell*, **5**, 887-896
- Janssen, B.J., Drummond, R.S.M., Snowden, K.C. (2014) Regulation of axillary shoot development. *Curr. Opin. Plant Biol.* **17**, 28-35
- Jiang, L., Liu, X., Xiang, G., Liu, H., Chen, F., Wang, L., Meng, X., Liu, G., Yu, H., Yuan, Y. *et al* (2013) DWARF53 acts as a repressor of strigolactone signalling in rice. *Nature*, **504**, 401-405
- Jiang, W., Yang, B., Weeks, D.P. (2014) Efficient CRISPR/Cas9-Mediated Gene Editing in *Arabidopsis thaliana* and Inheritance of Modified Genes in the T2 and T3 Generations. *PLoS One.* **9**(6), e99225
- Johnson, X., Brchich, T., Dun, E.A., Groussot, M., Haurongé, K., Beveridge, C.A., Rameau, C. (2006) Branching genes are conserved across species. Genes controlling a novel signal in pea are coregulated by other long-distance signals. *Plant Physiol.*, **142**, 1014-1026
- Jones, B., Gunnerås, S.A., Petersson, S.V., Tarkowski, P., Graham, N., May, S., Dolezal, K., Sandberg, G., Ljung, K. (2010) Cytokinin regulation of auxin synthesis in *Arabidopsis* involves a homeostatic feedback loop regulated via auxin and cytokinin signal transduction. *Plant Cell*, **22**, 2956-2969
- de Jong, M. and Leyser, O. (2012) Developmental plasticity in plants. *Cold Spring Harb. Symp. Quant. Biol.* **77**, 63-73

- Kagiyama, M., Hirano, Y., Mori, T., Kim, S.Y., Kyojuka, J., Seto, Y., Yamaguchi, S., Hakashima, T. (2013) Structures of D14 and D14L in the in the strigolactone and karrikin signalling pathways. *Genes Cells*, **18**, 147-160
- Kakimoto, T. (2001) Identification of plant cytokinin biosynthetic enzymes as dimethylallyl diphosphate: ATP/ADP isopentenyltransferases. *Plant Cell Physiol.* **42**, 677-685
- Kalousek, P., Buchtová, D., Balla, J. (2010) Cytokinin and polar transport of auxin in axillary pea buds. *Acta. Universitatis Agriculturae et Silviculturae Mendelianae Brunensis*, **LVIII**, 79-88
- Kang, J., Hwang, J.U., Lee, M., Kim, Y.Y., Assmann, S.M., Martinoia, E., Lee, Y. (2010) PDR-type ABC transporter mediates cellular uptake of the phytohormone abscisic acid. *Proc. Natl Acad. Sci. USA*, **107**, 2355-2360
- Kapulnik, Y., Delaux, P.M., Resnick, N. *et al.* (2011) Strigolactones affect lateral root formation and root-hair elongation in Arabidopsis. *Planta*, **233**, 209-216
- Keller, T., Abbott, J., Moritz, T., Doerner, P. (2006) *Arabidopsis* *REGULATOR OF AXILLARY MERISTEMS1* controls a leaf axil stem cell niche and modulates vegetative development. *Plant Cell*, **18**, 598-611
- Kerstetter, R.A. *et al.* (2001). KANADI regulates organ polarity in Arabidopsis. *Nature*. **411(6838)**, 706-709
- Kerstetter, R.A. and Hake, S. (1997) Shoot meristem formation in vegetative development. *Plant Cell*, **9**, 1001-1010
- Kim, J., Harter, K., and Theologis, A. (1998) Protein-protein interactions among the Aux/IAA proteins. *Proceedings of the National Academy of Science USA*. **94(22)**, 11786-11791
- Kohlen, W., Charnikhova, T., Liu, O., Bours, R., Domagalska, M.A., Beguerie, S., Verstappen, F., Leyser, O., Bouwmeester, H., Ruyter-Spira, C. (2011) Strigolactones are transported through the xylem and play a key role in shoot architectural response to phosphate deficiency in nonarbuscular mycorrhizal host *Arabidopsis*. *Plant Physiol.*, **155**, 974-987
- Kohlen, W., Charnikhova, T., Lammers, M. *et al.* (2012) The tomato *CAROTENOID CLEAVAGE DIOXYGENASE8 (SICCD8)* regulates rhizosphere signalling, plant architecture and affects reproductive development through strigolactone biosynthesis. *New Phytol.*, **196**, 535-547
- Komatsu, K., Maekawa, M., Ujiie, S., Satake, Y., Furutani, I., Okamoto, H. *et al.* (2003) LAX and SPA: major regulators of shoot branching in rice. *Proc. Natl. Acad. Sci. USA*, **100**, 11765-11770
- Konieczny, A. and Ausubel, F.M. (1993) A procedure for mapping *Arabidopsis* mutations using co-dominant ecotype-specific PCR-based markers. *Plant J.* **4(2)**, 403-410

- Koorneef, M. and Mienke, D. (2010) The development of *Arabidopsis* as a model plant. *Plant J.* **69**, 909-921
- Kretschmar, T., Kohlen, W., Sasse, J., Borghi, L., Schlegel, M., Bachelier, J.B., Reinhardt, D., Bours, R., Bouwmeester, H.J., Martinoia, E. (2012) A petunia ABC protein controls strigolactone-dependent symbiotic signalling and branching. *Nature*, **483**, 341-U135
- Kuromori, T., Miyaji, T., Yabuuchi, H., Shimizu, H., Sugimoto, E., Kamiya, A., Moriyama, Y., Shinozaki, K. (2010) ABC transporter AtABCG25 is involved in abscisic acid transport and responses. *Proc. Natl Acad. Sci. USA*, **107**, 2361-2366
- Laplaze, L., Benkova, E., Casimiro, I., Maes, L., Vanneste, S., Swarup, R., Weijers, D., Calvo, V., Parizot, B., Herrera-Rodriguez, M.B., *et al.* (2007) Cytokinins act directly on lateral root founder cells to inhibit root initiation. *Plant Cell*, **19**, 3889-3900
- Leyser, H.M. *et al.* (1993) *Arabidopsis* auxin-resistance gene *AXR1* encodes a protein related to ubiquitin-activating enzyme E1. *Nature*. **364(6433)**, 161-164
- Leyser, O. (2003) Regulation of shoot branching by auxin. *Trends Plant Sci.*, **8**, 541-545
- Leyser, O. (2005) The fall and rise of apical dominance. *Curr. Opin. Genet. Dev.* **15**, 468-471
- Li, C.J. and Bangerth, F. (1999) Autoinhibition of indoleacetic acid transport in the shoots of two-branched pea (*Pisum sativum*) plants and its relationship to correlative dominance. *Physiol. Plant*, **106**, 415-420
- Li, X.Y., Qian, Q., Fu, Z.M., Wang, Y.H., Xiong, G.S., Zeng, D.L. *et al.* (2003) Control of tillering in rice. *Nature*, **422**, 618-621
- Lin, H., Wang, R., Qian, O. *et al.* (2009) DWARF27, an iron-containing protein required for the biosynthesis of strigolactones, regulates rice tiller bud outgrowth. *Plant Cell*, **21**, 1512-1525
- Linkhor, B. *et al.* (2002). Nitrate and phosphate availability and distribution have different effects on root system architecture of *Arabidopsis*. *Plant J*, **29(6)**, 751-760
- Liu, W., Wu, C., Fu, Y., Hu, G., Si, H., Zhu, L., Luan, W., He, Z., Sun, Z. (2009) Identification and characterisation of *HTD2*: a novel gene negatively regulating tiller bud outgrowth in rice. *Planta*, **230**, 649-658
- Liu, Y., Gu, D.D., Ding, Y.F., Wang, Q.S., Li, G.H., Wang, S.H. (2011) The relationship between nitrogen, auxin and cytokinin in the growth regulation of rice (*Oryza sativa L.*) tiller buds. *Aust. J. Crop Sci.*, **5**, 1019-1026
- Ljung, K. *et al.* (2001) Sites and homeostatic control of auxin biosynthesis in *Arabidopsis* during vegetative growth. *Plant J.* **28**, 465-474

- Long, J.A., Moan, E.I., Medford, J.I., Barton, M.K. (1996) A member of the KNOTTED class of homeodomain proteins encoded by the *STM* gene of *Arabidopsis*. *Nature*, **379**, 66-69
- Long, J. and Barton, M.K. (2000) Initiation of axillary and floral meristems in *Arabidopsis*. *Dev. Biol.* **218**, 341-353
- Lopez-Bucio, J., Hernandez-Abreu, E., Sanchez-Calderon, L., Nieto-Jacobo, M.F., Simpson, J., Herrera-Estrella, L. (2002) Phosphate availability alters architecture and causes changes in hormone sensitivity in the *Arabidopsis* root system. *Plant Physiol.*, **129**, 244-256
- Mangnus, E.M., Dommerholt, F.J., Dejong, R.L.P., Zwanenburg, B. (1992) Improved synthesis of strigol analog GR24 and evaluation of the biological-activity of its diastereomers. *J. Agric. Food Chem.*, **40**, 1230-1235
- Mano, Y. and Nemoto, K. (2012) The pathway of auxin biosynthesis in plants. *J. Exp. Bot.* **63(8)**, 2853-2872
- Mashiguchi, K., Sasaki, E., Shimada, Y., Asami, T. (2009) Feedback-regulation of strigolactone biosynthetic genes and strigolactone-regulated genes in *Arabidopsis*. *Biosci. Biotechnol. Biochem.* **73**, 2460-2465
- Matsumoto-Kitano, M., Kusumoto, T., Tarkowski, P., Kinoshita-Tsujimura, K., Václavíková, K., Miyawaki, K., Kakimoto, T. (2008) Cytokinins are central regulators of cambial activity. *Proc. Natl Acad. Sci. USA*, **105**, 20027-20031
- Matusova, R. *et al.* (2005) The strigolactone germination stimulants of the plant-parasitic *Striga* and *Orobancha* spp. are derived from the carotenoid pathway. *Plant Physiol.* **139(2)**, 920-934
- McIntyre, G.I. (2001) Control of plant development by limiting factors: a nutritional perspective. *Physiol. Plantarum*, **113**, 165-175
- McIntyre, G.I. and Cessna, A.J. (1991) Apical dominance in *Phaseolus vulgaris* – effect of the nitrogen supply. *Can. J. Bot.*, **69**, 1337-1343
- McIntyre, G.I. and Hunter, J.H. (1975) Some effects of nitrogen supply on growth and development of *Cirsium arvense*. *Can. J. Bot.*, **53**, 3012-3021
- McSteen, P. and Leyser, O. (2005) Shoot Branching. *Annu. Rev. Plant Biol.* **56**, 353-374
- Mienke, D.W., Cherry, J.M., Dean, C., Rounsley, S.D., Koorneef, M. (1998) *Arabidopsis thaliana*: A model plant for genome analysis. *Science*. **282**, 662-682
- Miyawaki, K., Matsumoto-Kitano, M., Kakimoto, T. (2004) Expression of cytokinin biosynthetic *isopentenyltransferase* genes in *Arabidopsis*: tissue specificity and regulation by auxin, cytokinin, and nitrate. *Plant J.* **37**, 128-138

- Mok, D.W. and Mok, M.C. (2001) Cytokinin metabolism and action. *Annu. Rev. Plant Physiol. Plant Mol. Biol.*, **52**, 89-118
- Mooney, K.A. (2010) Evolutionary Trade-Offs in Plants Mediate the Strength of Trophic Cascades. *Science*, **327**, 1642-1644
- Morris, D.A. (1977) Transport of exogenous auxin in 2-branched dwarf pea-seedlings (*Pisum sativum* L)-some implications for polarity and apical dominance. *Planta*, **136**, 91-96
- Morris, S.E., Turnbull, C.G., Murfet, I.C., Beveridge, C.A. (2001) Mutational analysis of branching in pea. Evidence that *RMS1* and *RMS5* regulate the same novel signal. *Plant Physiol.*, **126**, 1205-1213
- Müller, D., Waldie, T., Miyawaki, K., To, J.P.C., Melnyk, C.W., Kieber, J.J., Kakimoto, T., Leyser, O. (2015) Cytokinin is required for escape but not release from auxin mediated apical dominance. *Plant J.*, **82**, 874-886
- Nakamura, H., Xue, Y.L., Miyakawa, T., Hou, F., Qin, H.M., Fukui, K., Shi, X., Ito, E., Ito, S., Park, S.H. *et al* (2013) Molecular mechanism of strigolactone perception by DWARF14. *Nat. Commun.* **4**, 2613
- Napoli, C. (1996) Highly branched phenotype of the petunia *dad1-1* mutant is reversed by grafting. *Plant Physiol.*, **111**, 27-37
- Nelson, D.C., Scaffidi, A., Dun, E.A., Waters, M.T., Flematti, G.R., Dixon, K.W., Beveridge, C.A., Ghisalberti, E.L., Smith, S.M. (2011) F-box protein MAX2 has dual roles in karrikin and strigolactone signalling in *Arabidopsis thaliana*. *Proc. Natl Acad. Sci. USA*, **108**, 8897-8902
- Nordström, A., Tarrkowski, P., Tarkowska, D., Norbaek, R., Åstot, C., Dolezal, K., Sandberg, G. (2004) Auxin regulation of cytokinin biosynthesis in *Arabidopsis thaliana*: a factor of potential importance for auxin-cytokinin-regulated development. *Proc. Natl Acad. Sci. USA*, **101**, 8039-8044
- Okada, K. *et al.* (1991) Requirement of the Auxin Polar Transport System in Early Stages of Arabidopsis Floral Bud Formation. *Plant Cell*. **3(7)**, 677-684
- Otsuga, D., DeGuzman, B., Prigge, M.J., Drews, G.N., Clark, S.E. (2001) REVOLUTA regulates meristem initiation at lateral positions. *Plant J.* **25(2)**, 223-236
- Paciorek, T., Zazimalova, E., Ruthardt, N., Petrasek, J., Stierhof, Y.D., Kleine-Vehn, J. *et al.* (2005) Auxin inhibits endocytosis and promotes its own efflux from cells. *Nature*, **435**, 1251-1256
- Pandya-Kumar, N., Shema, R., Kumar, M., Mayzlish-Gati, E., Levy, D., Zemach, H., Belausov, E., Wininger, S., Abu-Abied, M., Kapulnik, Y., Koltai, H. (2014) Strigolactone analog GR24 triggers changes in PIN2 polarity, vesicle trafficking and actin filament architecture. *New Phytol.*, **202(4)**, 1184-1196

- Pekker, I., Alvarez, J.P., Eshed, Y. (2005) Auxin response factors mediate *Arabidopsis* organ asymmetry via modulation of KANADI activity. *Plant Cell*. **17(11)**, 2899-2910
- Petrášek, J. and Friml, J. (2009) Auxin transport routes in plant development. *Development*, **136**, 2675-2688
- Pierik, R. and de Wit, M. (2014) Shade avoidance: phytochrome signalling and other aboveground neighbour detection cues. *J. Exp. Bot.* **65(11)**, 2815-2824
- Postma, J.A., Schurr, U., Fiorani, F. (2014) Dynamic root growth and architecture responses to limiting nutrient availability: linking physiological models and experimentation. *Biotechnol. Adv.* **32(1)**, 53-65
- Pozo, J.C. *et al.* (1998) The ubiquitin-related protein RUB1 and auxin response in *Arabidopsis*. *Science*. **280(5370)**, 1760-1763
- Prigge, M.J. *et al.* (2005) Class III homeodomain-leucine zipper gene family members have overlapping, antagonistic, and distinct roles in *Arabidopsis* development. *Plant Cell*. **17(1)**, 61-76
- Prusinkiewicz, P., Crawford, S, Smith, R.S., Ljung, K., Bennet, T., Ongaro, V., Leyser, O. (2009) Control of bud activation by an auxin transport switch. *Proc. Natl Acad. Sci. USA*, **106**, 17431-17346
- Qi, J., Wang, Y., Yua, T., Cunhae, A., Wua, B., Vernoux, T., Meyerowitz, E., Jiaoa, Y. (2014) Auxin depletion from leaf primordia contributes to organ patterning. *PNAS*. **111(52)**, 18769-18774
- Rasmussen, A., Mason, M.G., De Cuyper, C. *et al.* (2012) Strigolactones suppress adventitious rooting in *Arabidopsis* and Pea. *Plant Physiol.*, **158**, 1976-1987
- Reinhardt, D., Frenz, M., Mandel, T., Kuhlemeier, C. (2005) Microsurgical and laser ablation analysis of leaf positioning and dorsoventral patterning in tomato. *Development*. **132(1)**, 15-26
- Ritter, M.K., Padilla, C.M., Schmidt, R.J. (2002) The maize mutant barren stalk1 is defective in axillary meristem development. *Am. J. Bot.*, **89**, 203-210
- Ruegger, M. *et al.* (1998) The TIR1 protein of *Arabidopsis* functions in auxin response and is related to human SKP2 and yeast grr1p. *Genes Dev.* **12(2)**, 198-207
- Ruyter-Spira, C., Kohlen, W., Charnikhova, T.V. *et al.* (2011) Physiological effects of the synthetic strigolactone analogue GR24 on root system architecture in *Arabidopsis*: another belowground role for strigolactones? *Plant Physiol.*, **155**, 721-734
- Sachs, T. (1975) The induction of auxin channels by auxin. *Planta*. **127**, 201-206
- Sachs, T. (1981) The control of the patterned differentiation of vascular tissues. *Adv. Bot. Res.*, **9**, 151-262

- Sachs, T. and Thimann, K.V. (1964) Release of lateral buds from apical dominance. *Nature*, **201**, 939-940
- de Saint Germain, A., Ligerot, Y., Dun, E.A., Pillot, J.P., Ross, J.J., Beveridge, C.A., Rameau, C. (2013) Strigolactones stimulate internode elongation independently of gibberellins. *Plant Physiol.* **163**, 1012-1025
- Sakakibara, H. (2006) Cytokinins: activity, biosynthesis, and transduction. *Annu. Rev. Plant Biol.* **57**, 431-449
- Salmon J., Ward S.P., Hanley S.J., Leyser O, Karp A. (2014) Functional screening of willow alleles in Arabidopsis combined with QTL mapping in willow (*Salix*) identifies *SxMAX4* as a coppicing response gene. *Plant Biotechnol J.* **12(4)**, 480-491.
- Sato, D., Awad, A.A., Takeuchi, Y., Yoneyama, K. (2005) Confirmation and quantification of strigolactones, germination stimulants for root parasitic plants *Striga* and *Orobancha*, produced by cotton. *Biosci. Biotechnol. Biochem.*, **69**, 98-102
- Sawa, S. *et al.* (1999) FILAMENTOUS FLOWER, a meristem and organ identity gene of Arabidopsis, encodes a protein with a zinc finger and HMG-related domains. *Genes and Development.* **13(9)**, 1079-1088
- Scaffidi, A., Waters, M.T., Ghisalberti, E.L., Dixon, K.W., Flematti, G.R., Smith, S.M. (2013) Carlactone-independent seedling morphogenesis in *Arabidopsis*. *Plant J.*, **76**, 1-9
- Scarpella, E. *et al.* (2006). Control of leaf vascular patterning by polar auxin transport. *Genes and Development.* **20(8)**, 1015-1027
- Scheible, W.R., González-Fontes, A., Lauerer, M., Müller-Röber, B., Caboche, M., Stitt, M. (1997) Nitrate acts as a signal to induce organic acid metabolism and repress starch metabolism in tobacco. *Plant Cell.* **9**, 783-798
- Schmitz, G., Tillmann, E., Carriero, F., Fiore, C., Cellini, F., Theres, K. (2002) The tomato blind gene encodes a MYB transcription factor that controls the formation of lateral meristems. *Proc. Natl. Acad. Sci. USA*, **99**, 1064-1069
- Schmitz, G. And Theres, K. (2005) Shoot and inflorescence branching. *Curr Opin. Plant Biol.*, **8**, 506-511
- Schmülling, T., Werner, T., Riefler, M., Krupková, E., Bartrinay-Manns, I. (2003) Structure and function of cytokinin oxidase/dehydrogenase genes of maize, rice, *Arabidopsis* and other species. *J. Plant Res.* **116**, 241-252
- Schumacher, K., Schmitt, T., Rossberg, M., Schmitz, C., Theres, K. (1999) The lateral suppressor (Ls) gene of tomato encodes a new member of the VHIID protein family. *Proc. Natl Acad. Sci. USA*, **96**, 290-295

- Sclereth, A. *et al.* (2010) MONOPTEROS controls embryonic root initiation by regulating a mobile transcription factor. *Nature*. **464**, 913-916
- Seto, Y., Sado, A., Asami, K., Hanada, A., Umehara, M., Akiyama, K., Yamaguchi, S. (2014) Carlactone is an endogenous biosynthetic precursor for strigolactones. *Proc. Natl Acad. Sci. USA*, **111**, 1640-1645
- Sharda, J.N. and Koide, R.T. (2008) Can hypodermal passage cell distribution limit root penetration by mycorrhizal fungi? *New Phytol.*, **180**, 696-701
- Shimizu-Sato, S. and Mori, H. (2001) Control of outgrowth and dormancy in axillary buds. *Plant Physiol.* **127(4)**, 1405-1413
- Shinohara, N., Taylor, C., Leyser, O. (2013) Strigolactone can promote or inhibit shoot branching by triggering rapid depletion of the auxin efflux protein PIN1 from the plasma membrane. *PLoS Biol*, **11**, e1001474
- Siegfried, K.R. *et al.* (1999). Members of the YABBY gene family specify abaxial cell fate in *Arabidopsis*. *Development*. **126(18)**, 4117-4128
- Simons, J.L., Napoli, C.A., Janssen, B.J., Plummer, K.M., Snowden, K.C. (2007) Analysis of the *DECREASED APICAL DOMINANCE* genes of petunia in the control of axillary branching. *Plant Physiol.*, **143**, 697-706
- Skoog, F., and Miller, C.O. (1957) Chemical regulation of growth and organ formation in plant tissues cultured *in vitro*. *Symp. Soc. Exp. Biol.* **11**, 118-130
- Snowden, K.C., Simkin, A.J., Janssen, B.J., Templeton, K.R., Loucas, H.M., Simons, J.L., Karunairetnam, S., Gleave, A.P., Clark, D.G., Klee, H.J. (2005) The *DECREASED APICAL DOMINANCE/ Petunia hybrida CAROTENOID CLEAVAGE DIOXYGENASE* gene affects branch production and plays a role in leaf senescence, root growth, and flower development. *Plant Cell*, **17**, 746-759
- Sorefan, K., Booker, J., Haurogné, K., *et al.* (2003) *MAX4* and *RMS1* are orthologous dioxygenase-like genes that regulate shoot branching in *Arabidopsis* and pea. *Genes Dev.*, **17**, 1469-1474
- Soundapanna, I., Bennett, T., Morffy, N., Liang, Y., Stanga, J.P., Abbas, A., Leyser, O., Nelson, D.C. (2015) *SMAX1-LIKE/D53* Family Members Enable Distinct MAX2-Dependent Responses to Strigolactones and Karrikins in *Arabidopsis*. *Plant Cell*. **27(11)**, 3143-3159
- Spinelli, S.V., Martin, A., Viola, I.L., Gonzalez, D.H., Palatnik, J.F. (2011) A meristematic link between STM and CUC1 during *Arabidopsis* development. *Plant Physiol.* **156**, 1894-1904
- Stanga, J.P., Smith, S.M., Briggs, W.R., Nelson, D.C. (2013) *SUPPRESSOR OF MORE AXILLARY GROWTH2 1* controls seed germination and seedling development in *Arabidopsis*. *Plant Physiol.*, **163**, 318-330

- Stirnberg, P. *et al.* (2002) *MAX1* and *MAX2* control shoot lateral shoot branching *Development* **129**, 1131-41
- Stirnberg, P. *et al.* (2007) *MAX2* participates in an SCF complex which acts locally at the node to suppress shoot branching. *The Plant Journal*. **50**, 80-94
- Stirnberg, P., Liu, J.P., Ward, S., Kendall, S.L., Leyser, O. (2012) Mutation of the cytosolic ribosomal protein-encoding *RPS10B* gene affects shoot meristematic function in *Arabidopsis*. *BMC Plant Biol.* **12**:160
- Sugawara, S. *et al.* (2009) Biochemical analyses of indole-3-acetaldoxime-dependent auxin biosynthesis in *Arabidopsis*. *Proc. Natl. Acad. Sci. USA*. **106(13)**, 5430-5435
- Sugimoto-Shirasu, K. and Roberts, K. (2003) “Big it up”: endoreduplication and cell-size control in plants. *Curr. Opin. Plant Biol.* **6(6)**, 544-555
- Sussex, I.M. (1951) Experiments on the cause of dorsiventrality. *Nature*. **167(4251)**, 651-652
- Sussex, I.M. and Kerk, N.M. (2001) The evolution of plant architecture. *Curr. Opin. Plant Biol.*, **4**, 33-37
- Takei, K., Sakakibara, H., and Sugiyama, T. (2001a) Identification of genes encoding adenylate isopentenyltransferase, a cytokinin biosynthesis enzyme, in *Arabidopsis thaliana*. *J. Biol. Chem.* **276**, 26405-26410
- Takei, K., Sakakibara, H., Taniguchi, M., Sugiyama, T. (2001b) Nitrogen-dependent accumulation of cytokinins in root and the translocation to leaf: implication of cytokinin species that induces gene expression of maize response regulator. *Plant Cell Physiol.* **42**, 85-93
- Takei, K., Takahashi, T., Sugiyama, T., Yamaya, T., Sakakibara, H. (2002) Multiple routes communicating nitrate availability from roots to shoots: a signal transduction pathway mediated by cytokinin. *J. Exp. Bot.* **53**, 971-977
- Takei, K., Yamaya, T. and Sakakibara, H. (2004) *Arabidopsis CYP735A1* and *CYP735A2* encode cytokinin hydroxylases that catalyse the biosynthesis of trans-Zeatin. *J. Biol. Chem.* **279**, 41866-41872
- Tameshige, T., Fujita, H., Watanabe, K., Toyokura, K., Kondo, M., Tatematsu, K., Matsumoto, N., Tsugeki, R., Kawaguchi, M., Nishimura, M. (2013) Pattern Dynamics in Adaxial-Abaxial Specific Gene Expression Are Modulated by a Plastid Retrograde Signal during *Arabidopsis thaliana* Leaf Development. *PLOS genetics*. **9(7)**, e1003655
- Tanaka, M., Takei, K., Kojima, M., Sakakibara, H., Mori, H. (2006) Auxin controls local cytokinin biosynthesis in the nodal stem in apical dominance. *Plant J.* **45**, 1028-1036
- Tao, Y. *et al.* (2008) Rapid synthesis of auxin via a new tryptophan-dependent pathway is required for shade avoidance in plants. *Cell*. **133(1)**, 164-176

- Thimann, K.V. and Skoog, F. (1933) Studies on the growth hormones of plants III. The inhibiting action of the growth substance on bud development. *Proc. Natl. Acad. Sci. USA*. **19**, 714-716
- Tiwari, S.B. *et al.* (2003) The roles of auxin response factor domains in auxin-responsive transcription. *Plant Cell*. **15(2)**, 533-543
- To, J.P.C., Deruère, J., Maxwell, B.B., Morris, V.F., Hutchison, C.E., Ferreira, F.J., Schaller, G.E., Keiber, J.J. (2007) Cytokinin regulates type-A Arabidopsis Response Regulator activity and protein stability via two-component phosphorelay. *Plant Cell*, **19**, 3901-3914
- Toyokura, K., Watanabe, K., Oiwa, A., Kusano, M., Tameshige, T., Tatematsu, K., Matsumoto, N., Tsugeki, R., Saito, K., Okada, K. (2011) Succinic semialdehyde dehydrogenase is involved in the robust patterning of *Arabidopsis* leaves along the adaxial-abaxial axis. *Plant Cell Physiol*. **52(8)**, 1340-1353
- Turnbull, C.G., Raymond, M.A.A., Dodd, I.C., Morris, S.E. (1997) Rapid increases in cytokinin concentration in lateral buds of chickpea (*Cicer arietinum* L) during release of apical dominance. *Planta*, **202**, 271-276
- Turnbull, C.G., Booker, J.P., Leyser, H.M. (2002) Micrografting techniques for testing long-distance signalling in *Arabidopsis*. *Plant J.*, **32**, 255-262
- Ueguchi-Tanaka, M. and Matsuoka, M. (2010) The perception of gibberellins: clues from receptor structure. *Curr. Opin. Plant Biol.* **13(5)**, 503-508
- Ulmasov, T. *et al.* (1995). Composite structure of auxin response elements. *Plant Cell*. **7(10)**, 1611-1623
- Ulmasov, T. *et al.* (1997) Aux/IAA proteins repress expression of reporter genes containing natural and highly active synthetic auxin response elements. *Plant Cell*. **9(11)**, 1963-1971
- Umehara, M., Hanada, A., Yoshida, S. *et al.* (2008) Inhibition of shoot branching by new terpenoid plant hormones. *Nature*, **455**, 195-200
- Vierstra, R.D. (2003) The ubiquitin/26S proteasome pathway, the complex last chapter in the life of many plant proteins. *Trends Plant Sci.* **8(3)**, 135-142
- Vogel, J.T., Walter, M.H., Giavalisc, P. *et al.* (2010) *SICCD7* controls strigolactone biosynthesis, shoot branching and mycorrhiza-induced apocarotenoid formation in tomato. *Plant J.*, **61**, 300-311
- Waldie, T., McCulloch, H., Leyser, O. (2014) Strigolactones and the control of plant development: lessons from shoot branching. *Plant J.* **79**, 607-622
- Wang, H. *et al.* (2005) The tomato Aux/IAA transcription factor IAA9 is involved in fruit development and leaf morphogenesis. *Plant Cell*. **17**, 2676-2692

- Wang, L., Wang, B., Jiang, L., Liu, X., Li, X., Lu, Z., Meng, X., Wang, Y., Smith, S.M., Li, J. (2015) Strigolactone Signaling in *Arabidopsis* Regulates Shoot Development by Targeting D53-Like SMXL Repressor Proteins for Ubiquitination and Degradation. *Plant Cell*, **27(11)**, 3128-3142
- Wang, Q., Kohlen, W., Rossmann, S., Vernoux, T., Theres, K. (2014) Auxin depletion from the leaf axil conditions competence for axillary meristem formation in *Arabidopsis* and tomato. *Plant Cell*, **26**, 2068-2079
- Wang, Y., Sun, S., Zhu, W., Jia, K., Yang, H., Wang, X. (2013) Strigolactone/MAX2-induced degradation of brassinosteroid transcriptional effector BES1 regulates shoot branching. *Dev. Cell* **27**, 681-688
- Wang, Y., Wang, J., Shi, B., Yu, T., Qi, J., Meyerowitz, E.M. *et al.* (2014) The stem cell niche in leaf axils is established by auxin and cytokinin in *Arabidopsis*. *Plant Cell*, **26**, 2055-2067
- Ward, S.P., Salmon, J., Hanley, S.J., Karp, A., Leyser, O. (2013) Using *Arabidopsis* to study shoot branching in biomass willow. *Plant Physiol.*, **162**, 800-811
- Waters, M.T., Brewer, P.B., Bussell, J.D., Smith, S.M., Beveridge, C.A. (2012a) The *Arabidopsis* ortholog of DWARF27 acts upstream of MAX1 in the control of plant development by strigolactones. *Plant Physiol.*, **159**, 1073-1085
- Waters, M.T., Nelson, D.C., Scaffidi, A., Flematti, G.R., Sun, Y.K., Dixon, K.W., Smith, S.M. (2012b) Specialisation within the DWARF14 protein family confers distinct responses to karrikins and strigolactones in *Arabidopsis*. *Development*, **139**, 1285-1295
- Werner, T., Motyka, V., Laucou, V., Smets, R., Van Onckelen, H., Schmülling, T. (2003) Cytokinin-deficient transgenic *Arabidopsis* plants show multiple developmental alterations indicating opposite functions of cytokinins in the regulation of shoot and root meristem activity. *Plant Cell*, **15**, 2532-2550
- Werner, T., Köllmer, I., Bartrina, I., Holst, K., Schmülling, T. (2006) New insights into the biology of cytokinin degradation. *Plant Biol. (Stuttg.)*, **8**, 371-381
- Wickson, M. & Thimann, K. (1958) The Antagonism of Auxin and Kinetin in Apical Dominance. *Physiologia Plantarum*. **11(1)**, 62-74
- Wilson, A.K. *et al.* (1990) A dominant mutation in *Arabidopsis* confers resistance to auxin, ethylene and abscisic acid. *Mol Gen Genet*. **222(2-3)**, 377-383
- Woo, H.R., Chung, K.M., Park, J.H., Oh, S.A., Ahn, T., Hong, S.H., Jang, S.K., Nam, H.G. (2001) ORE9, an F-box protein that regulates leaf senescence in *Arabidopsis*. *Plant Cell*, **13**, 1779-1790
- Xie, X., Yoneyama, K., Kasumoto, D., Yamada, Y., Yokota, T., Takeuchi, Y., Yoneyama, K. (2008) Isolation and identification of alectrol as (+)-orobanchyl acetate, a germination stimulant for root parasitic plants. *Phytochemistry*, **69**, 427-431

- Xie, X. *et al.* (2010) The strigolactone story. *Annual Review of phytopathology*. **48**, 93-117
- Yang, F., Wang, Q., Schmitz, G., Mueller, D., Theres, K. (2012) The bHLH protein ROX acts in concert with RAX1 and LAS to modulate axillary meristem formation in *Arabidopsis*. *Plant J.*, **71**, 61-70
- Yang, Y. *et al.* (2006) High-affinity auxin transport by the AUX1 influx carrier protein. *Current Biology* **6**, 16(11):1123-7
- Yang, Y., Xu, R., Ma, C., Vlot, C., Klessig, D., Pichersky, E. (2008) Inactive Methyl Indole-3-Acetic Acid Ester Can Be Hydrolyzed and Activated by Several Esterases Belonging to the AtMES Esterase Family of *Arabidopsis*. *Plant Physiol.*, **147**, 1034-1045
- Yao, X., Wang, H., Li, H., Yuan, Z., Li, F., Yang, L., Huang, H. (2009) Two types of cis-acting elements control the abaxial epidermis-specific transcription of the *MIR165a* and *MIR166a* genes. *FEBS Lett.* **583(22)**, 3711-3717
- Yoneyama, K., Xie, X., Sekimoto, H., Takeuchi, Y., Ogasawara, S., Akiyama, K., Hayashi, H., Yoneyama, K. (2008) Strigolactones, host recognition signals for root parasitic plants and arbuscular mycorrhizal fungi, from *Fabaceae* plants. *New Phytol.*, **179**, 484-494
- Yoneyama, K., Xie, X., Kisugi, T., Nomura, T., Yoneyama, K. (2013) Nitrogen and phosphorous fertilization negatively affects strigolactone production and exudation in sorghum. *Planta*, **238**, 885-894
- Zadnikova, P. and Simon, R. (2014) How boundaries control plant development. *Curr. Opin. Plant Dev.* **17**, 116-125
- Zhao, L.H., Zhao, X.E., Wu, Z.S., Yi, W., Xu, Y., Li, S., Xu, T.H., Lui, Y., Chen, R.Z., Kovach, A. *et al.* (2013) Crystal structures of two phytohormone signal-transducing α/β hydrolases: karrikin-signalling KAI2 and strigolactone-signalling DWARF 14. *Cell Res.* **23**, 436-439
- Zhou, F., Lin, Q., Zhu, L., Ren, Y., Zhou, K., Shabek, N., Wu, F., Mao, H., Dong, W., Gan, L., *et al.* (2013) D14-SCF(D3)-dependent degradation of D53 regulates strigolactone signalling. *Nature*, **504**, 406-410
- Zou, J.H., Zhang, S.Y., Zhang, W.P., Li, G., Chen, Z.X., Zhai, W.X., Zhao, X.F., Pan, X.B., Xie, Q., Zhu, L.H. (2006) The rice *HIGH-TILLERING DWARF1* encoding ortholog of *Arabidopsis* *MAX3* is required for negative regulation of the outgrowth of axillary buds. *Plant J.*, **48**, 687-696
- Zwanenburg, B., Mwakaboko, A.S., Reizelman, A., Anilkumar, G., Sethumadhavan, D. (2009) Structure and function of natural and synthetic signalling molecules in parasitic weed germination. *Pest Manag. Sci.*, **65**, 478-491
- Zwanenburg, B., Nayak, S.K., Charnikhova, T.V., Bouwmeester, H.J. (2013) New strigolactone mimics: structure-activity relationship and mode of action as germinating stimulants for parasitic weeds. *Bioorg. Med. Chem Lett.*, **23**, 5182-5186

(2000) *A.thaliana* genome. *Nature*, **408**, 791